ISTANBUL TECHNICAL UNIVERSITY ★ GRADUATE SCHOOL OF SCIENCE ENGINEERING AND TECHNOLOGY

IMPACT OF ADDITIVES ON WELL CEMENT SETTING TEMPERATURE AND CASING DESIGN

M.Sc. THESIS

Sardar ASADOV

Department of Petroleum and Natural Gas Engineering

Petroleum and Natural Gas Engineering Programme

Thesis Advisor: Asst. Prof. Dr. M. Hakan OZYURTKAN

MAY 2017

ISTANBUL TECHNICAL UNIVERSITY ★ GRADUATE SCHOOL OF SCIENCE ENGINEERING AND TECHNOLOGY

IMPACT OF ADDITIVES ON WELL CEMENT SETTING TEMPERATURE AND CASING DESIGN

M.Sc. THESIS
Sardar Asadov
(505141504)

Department of Petroleum and Natural Gas Engineering

Petroleum and Natural Gas Engineering Programme

Thesis Advisor: Asst. Prof. Dr. M. Hakan OZYURTKAN

MAY 2017

ISTANBUL TEKNİK ÜNİVERSİTESİ ★ FEN BİLİMLERİ ENSTİTÜSÜ

KATKI MADDELERİNİN KUYU ÇİMENTOSU DONMA SICAKLIĞINA VE KORUMA BORUSU TASARIMINA ETKİSİ

YÜKSEK LİSANS TEZİ
Sardar Asadov
(505141504)

Petrol ve Doğal Gaz Anabilim Dalı

Petrol ve Doğal Gaz Mühendisliği Programı

Tez Danışmanı: Yrd. Doç. Dr. M. Hakan ÖZYURTKAN

MAYIS 2017

Sardar Asadov, a M.Sc. student of ITU Graduate School of Science Engineering and Technology student ID 505141504, successfully defended the thesis/dissertation entitled “Impact of additives on well cement setting temperature and on casing design”, which he prepared after fulfilling the requirements specified in the associated legislations, before the jury whose signatures are below.

Thesis Advisor : **Asst. Prof. Dr. M. Hakan OZYURTKAN** ....
Istanbul Technical University

Jury Members : **Asst. Prof. Dr. Ihsan M. GOK** ....
Istanbul Technical University

Asst. Prof. Dr. Ali ETTEHADI ....
Izmir Katip Çelebi University

Asst. Prof. Dr. M. Hakan OZYURTKAN ....
Istanbul Technical University

Date of Submission : 3 May 2017
Date of Defense : 9 June 2017

To my family and friends,

FOREWORD

First and foremost, I would like to express my sincere gratitude to my advisor Asst. Prof. Dr. M. Hakan Özyurtkan for the continuous support of my MSc. study, for his patience, motivation, enthusiasm and immense knowledge. His guidance helped me in all the time for writing of this thesis. Besides my advisor, I would like also to thank the rest of my professors and department staff for their invaluable time and guidance in my studies, and as well as my thesis committee for their extreme patience and insightful comments.

Special thanks to Specialist Eda Ay for helping me at the bench throughout my analyses, as well as Özge Ramazanoğlu and Yalçın Yaradılmış to provide additives.

I want to thanks to all my friends for sharing my happiness when starting to my postgraduate degree and following with encouragement when it seemed too difficult to be completed. I would have probably give up without their support and example on what to do when you really want something.

Last but not the least, thanks to my family for having the patience with me for having taking yet another challenge which did not let me to spend time with them because of distances. Specially Minayə, my mother, who has taken a big part of that sacrifice, and also Səbinə, my sister, who gives encouragement in her particular way. Lastly, I want to thank my father, Israyil, for all of the support he has given through all of these years while I am in Istanbul.

May 2017

Sardar Asadov
(M.Sc. Petroleum and Natural Gas Engineer)

TABLE OF CONTENTS

Page

ABBREVIATIONS

API : American Petroleum Institute
ASTM : American Society for Testing and Materials
BWOC : By Weight of Cement
HEC : HydroxyEthyl Cellulose
HSR : High Sulfate Resistant
MSR : Moderate Sulfate Resistant
OLS : Ordinary Least Squares
RPM : Revolution per Minute
WOC : Wait On Cement

SYMBOLS

$\mathbf{D}$: Diameter
$\mathbf{T}$: Temperature
$\mathbf{A_t}$: Cross – sectional area of casing string
$\mathbf{E}$: Young’s elastic modulus
$\mathbf{l}$: Length
$\mathbf{T_o}$: Triaxial stress
$\mathbf{F_o}$: Tensile force
$\mathbf{F_m}$: Maximum load
$\Delta \mathbf{T}$: Temperature difference
$\boldsymbol{\alpha}$: Thermal expansion
$\boldsymbol{\sigma_z}$: Axial stress in z direction
$\boldsymbol{\varepsilon_z}$: Uniaxial strain (change in length/original length)
$\boldsymbol{\omega}$: Nominal weight

LIST OF TABLES

LIST OF FIGURES

THE IMPACT OF ADDITIVES ON WELL CEMENT SETTING TEMPERATURE AND CASING DESIGN

SUMMARY

Cement is composition of several raw materials such alumina, silica, iron and magnesium oxide that burned together in the kiln and as a result of whole process the powder is obtained. This raw material is widely used in many industries, including petroleum industry as well. In drilling operations, cement is used to provide isolation between casing and formation. It helps to hold casing string in the well properly and eliminate fluid migration from the formation in to the wellbore.

In the petroleum industry, cement slurries are prepared at the surface where mainly cement is combined with water and some other additives for various purposes. According to the problems raised in the well, cement slurries are designed and pumped behind the casing throughout the well. Whereas these additives help to eliminate encountered problems in the well but meanwhile inverse effect of these components change other properties as well. For instance to additives, accelerators help to increase the rate of hydration at the early ages while retarders prevent hydration and slow hardening or having extenders in the slurries are resulted to an increase at the rate of pumpability.

Particularly, in permafrost zones and in extremely deep wells designing of slurries at the surface become more challenged. Abnormal pressures and thermal loads directly affect the cement slurries or reverse, added agents in cement composition at the surface may change the physical properties of the slurry in these particular cases. In other words, internal and external alterations may affect the wellbore cement stability throughout the setting period.

Natively, combination of the cement with water is an exothermic chemical reaction. However, in this study, the effects of some additives on the extra heat generation of the cement slurry has been investigated experimentally. Two different broadly used additives, friction reducer, CFR–3 and fluid – loss additive, Halad9 had been used throughout tests. Approximately 120 different samples were prepared to observe temperature track during 24 hours. Samples divided into 12 different sets where in each set of experiment, concentration of friction reducer was kept constant while concentrations of fluid – loss agent looped from 0.1% by weight of cement up to 1.0%. It would be relevant to note that all of samples are performed in the laboratory according to the API 10 B – Recommended Practice for Testing Well Cements.

Obtained results from the experiments illustrated the direct effect of additives on the heat generation of cement during setting. At the different concentrations of agents, variety of temperature readings have been recorded. Maximum temperatures were recorded above 70 ^{0}C at the friction reducer concentrations of 0.3% by weight of cement. Furthermore, it was also monitored that addition of fluid – loss additive may cause to reach maximum temperatures lately and Halad9 did not let to raise temperatures in the experiments. The role of CFR–3 in the temperature contributions is higher than Halad9.

After all, obtained maximum temperature readings were assessed and statistical approach applied to them. Hence variety of readings existed among the samples, a reasonable results could not be yielded from them. Nonetheless, using statistical evaluation for individual sets triggered to figure out some statistical relationship between them. Specially, the values of R - squared at the CFR-3 concentrations of 0.4% and 0.5% BWOC were high enough to set mathematical relationship between them. The value of R – squared was 0.955 for CFR-3 compositions at the 0.4 per cent concentration and 0.956 for 0.5 per cent by weight of cement.

Thermal loads due to additives in the cement slurries were taken under consideration as well, particularly in the casing design and/or formation during the time period of first 24 hours. Thermal loads regarding to maximum temperatures at the early times of hydration also was studied and the magnitude of the stresses were computed. In general, these effects are not so much to hazard the casing or formation, but shall not be neglected during the designing.

Key words: cementing, cementing job, additives impact, casing design, additives effect on heat of hydration, well cementing, well completion

KATKI MADDELERİNİN KUYU ÇİMENTOSU DONMA SICAKLIĞINA VE KORUMA BORUSU TASARIMINA ETKİSİ

ÖZET

Çimento, fırında bir arada yanan alümina, silis, demir ve magnezyum oksit gibi çeşitli hammaddelerin kompozisyonudur. Tüm prosedürün sonunda toz şeklinde elde edilir. Bu hammadde petrol endüstrisi de dâhil olmak üzere pek çok sanayide yaygın olarak kullanılmaktadır. Sondaj işlemlerinde çimento, koruma borusu ve formasyon arasında izolasyon sağlamak amacıyla kullanılır. Koruma borusunu desteklemeye yardımcı olur ve formasyondan kuyunun içine akışkan göçünü engelleme amacıyla kullanılır. Petrol endüstrisinde, çimento şerbeti çoğunlukla çimento ile su ve bazı katkı maddelerinin çeşitli amaçlarla yüzeyde karıştırılmasından oluşur.

Çimento şerbeti kuyudaki sorunların tipine göre hazırlanır ve kuyu boyunca koruma borusu ile formasyon arasında yer alır. Kuyuların derinliklerine ve maruz kaldıkları sıcaklık ve basınçlara göre katkı maddeleri de çimento şerbetine ilave edilir. Katkı maddeleri çimentonun kalınlaşma zamanı, viskozite, dayanım, donma zamanı gibi özelliklerinin ayarlanması amacıyla çimento şerbetine ilave edilir.

Katkı maddeleri kuyudaki karşılaşılan problemleri ortadan kaldırmaya yardımcı olurken bu bileşenlerin ters etkileri diğer özelliklerini de değiştirebilir. Örneğin hızlandırıcılar, erken dönemde hidratasyon oranını arttırmaya yardımcı olurken, geciktiriciler hidratasyonu ve dayanımı önler veya şerbetlerde kalınlaştırıcıların olması onun vizkozitesinin artmasına sebep olduğundan dolayı pompalanabilirliğini azaltır.

Özellikle, permafrost zonlarında ve son derece derin kuyularda, yüzeydeki şerbetlerin tasarımı daha da karmaşık hale gelebilir. Abnormal basınçlar ve termal yükler, çimento şerbetini doğrudan etkiler ve yüzeydeki çimento bileşimindeki ilave maddeler, bu belirli durumlarda bulamacın fiziksel özelliklerini de değiştirebilir.

Çimentonun karışımının donma süreci doğal ekzotermik bir kimyasal reaksiyondur. Bu çalışmada, iki farklı katkının çimento bulamacında ekstra ısı oluşumuna etkisi deneysel olarak araştırılmıştır. İki farklı yaygın olarak kullanılan katkılar, sürtünme azaltıcı, CFR – 3 ve sıvı kaybı katkı maddesi olan Halad9 testler boyunca kullanılmıştır. 120 farklı kompozsiyon için testler gerçekleştirilmiştir. Çimento bünyesindeki sıcaklık değişimleri 24 saat boyunca gözlemlenmiştir. Deneylerin her bir setinde, sıvı kaybı katkısı konsantrasyonları, çimento ağırlığının % 0.1'inden % 1.0'a kadar arttırılırken, sürtünme azaltıcı konsantrasyonunun her sette sabit tutulduğu 12 farklı grupta numuneler incelenmiştir. Tüm numunelerin testleri, API 10 B - Kuyu Çimentolarını Test Etmek İçin Tavsiye Edilen Uygulama Şartnamesine uygun olarak gerçekleştirilmiştir.

Sıcaklık davranışlarını gözlemlemek amacıyla hazırlanmış çimento bulamaçları çevrel ısıdan etkisinin en aza indirilmesi amacıyla özel izole kaba yerleştirilmiştir. Bununla beraber kap ve kapağı çevresindeki sıcaklık etkilerini ortadan kaldırmak için yalıtım bandı ile sarılmıştır. Sıcaklık veri kayıt cihazı çimento bulamacının üzerindeki kapaktan geçerek güvenli bir şekilde çimento şerbetinin hemen üstünde alıcı olacak şekilde kaba yerleştirilmiştir.

Deneylerden elde edilen sonuçlar, katkı maddelerinin, çimentonun ısınması üzerine direkt etkisini göstermektedir. Farklı katkılar için farklı konsantrasyonlarda çeşitli sıcaklık okumaları kaydedilmiştir.

Çimento, su ve CFR-3 karışımı deneylerinde sürtünme azaltıcının sıcaklık değişiminde etkisi bireysel olarak incelenmiş ve deney sonuçlarından 70.8 ^{0}C sonuç alınmıştır. Bu sonuç CFR-3'ün %0.9 oranında elde edilmiştir.

Bununla beraber, Halad9 sıvı kaybı kontrol katkısının çimento ve su karışımı üzerindeki etkisi de deneylerde ayrı ayrı incelenmiştir. CFR-3'den farklı olarak Halad9 katkı maddesinin sıcaklık üzerindeki etkisi daha düşük olup, onun %0.1 oranlı karışımında maksimum sıcaklığı 66.5 ^{0}C olarak ölçülmüştür. Halad9 katı maddesinin maksimum sıcaklığa ulaşılma zamanlarındaki etkisi de gözlemlenmiştir. Çimento, su ve Halad9 karışımlarındaki maksimum sıcaklık ötelemesi 1 saatten fazla olarak izlenmiştir.

Çimento ağırlığınca % 0.3'ü oranında sürtünme azaltıcı konsantrasyonlarında 70 °C'nin üzerinde maksimum sıcaklık kaydedilmiştir. Ayrıca, akışkan kaybı katkı maddesinin ilavesinin artan konsantrasyonlarında maksimum sıcaklığa ulaşması ve Halad9'un deneylerde sıcaklığın yükselmesine bir etkisi olmadığı izlenmiştir. CFR–3'ün sıcaklık değişimlerindeki etkisi Halad9'dan daha yüksektir.

Sonuçta, elde edilen maksimum sıcaklık okumaları değerlendirilmiş ve basit lineer regresyon analizi yapılarak katkı maddelerinin miktarı ve sıcaklık değişimi arasındaki ilişki incelenmiştir. Bütün deney sonuçları göz önünde bulundurulduğunda, maksimum sıcaklık okumalarının her sette farklı olması nedeniyle genel olarak lineer bir ilişki tespit edilememiştir. Bununla birlikte ayrı ayrı setler için lineer regresyon analizi kullanılarak bazı kompozisyonlar için lineer ilişki elde edilmiştir. Özellikle, çimento ağırlığının % 0.4 ve % 0.5 CFR-3 konsantrasyonlarında R - kare değerleri, aralarındaki matematiksel ilişki değerlendirilebilecek kadar yüksektir. R-kare değeri, çimento ağırlığının % 0.4 konsantrasyonlu CFR-3 bileşimleri için 0.955 ve çimento ağırlığının % 0.5'i için 0.956'dır. Bu kompozisyonlara sahip çimento şerbetlerinde katkı maddelerinin miktarı ile sıcaklıklardaki artış arasında lineer bir ilişki olduğu söylenebilir.

Deney sonuçlarının ayrıca koruma borusu tasarımı aşamasındaki etkileri incelenmiştir. Bunun için en yüksek, orta ve en düşük sıcaklık değişimine sahip çimento kompozisyonlarından elde edilen veriler kullanılmıştır. Çimento şerbetlerinde katkı maddeleri nedeniyle oluşan termal yükler, özellikle ilk 24 saatlik periyot boyunca koruma borusu tasarımı ve / veya formasyon için etkileri hesaplanmıştır. Bunun için 3 farklı koruma borusu: K – 55, C – 95, P – 110 tüm nominal ağırlıkları ile beraber hesaplamalarda kullanılmıştır. Koruma borusunun uzunluğu 3 000 ft, 10 000 ft ve 15 000 ft olup numunelerden elde edilmiştir.

Hidratasyonun erken dönemlerinde maksimum sıcaklık değişimine ilişkin termal yükler de incelenmiş ve gerilmelerin büyüklüğü hesaplanmıştır. En yüksek gerilim değeri 9765 psi olup C – 95 sınıf koruma borusunun 53.5 Ibm/ft nominal ağırlığında, 53 ^{0}C sıcaklık farkında hesaplanmıştır. Genel olarak, bu etkiler koruma borusu veya formasyon için çok fazla olmamakla birlikte, ancak tasarım sırasında ihmal edilmemelidir. Özellikle koruma borularındaki yüklerin sıkışmadan gerilmeye geçtiği bölgelerde bu etki bir fark yaratabilir ve göz ardı edilmemelidir.

Çimento katkı maddelerinin çimentonun donması sırasında ortaya çıkan ısıya önemli etkileri bulunmaktadır. Bu durum çimentonun asli görevi olan izolasyon özelliğini bozabilecek erken jelleşme, çimento bünyesinde çatlaklar oluşturma ve bağlanma problemleri gibi durumlara sebep olabilir.

Elde edilen sonuçlar katkı maddelerinin çimentonun donma reaksiyonunca oluşan ekzotermik ısının daha da arttırabileceğini ortaya koymaktadır. Bu çalışmanın amaçlarından biride kuyularda çimento donma sıcaklığı değişimi sebebiyle oluşabilecek olumsuzluklar için farkındalık yaratmaktır.

Anahtar kelimeler: çimentolama, çimento işi, katkıların etkisi, koruma borusu tasarımı, katkı malzemelerinin ısı üzerindeki etkisi, kuyu çimentolama, kuyu tamamlama

1. INTRODUCTION

Cement is determined as adhesive substances which is capable of uniting particles or masses of solid matter to a compact whole.

The first use of cement in building dates back, approximately 2600 years ago, to the relatively advanced stage of civilization. The earlier structures are composed of earth materials, sometimes were built in the form domes or walls by ramming successive layer, or of stone blocks, set one above another without using any cementing material, as in prehistoric megalithic structures, and in the Cyclopean masonry of Greece (Isaacs, 2008).

The simplest construction plan is found in the brick walls of ancient Egyptian buildings. The bricks were dried in the sun and each course is covered with a moist layer of the loam used for making the bricks, with or without the addition of chopped straw. The drying of this layer made the wall a solid mass of dry clay. Such a mode of construction was only possible in a rainless climate, as the unburnt possesses little power of resistance to water.

It is supposed that at the early stages Egyptians unknowingly used lime in their life, then the usage of cement found in the Greek buildings, and it is thought that Romans borrowed it from their neighbors.

Both the Greeks and Romans were familiar with the fact that using finely ground volcanic deposits and mixed with lime and sand yielded a mortar which not only leads to superior strength, but was also capable of withstanding the action of water, whether it is fresh or salty. For this purpose, the Greeks were worked with the volcanic tuff from the island of Thera (now called Santorin) and this material is known as Santorin earth, still enjoys a high reputation on the Mediterranean region.

The word of Pozzolana originates from the name of place called Pozzoh or PozzuoH (in Latin *Puteoli*) in ancient Romania and that has been extended to the whole class of mineral matters of which it is a type. We know that the soil from Pozzuoli or Pozzolan consists of 60 to 90% clay and nearly 10 to 40% lime, depending on the source.

Figure 1.1: Facade view of the Colosseum in Rome, Italy (Url-1).

The Roman combination of lime and natural or artificial pozzolona long kept its position as the only suitable material for work when exposed to water. Roman cement was a quick-setting cement and its applications in work in contact with water were found very useful. Its popularity for civil engineering work lasted until the beginning of 19th century, after which was gradually replaced by Portland cement.

On Figure 1.1 the great Colosseum Museum in Rome is shown where it is supposed that cement material was used during its building.

Since that the investigations had been started to prepare an artificial hydraulic cement. A young engineer, Louis Vicat, was working on the hydraulic features of a “lime-volcanic ash” mixture in 1817 and was the first to determine in a precise, controlled and reproducible manner the proportions of limestone and silica needed to obtain a mixture which, after burning at a specific temperature and after grinding, produced a hydraulic binder for industrial applications. In other words, cement.

Nonetheless the numerous of publications and patents in the early stage of 19th century, Aspdin’s famous patent was standing out in historic importance to others. Aspdin was from Leeds in England and builder or bricklayer who professionally acquainted with building stones, in his patent he described his material as “Portland Cement”, dated 21 October 1824. He called it **portland**, because it resemblances to a type of rock found in the region of Portland in southern England.

Aspdin’s early cement did not differ than a hydraulic Hme, but his 1824 patent gave him the priority for the use of the term Portland cement even though his product was not the Portland cement that it is known today. Its mineralogy was completely different, as was its hydraulic activity. Nevertheless, his patent was spark to the development of the cement industry through technological advancement and led to the calcium silicates of today’s market call it Portland cement (Hewlett, 2001).

In the history of Portland cement one of the most important situation was the shifting from the shaft kiln technique to the rotary skin. Cement manufacture started to a continuous production process instead of using a batch process. Moving to the new techniques occurred slowly at the beginning of the twentieth century and lasted nearly 70 years until the implementation of computer monitoring system introduced due to improvements in quality control.

Development stages and changing of mineralogy constitution of Portland cement following classifications was historically suggested:

- prosto – Portland cement;
- meso – Portland cement;
- normal Portland cement;

Proto-Portland cement is essentially a calcined mixture of limestone and clay with little evidence of $CaO \cdot SiO_2$ interaction, because the burning temperature is too low for compound synthesis. Joseph Aspdin's original patent cement which was discovered at Wakefield may be termed proto-Portland cement (Figure 1.2).

Meso - Portland cement is an extremely heterogeneous material but with definite evidence of $CaO\text{-}SiO_2$ interaction (producing $\beta\text{-}2CaO \cdot SiO_2$ and a small content of $3CaO \cdot SiO_2$) and poorly defined flux phases. Meso-Portland cement displays clear evidence of slow cooling, the presence of low temperature ternary solid solution occasionally with unreacted grains of silica (grinding the raw material with grinding stones) and flakes of iron (from bars in the vertical kiln).

Normal Portland cement, as broadly used today, is a quality calcareous cement manufactured in a rotary kiln and a definition of this product can be made. Normal Portland cement is a synthetic mixture of calcium silicates formed in a molten matrix from a suitably proportioned and homogeneously prepared mixture of calcareous and argillaceous components.

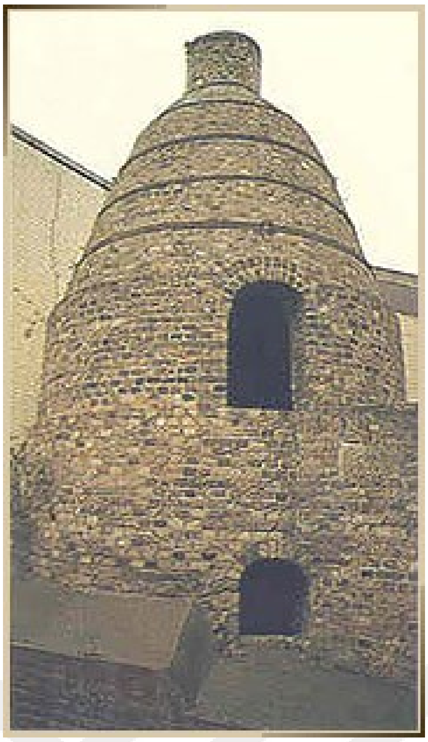

Figure 1.2: Aspdin’s Beehive kiln used to make first genuine Portland cement (Url – 2).

The calcination period, the reaction temperature and the residence time in the burning zone of the rotary kiln should be such as to minimize the uncombined Hme and maximize the calcium silicates in the product which will yield a suitable ratio of $3CaO{\cdot}SiO_2$ to $2CaO{\cdot}SiO_2$. The product, when ground to an optimum particle size distribution can then be hydrated under certain conditions to agree with commercial requirements within the relevant national standard specifications Normal Portland cement (unlike earlier proto- or meso-Portland cement) will contain a controlled amount of interground calcium sulfate as a setting retarder.

Combinability efficiency and mineral homogeneity is the chief difference between the meso – Portland cement of the Aspdin era and modern Portland cement. As a result of the applied technology ordinary Portland cement has been changed its properties throughout twentieth century. Remarkable changes are in the ratio of tricalcium silicate to dicalcium silicate, tough the total amount of calcium silicate in cement composition has remained nearly constant (Hewlett, 2001).

At present, it can define Portland cement as a combination of some number of hydraulic compounds and each specifically reacts with water specifically, and result of the reactions leads to the setting and hardening of the cement.

1.1 Cement Consumption in the World

Excessive use of cement cause to increase in the demand of production at the world market. Regarding to Cembureau it can be clearly state that the amount of cement usage is forecasted to rise up significantly at least during the next 5 years. Figure 1.3 shows that a consistent increase was observed in Asia. The consumption went up at least three times for this particular region. Africa and CIS countries followed Asia during the last 15 years.

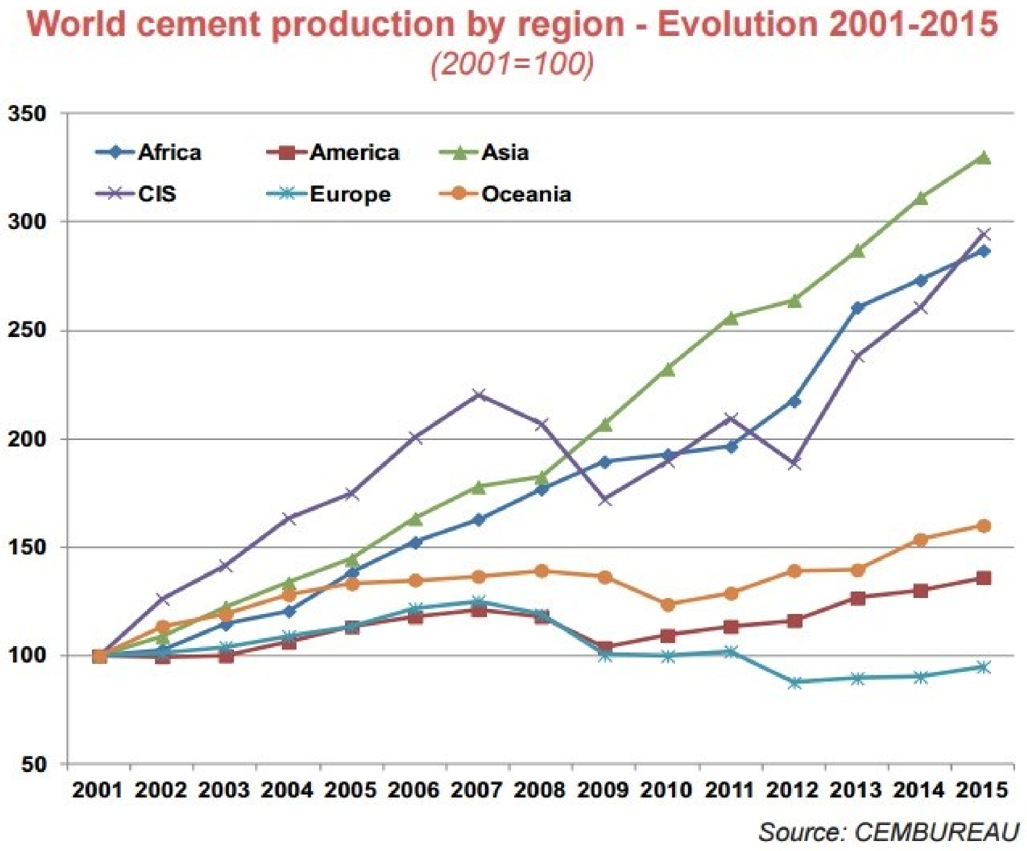

Figure 1.3: World Cement production by region between 2001 and 2015 (Url–3).

Moreover, Figure 1.4 depicts the cement supply and consumption in the USA from 2002 to 2021. The domestic production and import capacity just climbed up 130.000 thousands metric tons and it is predicted that it will stay constantly over that figure until 2021. Another interesting fact about the Portland and Masonry cement consumption. While they peaked by 128.000 thousands metric tons in the mid of 2015 but then consumption decreased dramatically until 70.000 thousand metric tons. Steady increase has been observing in the consumption of portland and masonry cement in USA and estimation says it will overcome 110.000 thousands metric tons in 2021.

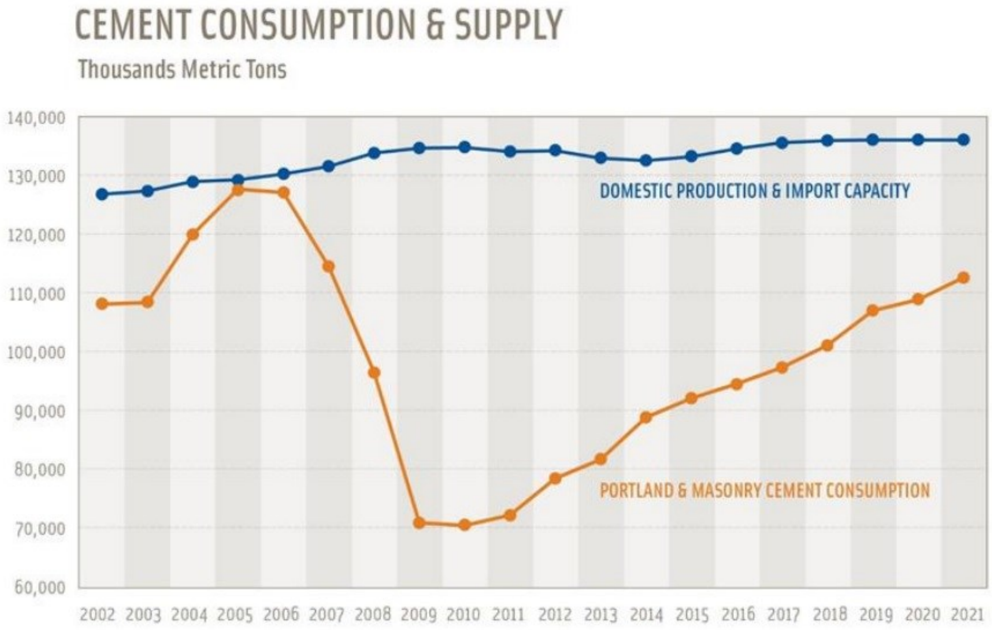

Figure 1.4: Cement Consumption and Supply in USA between 2002 and 2021 [Url - 3].

Following CEMEX's Figure 1.5 illustrates cement demand outlook between 2017 – 2021. Strong growth is exptected in Spain, India and some Asian countries. The degree of growth is estimated from 2% to 5% in the United States. This scale growth also expected in some Latin American countries and as well as in Australia.

1.2 Composition and Constitution of Cement

Since cement contains adhesive and cohesive properties, it would be worthwhile to know which components make up its structure. The Portland cement's chemical composition can be easily determined through the laboratory to selecting appropriate composition in implementations.

Composition of the Portland cement consists of commonly Calcarous materials such as chalk or limestone (as a source of lime (CaO)) and mostly Clayey materials such as shale or pure clay (as a source of silica and alumina). In the kiln, these elements interact

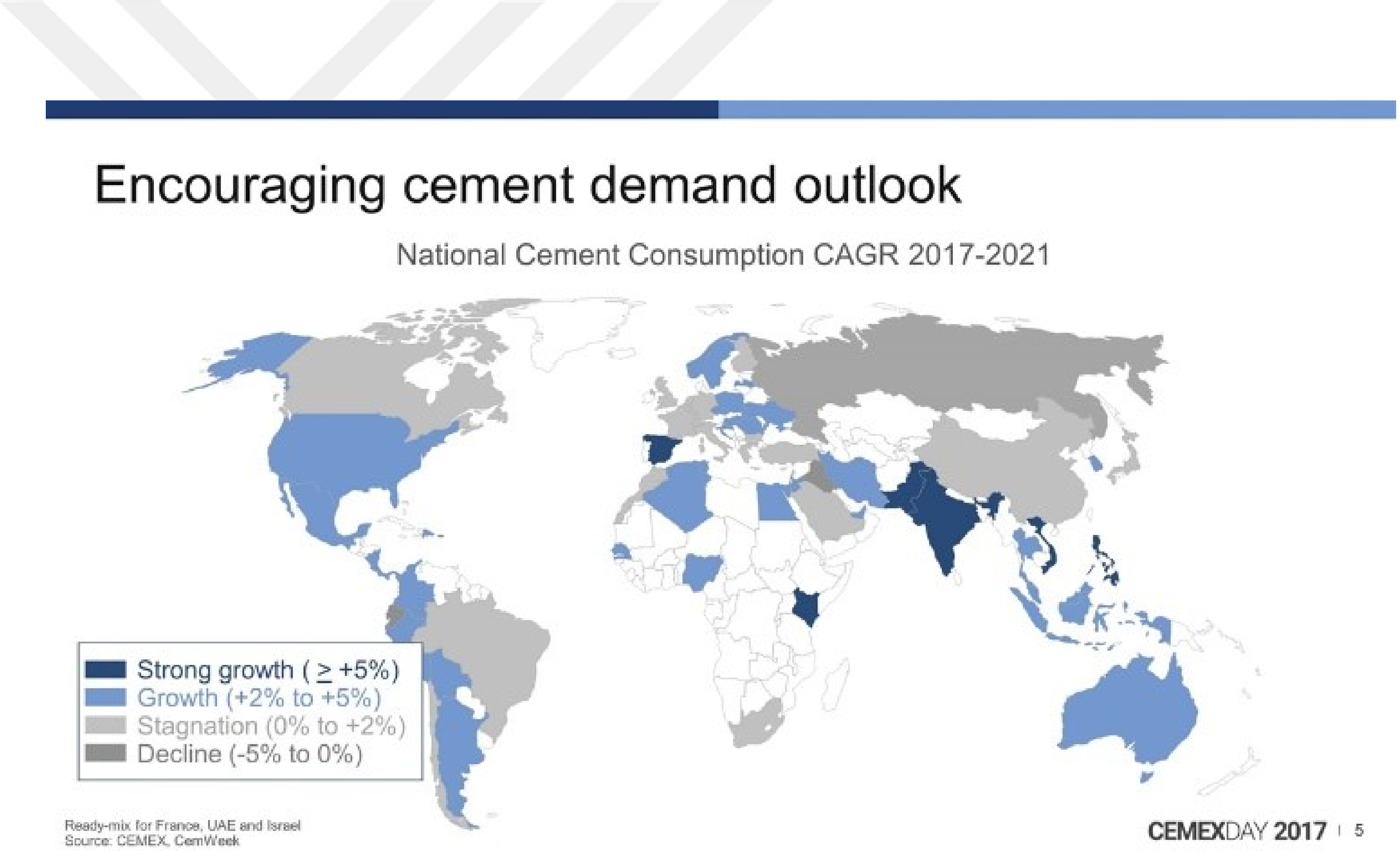

Encouraging cement demand outlook

National Cement Consumption CAGR 2017-2021

Ready-mix for France, UAE and Israel
Source: CEMEX, CemWeek

CEMEXDAY 2017 | 5

Figure 1.5: Cement demand outlook from 2017 to 2021 (Url-4).

each other to form a series of more complex products. Thus, following major chemical components are the constituents of cement:

1. Tricalcium silicate $3CaO \cdot SiO_2$ – (C_3S)
2. Dicalcium silicate $3CaO \cdot SiO_2$ – (C_2S)
3. Tricalcium aluminate $3CaO \cdot Al_2O_3$ – (C_3A)
4. Tetracalcium aluminoferrite $4CaO \cdot Al_2O_3 \cdot Fe_2O_3$ – (C_4AF)

Generally, ideal Portland cements are taken as pure tircalcic – silicate ($3CaO \cdot SiO_2$) where nearly 73.5% correspond for CaO, and rest 26.5% remains for SiO_2. However, actual Portland cement noticeably differ in composition. Table 1.1 shows typical compound composition for ordinary cement in the market. Considerable proportion of alumina and some part of the lime together form dicalcic aluminate ($3CaO \cdot SiO_2$). This statement formulated by Newberry as general formula of a pure Portland cement (Eckel, 1905):

$$x\ (3CaO \cdot SiO_2) + y\ (2CaO \cdot Al_2O_3)$$

Table 1.1: Shows typical compound composition in ordinary cement (Edwin, 1905).

Compound	Content, %
C_3S	54
C_2S	17
C_3A	11
C_4AF	9

Composition becomes further complicated by the existence of some intentional and unintentional added elements. In addition to the main compounds mentioned above (Table 1.1), there exist minor compounds, such as **MgO, TiO_2, Mn_2O_3, K_2O and Na_2O**. Two of the minor compounds are of particular interest: K_2O and Na_2O, known as the **alkalis** (about 0.4-1.3% by weight of cement). The usage of these minerals in Portland cement composition is tabulated in Table 1.2.

Some additional minor components or ingredients can be useful in the composition of Portland cement. Calcium sulfate can be an example which serves to retard the set of the cement without any harmful effect during operations. Furthermore, the presence of small portions of Magnesium-carbonate comes upon in limestone or clays and magnesia is invariably present in the cement (Hewlett, 2001).

Table 1.2: The limits of usual composition of Portland cement.

Oxide	Content, %
CaO	60 – 67
SiO_2	17 – 25
Al_2O_3	3 – 8
Fe_2O_3	0.5 – 6
MgO	0.5 – 4
Alkalis (as Na_2O)	0.3 – 1.2
SO_3	2.0 – 3.5

1.3 Manufacturing of Cement

Manufacturing of Portland cement involves different raw materials and processes. Each process covers chemical reactions. The manufacture of Portland cement is passing through 4 main stages:

1. Mixing of raw material
2. Heat and Cooling Treatment
3. Grinding
4. Storage and packaging

1.3.1 Mixing of raw material

Although each cement plant has its own specific method, there are two general processes in use today: Dry process and Wet process.

1.3.1.1 Dry process

In the dry process, grinding and blending are performed using dry materials. As shown on Figure 1.6 calcareous and argillaceous raw materials are firstly crushed in the Gyratory crushers to get 2-5 cm size pieces separately and are dried in rotary driers. Raw materials are proportioned to obtain the correct bulk composition, and then ground in tube mills consisting of rotating steel cylinders containing steel balls or other grinding media. The ground material goes through a pneumatic size classifier, in which the air velocity is sufficient to carry ground material of the required fineness. Coarser particles are thrown out by centrifugal action. The ground material is stored in several silos. The chemical constitution differs from silo to silo; therefore, another opportunity exists to blend again and “fine tune” the mixture which will come to the kiln (Nelson et al, 1990).

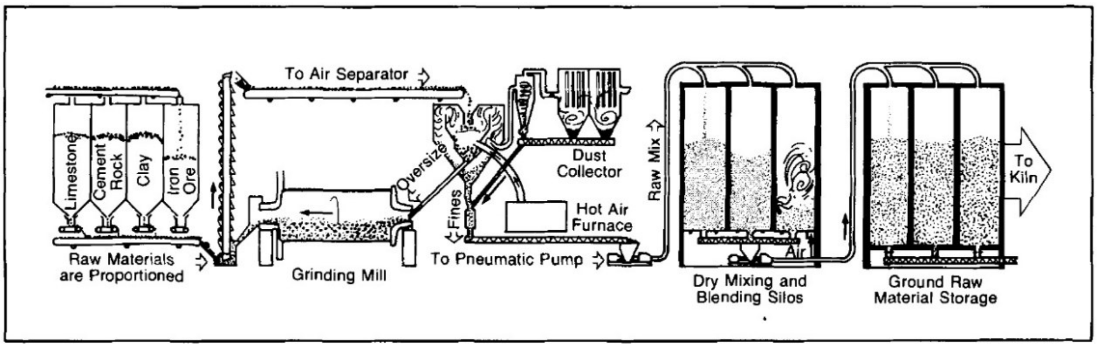

Figure 1.6: Schematic flow diagram of the Dry Process (Portland Cement Association & Skokie, 1969).

1.3.1.2 Wet process

First of all, the raw materials are proportionally balanced in the dry media and made into powdered form. Powder is stored in soils. Unless dry process, at the next stage water is added in to the system. For the purpose of further size reduction, composition goes into a grinding mill where the paste – known as slurry is formed. Size classification is performed by pumping the resulting slurry through a vibrating screen. Coarser material is returned to the mill for regrinding. Mixture is stored in silos equipped with rotating arms and compressed air agitation to keep the mixture homogeneous. Thus final adjustments of mixtures can be performed by blending the slurries from various basins. Procedure has been described on the Figure 1.7.

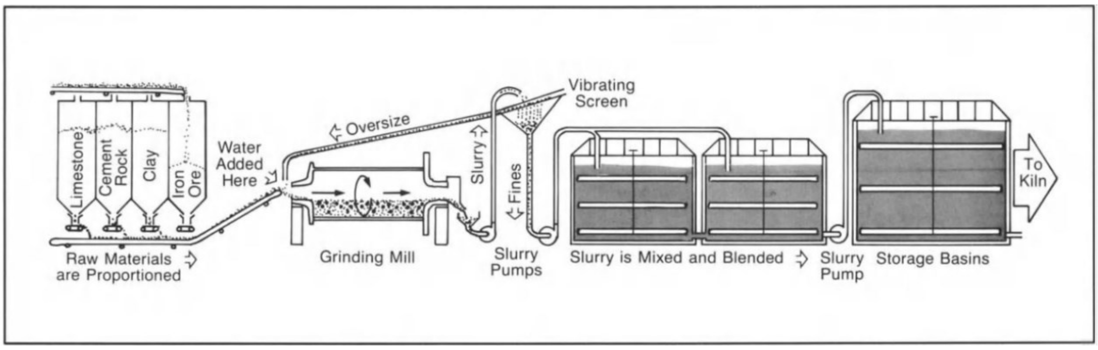

Figure 1.7: Schematic flow diagram of the Wet Process (Portland Cement Association & Skokie, 1969).

Significant amount of fuel was consumed in the kiln to evaporate the water and previously it was preferred to use wet method to get accurate results. However, development in technology allows the industry to turn back again to dry process. Advanced technology let the industry save fuel consumption and by using technology it is possible to gain more accurate results as well.

1.3.2 Heat and cooling treatment

The processes heating and cooling is important stages at the production of cement and will be explained broadly in the following 1.3.2.1 and 1.3.2.2 parts.

1.3.2.1 Heat treatment

After being reached to desirable size reduction, classification and blending of materials, heat treatment is carried out in the slightly inclined rotary kiln while the raw materials are rotated at 1 – 4 RPM (Revolution Per Minute) at its longitudinal axis (Figure 1.8). The rotary kiln is made up of steel tubes having diameter of 2.5 – 3.0 meter and the length varies from 90 – 120 meter. Refractory bricks lay down inside the kiln. It is heated with the help of powdered coal or oil or hot gases from the lower end of the kiln so that the long hot flames are produced.

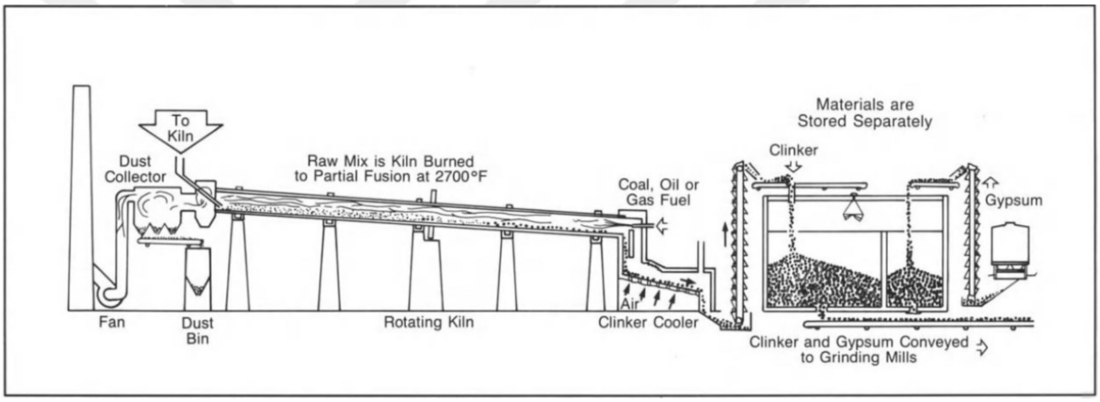

Figure 1.8: Schematic flow diagram of the burning process (Portland Cement Association & Skokie, 1969).

Many chemical reactions take place throughout the kiln, whereby the raw materials are converted to “clinker”. Kiln can be divided six zones where the temperatures and reaction profiles are totally different. The information about zones is given in Table 1.3.

At the first zone, free water evaporates from the mixture. Removing water from the mixtures performed quickly at the dry process. However, one and half length of the kiln could be used for removing water from the mixture particularly at wet process. After being materials are dried, they go to Zone II, called preheating phase where dehydroxylation of the clay minerals occur. Temperature ranges 200 ^{o}C to 800 ^{o}C. In Zones III and IV some chemical reactions occur and temperate raises from 800 ^{o}C up to 1100 ^{o}C and 1100 ^{o}C up to 1300 ^{o}C respectively.

Table 1.3: Information about temperatures and reactions in the kiln.

Zone	Temperature Range, (^oC)	Reaction Profile
I	Up to 200	Evaporation
II	200 – 800	Preheating
III	800 – 1100	Decarbonation
IV	1100 – 1300	Exothermic Reactions
V	1300 to 1500 to 1300	Sintering
VI	1300 – 1100	Cooling

Calcium carbonate breaks up to free lime, big amount of carbon dioxide releases. At this stage, various calcium aluminate compositions and ferrites might be produced as well. Zone V is very crucial since most of cement phases are manufactured at this level whereas zone is engaged small portion of kiln. At this point, some part of the reaction mixture liquefies. Maximum temperature in the kiln occurs in this zone by 1500 ^{0}C and picked temperature is called “clinkering temperature” or “clinkering zone” where lime and clay react to produce calcium aluminates and calcium silicates. Finally, at the stage Zone VI, C_3A and C_4AF crystallize as the liquid phase reduced.

1.3.2.2 Cooling treatment

Cooling is an important stage in production of cement since it determines the quality of the clinker and the final cement product. The good quality clinker can be produced when cooling occurs, firstly, slowly from peak to nearly 1250 ^{0}C and followed by rapid cooling to 18 – 20 ^{0}C/min.

Slower cooling rate (4^o – 5 ^{o}C/min) leads to develop a high degree of C_3A and C_4AF crystallinity, to high ordered C_3S and C_2S crystals and free MgO (periclase). This creates less hydraulically active cement. However, the degree of early compressive strength is high, but longer term strength is low.

On the other hand, faster cooling rate in the Zone V liquid phase becomes solid in the kiln. C_3A and C_4AF deposited in the glassy phase and less ordered C_2S and C_3S are released. The free MgO trapped in the glassy phase as well. As a result, cement is obtained which has properties such as being less active and having high longer term strength (Nelson et al., 1990).

1.3.2.3 Grinding

After being cooled at the cooling stage, the clinkers are sent into mills and produced with 2 – 3 % gypsum (CSH_2). The clinkers are grinded finely into powder, having particle size between 1 – 100 µm by using hard steel balls in tubular mills (Figure 1.9).

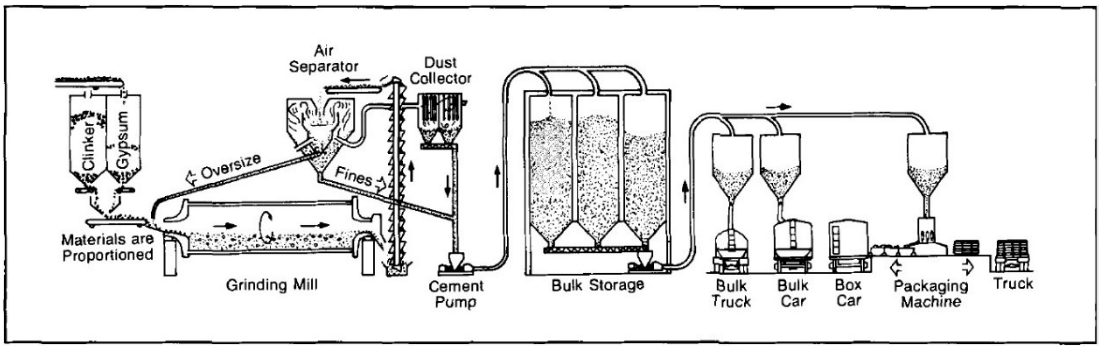

Figure 1.9: Schematic flow diagram of the grinding process and storage (Portland Cement Association & Skokie, 1969).

After the initial setting time of the cement, the cement becomes stiff and the gypsum retards the dissolution of tri-calcium aluminates by forming tricalcium sulfoaluminate which is insoluble and prevents too early further reactions of setting and hardening.

$$3CaO \cdot\ Al_2O_3 + xCaSO_4 \cdot 7H_2O = 3CaO \cdot Al_2O_3 \cdot xCaSO_4 \cdot 7H_2O$$

Eventually, after grinding cement is reserved in silos, from here for marketing purposes it can be loaded to containers or 50 kg bags. It is important to protect the cement products from humidity and CO_2 effects.

1.4 Cement Types

According to the needs and based on the required performance or the placement conditions different types of cements can be produced.

Types of the cement is defined by twisting internal mix ratio or by altering the chemical inputs. Different type of Portland cements now is available in the market, these are:

Rapid hardening cement, Sulfate resisting cement, Low heat cement, Quick setting cement, Pozzolanic cement, Blast furnace cement, High alumina cement, White cement, Colored cement, Air entraining cement, Hydrophobic cement.

1.4.1 Rapid hardening cement

The initial and final setting times of Rapid Hardening Cement does not differ from the ordinary Portland cement, manufactured by combining limestone and shale at high temperature. It reaches its maximum strength in early days. Rapid Hardening Cement is used mainly at road pavement works and precast concrete casting. The chemical constitution of this particular cement is mainly tricalcium silicate (C_3S) and it consists of approximately 56% in compositions (Url-5).

1.4.2 Sulfate resisting cement

The amount of tricalcium aluminate C_3A in the composition is reduced to 5% in this kind of cement. Lower percentage of tricalcium aluminate leads to increase in resisting power against sulfate attacks. Sulfate Resisting Cement stands against these attacks where the concrete is direct contact with soil. Generally, its usage areas are accounted for pile foundation, coastal area works, and water and sewage treatment plants (Url-5).

1.4.3 Low heat cement

During the setting time of cement exothermic reactions occurs and the significant amount of heat is released. This is issue is taken under the consideration in some applications such as marine constructions, hydraulic engineering applications, retaining wall construction and etc. In order to reduce the measure of heat, Low Heat Cement is used. Like Sulfate Resisting cement lower percentage of tricalcium aluminate is added and approximately 46% dicalcium silicate exists in the composition. The initial and final setting times take place nearly one hour and 10 hours respectively (Url-6).

1.4.4 Quick setting cement

Composition of quick setting cement contains small amount of gypsum and low percentage of Aluminum sulfate. The addition of aluminum sulfate and finely grinded cement serve for accelerating the setting time of cement. The setting of cement starts within 5 minutes immediately after addition of water and after 30 minutes later it turns to hard substance. As be seen from the name it is used where works must be completed within the short time period. In underwater work projects, in cold and humidity weather conditions this kind of cement could be very useful (Url-6).

1.4.5 Pozzolanic cement

Pozzolanic Cement is product of some mixed materials such as fly ash, shale, clay and prepared by grinding clinker with Portland cement. Unlike Rapid Hardening cement high compressive strength is achieved after certain time period later. The price of the pozzolanic cement in the market is lower compare than other types and frequently used to prepare mass concrete of lean mix, in sewage works, bridge constructions (Taylor, 1990).

1.4.6 Blast furnace cement

It is made by grinding the clinkers with approximately 60-65% slag. The properties of the blast furnace cement are more or less the same as ordinary cement is. Basic components involving alumina, lime and silica made up the chemical composition of this type of cement. Hardening slowly occurs hence it demands longer curing period (Url-5).

1.4.7 High alumina cement

This cement is prepared by grinding clinkers formed by calcining bauxite and lime. According to the industrial standards total alumina content in the composition should not be below 32% and weigh ration alumina to lime must be between 0.85 – 1.30. Because if its endurance against high temperature, acidic action the cement is mostly used is construction of refineries, factories and other workshop type (Taylor, 1990).

1.4.8 White cement

It is just Portland cement but without color while during its production raw materials are tended to be free from coloring oxides of iron, manganese or chromium. Oil fuel is replaced by coal as well for burning of this cement. Owing to its color, white cement particularly is used for floor finish, plaster work, ornament work etc. The following Figure 1.10 shows white cement on facade of building.

Figure 1.10: White cement has been used on the facade of building (Url-7).

1.4.9 Colored cement

The desired color of cement may be achieved by intimately mixing mineral pigments with ordinary cement. The scope of the color in the cement may vary from 5 – 10 percent. Above the threshold the strength of cement is affected.

Chromium oxide changes cement’s color to green, while cobalt gives blue and having iron oxide in various proportions may result in brown, red or yellow color. Colored cement is extensively used in artificial marble or floor finishing (Url-5).

1.4.10 Air entraining cement

It is produced by adding certain amount of air entraining agents as resins, glues, sodium salts of sulfates during the grinding of clinker. It is used to fill up the gap in concrete which are produced by excessive amount of water during casting. Use of air entraining cement is particularly to improve frost resistance of concrete (Url-6).

1.4.11 Hydrophobic cement

Hydrophobic cement is designed for wet climatic conditions. It is manufactured by mixing admixtures like oxidized petrolatum, naphthalene soap, acidol etc. When it is added to slurry the water resistance of the concrete goes up significantly. Hydrophobic cement is useful when cement is stored for longer duration in wet climatic conditions (Url-5).

1.5 Classification of Portland Cement

Portland cements are produced according to certain chemical and physical standards for the purpose of meeting demands of the applications. To keep the consistency of performance among cement producers, classification systems and specifications have been created by some institutions. Best known classifications and systems have been framed by the American Society for Testing and Materials (ASTM) and the American Petroleum Institute (API) (Nelson et al., 1990).

1.5.1 Classification criteria

The classification of Portland cement principally based on its clinker phases which directly affects the chemical composition of final product, known as the "potential phase composition". In spite of numerous research over the last 100 years, a reliable direct method for calculating the concentrations of clinker phases in Portland cement has not been found out yet. The most well-known method for the determining the concentrations of Portland cement was suggested by Bogue that is based upon different phase equilibria relationships between the cement components. Bogue's method is limited in use but still considered one of the best approximation to determine cement class. Bogue's equations (ASTM Method from C 114) will be given as follows (Bogue, 1929):

When the ration of percentages of aluminum oxide to ferrio oxide is 0.64 or more, the percentages of tricalcium silicate, dicalcium silicate, tricalcium aluminate, and tetracalcium aluminoferrite shall be calculated from the chemical analysis as follows:

Tricalcium silicate = $(4.071 \times \%\ CaO) - (7.600 \times \%\ SiO_2) - (6.718 \times \%\ Al_2O_3) - (1.430 \times \%\ Fe_2O_3) - (2.852 \times \%\ SO_3)$

Dicalcium silicate = $(2.867 \times \%\ SiO_2) - (0.7544 \times \%\ C_3S)$

Tricalcium aluminate = $(2.650 \times \%\ Al_2O_3) - (1.692 \times \%\ Fe_2O_3)$

Tetracalcium aluminoferrite = $3.043 \times \%\ Fe_2O_3$

When the alumina – ferric oxide ration is less than 0.64, a calcium aluminoferrite solid solution (expressed as ss ($C_4AF + C_2F$)) is formed. Contents of this solid solution and of tricalcium silicate shall be calculated by the following formulas:

$ss(C_4AF + C_2F) = (2.100 \times \%\ Al_2O_3) + (1.702 \times \%\ Fe_2O_3)$

Tricalcium silicate = $(4.071 \times \%\ CaO) - (7.600 \times \%\ SiO_2) - (4.479 \times \%\ Al_2O_3) - (2.859 \times \%\ Fe_2O_3) - (2.852 \times \%\ SO_3)$

Specifications of physical parameters are considered the fineness of the cement and the performance of the cement regarding to standardized tests. The performance tests might be thickening time, compressive strength, free water and expansion.

1.5.2 API classification system

Oil – well cement standards has been established by the API since the conditions for oil wells differ radically from the civil engineering applications or constructions. According to API standards, currently eight classes, namely A through H are available in the market. Classes are arranged with respect to the depths of the wells and the temperatures and pressures to which they are exposed.

Class A: Intended for use from surface to a depth of 6,000 ft. (or 1,830 m), when special properties are not required. Available only in Ordinary type. Class A is similar to ASTM Type I.

Class B: Intended for use from surface to a depth of 6,000 ft. (1,830 m), when conditions require moderate to high sulfate resistance. Class B is similar to ASTM Type II, and has lower C_3A content than a Class A.

Class C: Intended for use from surface to a depth of 6,000 ft. (1,830 m), when conditions require high early strength. Class C is available in all three degrees of sulfate resistance, and is roughly equivalent to ASTM Type III. To achieve high early strength, the C_3A content and the surface area are relatively high.

Classes D, E and F are also known as “retarded cements”, intended for use in deeper wells. The retardation is accomplished by significantly reducing the amount of faster – hydrating phases (C3S and C3A), and increasing the particle size of the cement grains. Since these classes were first manufactured, the technology of chemical retarders has significantly improved; consequently, they are rarely found today.

Class D: Intended for use at depths from 6,000 ft. (1,830 m) to 10,000 ft. (3,050 m), under conditions of moderately high temperatures and pressures. It is available in MSR and HSR types.

Class E: Intended for use from 10.000 ft. (3.050 m) to 14,000 ft. (4,270 m) depth, under conditions of high temperatures and pressures. It is available in MSR and HSR types.

Class F: Intended for use from 10,000 ft. (3,050 m) to 16,000 ft. (4,880 m) depth, under conditions of extremely high temperatures and pressures. It is available in MSR and HSR types.

Classes G and H were developed in response to the improved technology in slurry acceleration and retardation by chemical means. The manufacturer is prohibited from adding special chemicals, such as glycols or acetates, to the clinker. Such chemicals improve the efficiency of grinding, but have been shown to interfere with various cement additives. Classes G and H are by far the most commonly used well cements today.

Class G: Intended for use as a basic well cement from surface to 8,000 ft. (2,440 m) depths as manufactured, or can be used with accelerators and retarders to cover a wide range of well depths and temperatures. No additions other than calcium sulfate or water, or both, shall be inter ground or blended with the clinker during manufacture of Class G and H well cements. They are available in MSR and HSR types.

The chemical compositions of Classes G and H are essentially identical. The principal difference is the surface area. Class H is significantly coarser than Class G, as evidenced by their different water requirements (Cartalos & Lecourtier, 1993).

Within some classes, cements with varying degrees of sulfate resistance (as determined by C_3A content) are sanctioned: ordinary (O), moderate sulfate resistance (MSR) and high sulfate resistance (HSR). The chemical and physical specifications are listed in Table 1.4 (Nelson et al., 1990).

1.5.3 Well cement

As cement is World's most widely used building material it also plays very pivotal role in petroleum industry. Cement is defined as compounds of mainly calcium silicates and other calcium components together having hydraulic features.

Cements are divided in two classes, namely as hydraulic or non-hydraulic. Hydraulic cements set and harden after being combined with water. They then keep their strength, even if they get wet. Earlier non-hydraulic cements, on the other hand, need to be kept dry after setting in order to keep their strength.

Principally hydraulic type cements are used in petroleum industry mostly, oil – gas, geothermal wells are completed by that where the process is called cementing and basically it is learnt in well completion division. Primary cementing is the process of filling and sealing the annulus between the casing string and the drilled hole (Figure 1.11) (Nelson & Guillot, 2006).

Table 1.4: Chemical requirements for API Portland cements (from API Spec 10: Materials and Testing for Well Cements) (Nelson et al., 1990).

Ordinary Cement

	A	B	C	D, E, F	G	H
Magnesium oxide (MgO), maximum %	6.0	-	6.0	-	-	-
Sulfur Trioxide (SO_3), maximum %	3.5	-	4.5	-	-	-
Loss on ignition, maximum %	3.0	-	0.75	-	-	-
Insoluble aluminate ($3CaO \cdot Al_2O_3$), max %	-	-	15	-	-	-

Moderate Sulfate – Resistant Type (MSR)

	A	B	C	D, E, F	G	H
Magnesium oxide (MgO), maximum %	-	6.0	6.0	6.0	6.0	6.0
Sulfur Trioxide (SO_3), maximum %	-	3.0	3.5	3.0	3.0	3.0
Loss on ignition, maximum %	-	3.0	3.0	3.0	3.0	3.0
Insoluble residue, maximum %	-	0.75	0.75	0.75	0.75	0.75
Tricalcium silicate ($3CaO \cdot SiO_2$), max %	-	-	-	-	58	58
Trialcium silicate ($3CaO \cdot SiO_2$), min %	-	-	-	-	48	48
Tricalcium aluminate ($3CaO \cdot Al_2O_3$), max %	-	8	8	8	8	8
Total alkali content expressed as sodium oxide (Na_2O) equivalent, max %	-	-	-	-	0.75	0.75

High Sulfate – Resistance Type (HSR)

	A	B	C	D, E, F	G	H
Magnesium oxide (MgO), maximum %	-	6.0	6.0	6.0	6.0	6.0
Sulfur Trioxide (SO_3), maximum %	-	3.0	3.5	3.0	3.0	3.0
Loss on ignition, maximum %	-	3.0	3.0	3.0	3.0	3.0
Insoluble residue, maximum %	-	-	-	-	65	65
Tricalcium silicate ($3CaO \cdot SiO_2$), max%	-	-	-	-	48	48
Trialcium silicate ($3CaO \cdot SiO_2$), min %	-	3	3	3	3	3
Tricalcium aluminate ($3CaO \cdot Al_2O_3$), max %	-	24	24	24	24	24
Tetracalcium aluminoferrite ($3CaO \cdot Al_2O_3 \cdot Fe_2O_3$) plus twice the tricalcium aluminate ($3CaO \cdot Al_2O_3$), maximum %	-	-	-	-	0.75	0.75
Total alkali content expressed as sodium oxide (Na_2O) equivalent, max%						

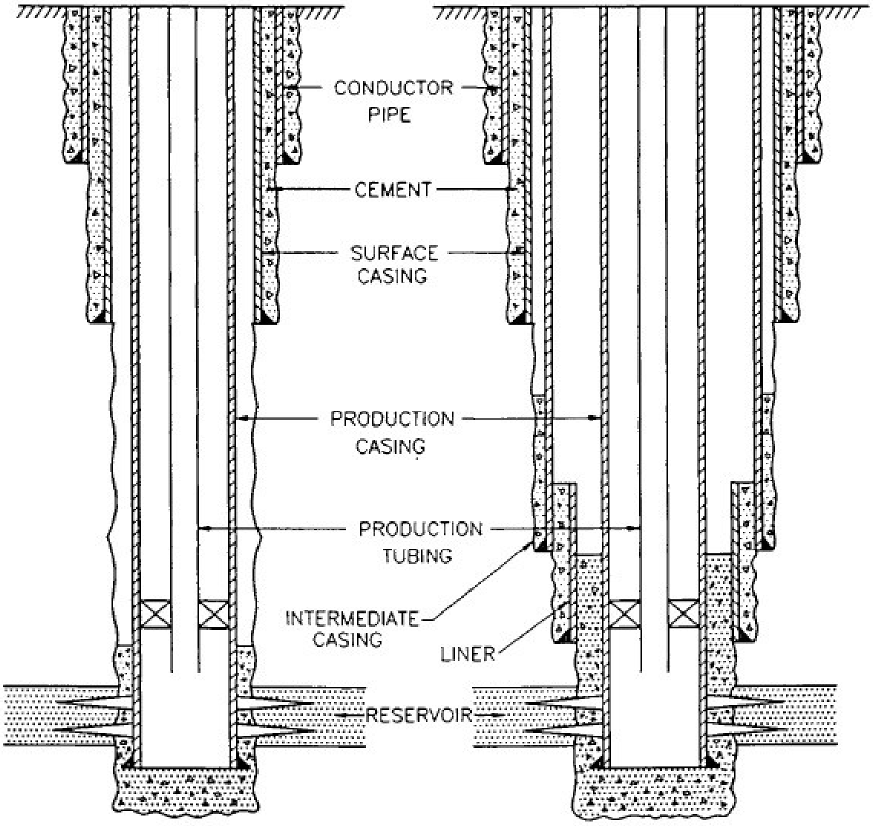

Figure 1.11: Typical casing program showing different casing sizes and their setting depths (Rahman & Chilingarian, 1995).

The purposes of using well cement are (1) zonal isolation and segregation, (2) corrosion control and (3) pipe strength improvement and formation stability.

Since its inception in 1903, the major objective of primary cementing has always been to provide zonal isolation in oil, gas and water wells. e.g., to exclude fluids such as water or gas in one zone from oil in another zone. Zonal isolation is surely the most important function of the cement sheath. To achieve this objective, a hydraulic seal must be obtained between casing and the cement, and between the cement and the formations, while at the same time preventing fluid channels in the cement sheath. Well may not reach its full producing potential without having complete zonal isolation.

The simplest cementing job procedures are performed by the two – plug method for pumping and displacement. For the first time this method used in California in shallow wells. After being reached to the desired depth, the drill – pipe is removed and a larger casing string is run into the well until it touches the bottom of the well. At the same time, drilling mud is circulated to eliminate cuttings from the wellbore. This mud must be removed from the well and replaced with hardened cement. The described whole process is called two – plug cementing method which is shown in the following Figure 1.12.

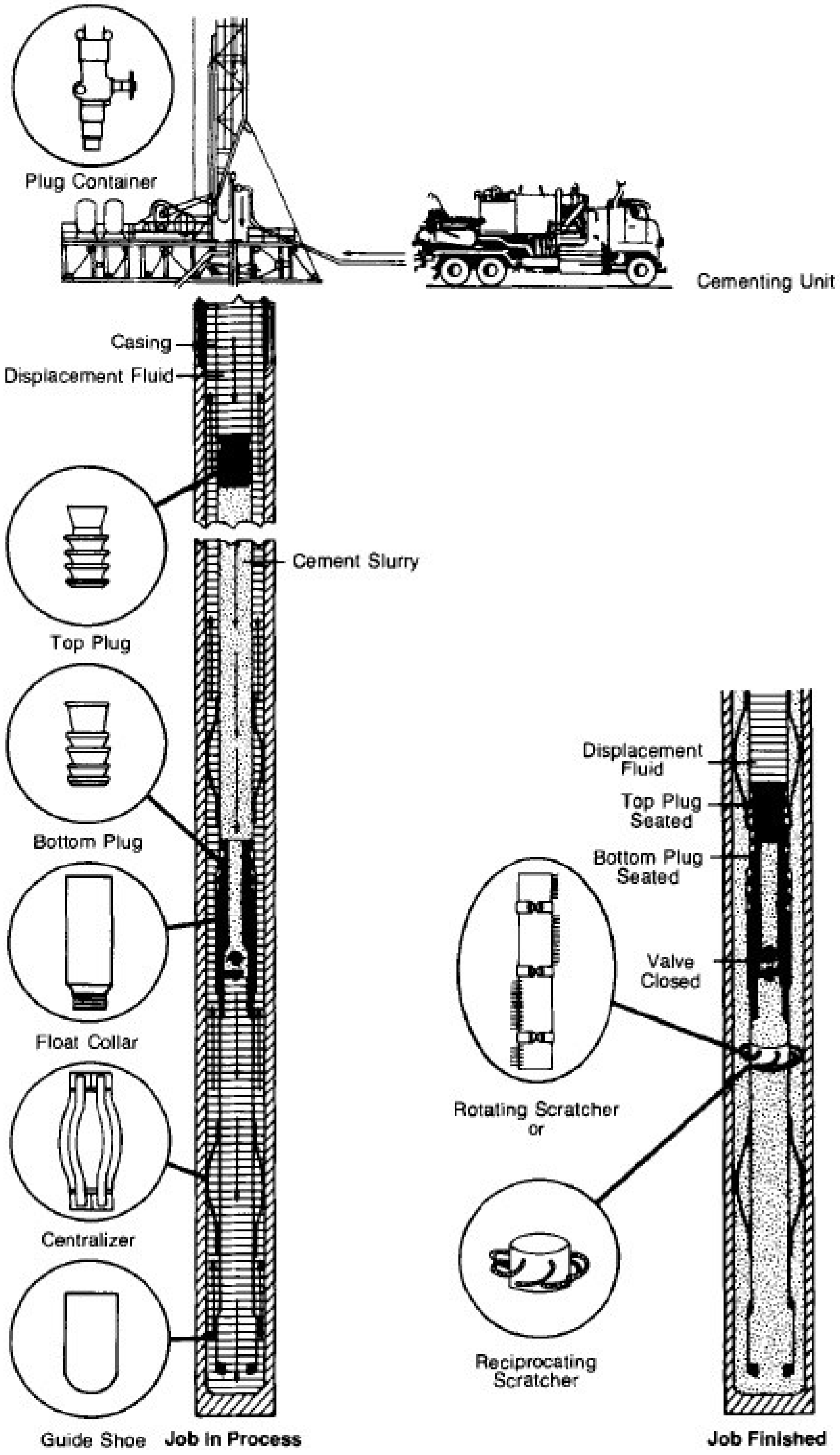

Figure 1.12: Typical Primary Cementing Job (Nelson et al., 1990).

Two – plugs are used to isolate the cement as it is pumped down the casing to prevent contamination with mud. Significant volume of cement is placed into the casing to fill the annular column from the bottom up to at least across the productive zones. The height of cemented zone may reach up to the surface in order to eliminate undesired fluids from the wellbore, to protect fresh water zones, and to defend the casing from corrosion. The completion of cementing process is understood when the gauges show immediate pressure increase at the surface which indicates the top plug has been placed over the landing collar or float collar. The well is kept under shut in mode for a time to let the cement to harden before beginning completion work or drilling out to drill deep zones (Nelson et al., 1990).

Although today's technology let the companies to drill deeper and cementing methods have changed, but the basic two – plug method described above still widely used in field.

1.6 Cement Additives

Portland cement is widely used hydraulic cement which set and develop compressive strength through hydration, not by drying out. When talked about hydration it is understood chemical reactions between water and the cement compounds. Sometimes, air could be left during hydration or it could be submerged in water though independently it sets and hardens. After being set, it has low permeability and high resistance against attack from water. All these elements make Portland cement unique for completing wells and maintaining isolation between zones (Michel et al., 1989).

As technology improved deeper wells in various conditions are drilled. Today's well cements are supposed to have to meet challenging downhole environments to complete wells successfully. In permafrost zones, the cement must confront below – freezing surroundings or in geothermal fields they must overcome the temperatures above 350 ^{0}C. Duty of cement in the well is to protect the casing from the weak or over – pressured formations where either lost circulation problem or corrosive problems could be encountered. Nowadays many service companies suggest wide range of chemicals and additives to customize any given slurry for the demands of each well. Though the number of additives exceed couple of hundreds today in the market, however they can be widely classified into 8 main different categories: Accelerators, Retarders, Extenders, Weighting agents, Friction reducers, Fluid – loss control agents, Lost – circulation agents, Special additives (Michel et al., 1989).

1.6.1 Accelerators

Cement setting time can be adjusted with accelerators. They serve to increase the rate of hydration at the early stages, especially, in shallow and low – temperature wells. On the other hand, accelerators are also used to contend when setting delay issue raises due to other additives like dispersants and fluid – loss agents.

Calcium Chloride ($CaCl_2$) is the mostly seen accelerator in the industry. The reason why it accelerates the hydration is explained as calcium chloride might increase the permeability of the C – S –H gel building around each silicate grain and let the water ready access to the grain's anhydrous surface.

Calcium Chloride reduces thickening time, help to raise early strength, and shortens setting time. Furthermore, it also reduces viscosity of slurry at low concentrations and an increase of slurry viscosity is observed at high concentrations. $CaCl_2$ becomes effective at temperatures between 4 ^{o} and 49 ^{o}C in concentrations of 2 – 4% by weight of cement. CaCl decreases viscosity and thickening time in low concentrations and vice – verse.

Halliburton suggests numerous accelerator products for use. Sodium Chloride, Calcium Chloride, Econolite Additive A – 4, Sodium Chloride Accelerator – A4, Cal – Seal 60 Cement Accelerator etc. could example for those (Url-8).

1.6.2 Retarders

Retarders prevent hydration and slow hardening that resulted to pump viscous slurry in deep and hot wells during the long time period. Retarders reduce the speed of cement hydration, showing opposite features that accelerators have.

Generally, retarders are made from wood pulp. They contain sodium and calcium salts of lignosulfonic acids and involve some saccharides. It is supposed that these retarders adsorb onto the initial layer C – S – H gel, rendering it hydrophobic and prolonging the induction period. The percentage of compounds in the slurry is 0.1 – 1.5 by weight of cement. They delay hydration at temperatures up to 122 ^{o}C. Addition of borax, lignosulfonates could allow to use cement slurries at 315 ^{o}C temperatures.

Addition some hydroxycarboxylic class components like gluconate and glucoheptonate salts help to decrease speed of hydration unless bottomhole temperature is below 93 ^{o}C. Else, the length of time for thickening becomes extremely long.

Products of Cellulose like Carboxymethyl Hyrdoxyethyl Cellulose (CMHEC) are also broadly used retarders in the petroleum wells. They are functional and effective to 120 ^{o}C. Meanwhile its retarding features CMHEC has also additional effects. It helps to improve fluid – loss control which could be desirable in some applications and yields higher slurry viscosity that could be unwanted property of the retarder.

Organophosphates are considered relatively new in its class and are functional at bottomhole circulating temperatures as high as 204 ^{o}C. The desired property of this class retarders is to let lower viscosity of high – density cement slurries (Url-9).

Component R™ Retarder, HR® – 12 Cement Retarder, HR® - 25 Cement Retarder, Sodium Citrate etc could be shown as an example for Halliburton retarders in the market (Url-8).

1.6.3 Extenders

Addition of extenders to cement slurries may result in lower slurry density that also increase the rate of pumpability of slurries to the deeper wells. In addition, Extenders help to reduce hydrostatic pressure during cementing operations as well. These properties become very helpful when drilling goes through weak formations. Dense cement slurry may break – down weak formations or loss of circulation may be observed at permeable zones. Adding extenders to the cement slurry lead to save the amount of cement needed for the cementing operations. Economically, extenders are less expensive than the cement (Michel et. al., 1989).

Extenders are classified into four main classes:

- Physical extenders (clays and organics)
- Pozzolanic extenders
- Chemical Extenders
- Gases

Any material which has lower specific gravity compare than that of the cement will act like an extender. As afore – mentioned these materials help to obtain lower dense of cement slurries by one of three means (Url-10).

1.6.4 Weighting agents

Pressure gradient increases as deeper in wells and high pressures can be reason for blow – out occasions. To prevent these kind of accidents effective cementing is applied. For the purpose of being effective in such situations the density of cement slurries is increased. Density can be increased by removing water from the mixture however a decrease of water volume in cement slurries raise pumpability issue whilst operation is going on. So that some weighting agents are added to cement slurry to get high density in the well (Hewlett, 2001).

Weighting agents move in at densities greater than 17 Ibm/gal where silica and dispersants are not any more effective. Weighting agents have specific requirements such as the specific gravity is greater than the cement, the particle size distribution is consistent, low amount of water is required and agents do not interfere with logging tools. Hematite, Ilmenite, Barite and Galena are most commonly used agents in petroleum industry.

Hematite's chemical formulation is Fe_2O_3, and is a brick – red mineral, usually co-exist with a dull metallic luster. It's composed by 70% of iron. The specific gravity of hematite changes from 4.9 to 5.3, depending on its quality.

Ilmenite ($FeO{\cdot}TiO_3$) behaves almost like hematite where it contains nearly 37% iron. It resembles magnetite in appearance but has very low magnetic character. Depending on its purity, the specific gravity varies from 4.5 to 5.

Another weighting agent is Barite (BaSO4). Due to its high surface area and high water demand, barite very occasionally is used in cementing operations. It is a soft, light gray and naturally exist nonmetallic material. Specific gravity starts from 4.0 up to 4.5, depending on its purity (Url-9)

Galena (PbS) is naturally found in nature and finely – ground mineral. Specific gravity of galena range from 6.7 to 7.0. In the industry is very seldom required agents since barite or hematite are capable to eliminate mud weighting problems in the wells (Url-2).

Many weighting agents are suggested by companies. For example, widely used Schlumberger products are M-I WATE high – quality barite, FER – OX hematite weighting agent, M-I BAR Barite (Url-11); Halliburton products such as Bentonite A-4, Spherelite™ Cement Additive, Econolite Additive, Barite Heavyweight Additive, Bentonite (Halliburton Gel), MICROMAX™ Weight Additive and etc (Url-8).

1.6.5 Friction reducers

Dispersants or with its other name friction reducers improve the flow properties of the cement slurry by breaking up cement agglomerates and freeing water. They are extensively used in cement mixtures to optimize rheological properties of the slurry during pumped in the well. Dispersant added slurries become lower viscous substances and reaching to turbulent flow conditions becomes easy task at lower pump pressures. Its usage in slurries lead to reduce pressures exerted on weak formations and preventing possibly circulation losses (Hewlett, 2001).

Therefore, dispersants is used to prevent flocculation of cement particles, because they adsorbs onto hydration cement particle, and particle surfaces are charged negatively and eventually, repel each other. Otherwise, water would have been entrained in the flocculated system also becomes available to further lubricate the slurry.

Polyunsulfonated naphthalene (PNS) and Hydroxycarboxylic acids are commonly used dispersants in cementing operations.

Polyunsulfonated naphthalene can be found in dust form as a calcium or sodium salt and from them solid and liquid form can be derived. The commercial liquid form typically has solids particles of nearly 40%. The advantage of using polyunsulfonated naphthalene in applications is that improved rheological properties can be gained and at the reduced pressures slurries are pumped easily.

Hydroxycarboxylic acids are accepted as the primary dispersant in freshwater slurries at temperatures above 95 ^{o}C. This acid is also used in salt and seawater cement applications. The concentration of use is restricted by the temperature and thickening time desired, furthermore concentrations of 0.5 to 1.0% by weight of cement are usually sufficient (Url-9).

CFR–3™, CFR–4™, CFR–6™, CFR–8™ Cement Friction Reducers are suggested by Halliburton and widely used in the petroleum wells.

CFR–3™ Friction Reducer is very useful to lower viscosity and improve the rheological parameters of the cement slurry. At lower pumping pressures turbulent flow regime is achieved. Nevertheless, CFR – 3 helps improve fluid – loss control and deliver slight slurry retardation. Bulk density of CFR – 3 is 38.00 Ib/ft^3 and specific gravity is 1.16. It is in red – brown solid form and packing in 50 Ib bags (Url-8).

1.6.6 Fluid – loss control agents

When slurry is pumped to the well, it is placed across a permeable formation under abnormally high pressure. In this case, fluid loss from the cement slurry toward permeable zone exists. In that permeable zones, water tends to escape from the slurry and the cement particles are left behind. Unless fluid loss is controlled and loss of only a proportion of this water can significantly alter the cement properties, some parameters such as rheology, thickening time and density of the slurry will change and the cementing job could be resulted in failure. If a high portion of the excess water is squeezed from the slurry, the cement may experience what many call a “flash set.” At this point, the cement is no longer pumpable and the job is terminated prematurely. For that Fluid Loss agents are added in the cement slurry in order to stop water loss and protect slurry properties. These additives help to reduce the permeability of cement filter cake that is accumulated on the formation surface when fluid loss exists. In addition, some fluid – loss agents may increase the viscosity of water in the cement slurry, thus reducing the rate of filtration (Hewlett, 2001).

Commonly used fluid loss agents are polyacrylamide, polyethyleneamines, carboxymethylhydroxyethylcellulose (CMHEC) and hydroxyethylcellulose (HEC) (Michel et al., 1989).

Carboxymethylhydroxyethylcellulose (CMHEC): Certain admixtures of carboxymethylhydroxyethyl cellulose or copolymers and copolymer salts of N, N-dimethylacrylamide and AMPS, together with a copolymer of AA, may provide fluid loss control to cement compositions under elevated temperature conditions (Patel and Bharat, 1990).

Hydroxyethylcellulose (HEC): An apparent viscosity in water of at least 15 c P should be adjusted to achieve an API fluid loss of less than 50 ml/30 min. Cross-linked

HEC is suitable for high-permeability formations (Parlar M. et. al., 1998 and Chang et al., 1999).

A derivatized HEC polymer gel exhibited excellent fluid loss control over a wide range of conditions in most common completion fluids. This particular grated gel was compatible with the formation material and caused little or no damage to original permeability (Nguyen et. al., 1996).

Detailed measurements of fluid loss, injection, and regained permeability were taken to determine the polymer particulate’s effectiveness in controlling fluid loss and to assess its ease of removal. HEC can be etherified or esterified with long chain alcohols or esters. An ether bond is more stable in aqueous solution than is an ester bond (Audibert et. al., 1997).

DeepFX™– L, Halad®– 200 L, Halad®– 23, Halad®-688 and Halad®–688 EXP, Halad®–9 Fluid Loss Additive are all fluid – loss additives in the market suggested by Halliburton.

Halad®–9 Fluid Loss Additive is more popular in comparison with others.

It is a blended material included to cellulose class and a dispersant. Generally, it is added in to cement slurry to provide fluid – loss control in all API cement classes.

Usage of this additive in wells are limited due to temperature effects and effective minimum temperature is 15.5^o up to maximum 149 ^{o}C. Halad – 9 provides adequate fluid – loss control at the concentrations up to 1%.

It helps keep horsepower requirements low by controlling viscosity and circulation pressures.

Halad®-9 helps control gas migration and can improve squeeze cementing results.

It helps protect water-sensitive formations.

This additive can allow a better cement/casing bond and helps maintain slurry density.

Halad – 9 is in red color and available as solid powder. Bulk density of the additive is 37.20 Ib/ft^3 (Url-8).

1.6.7 Lost – circulation agents

Lost circulation is a frequently observed issue during drilling and high pressure difference between permeable zones and cement slurry cause to raise that problem.

Loss usually occurs in fractured, vuggy or cavernous formations, and operator is awarded about expected lost circulation problems regarding drilling parameters. The term of loss circulation is defined as the total or partial loss of drilling fluids into the permeable zones and the voids of the formation while the cementing operations (Michel et al., 1989).

Lost circulation materials are basically divided into three groups: fibers (1), flakes (2) and granular materials (3). These materials are used when drilling goes through high – permeable zones to prevent fluid losses in order to continue operations (Boukadi et al., 2004).

Granular materials such as gilsonite and granular coal are highly effective bridging additives but ground walnut and pecan shells, coarse bentonite or even corn cobs are sometimes used. Another useful bridging additive is cellophane flake. The flakes form a mat that seals the face of the fracture and prevents cement from entering formation (Bourgoyne et al., 1991)

In case, the size of vugs or caverns are so large in the formation, bridging agents may not be effectible then thixotropic cement is moved in to operations. When thixotropic cement is entered to the formation and slows down, it experiences less shear force and begins to gel, becoming self – supporting and eventually plugging the cavern or vug (Michel et al., 1989).

Before a mud filter cake can be created, loss circulation additives must bridge across the large openings and provide a base upon which the mud cake can be built.

1.6.8 Special additives

At some operations special additives are mixed to prevent unwanted results in the well. Antifoam agents, fibrous additives and gas migration preventers can be very good examples for the special additives.

Antifoam agents help to reduce the amount of foam that often arises whilst additives are mixed into cement slurry. Uncontrolled foam can lead to loss in hydraulic pressure possibly wrecking the cementing job. For that purpose, polyethylene glycol is added which has the lowest price in the market and broadly used antifoaming agent. Better results obtained when antifoaming agent is mixed with water before slurry preparation.

The more expensive silicone emulsions will defeat a foam regardless of when they are added.

Fibrous materials serve to increase resistance of cement to stresses that develop around drill collars or when perforating is applied. Nylon fibers and particulate rubber are the two most commonly used strengthening agents.

In the gas wells special problems arises. During drilling and while cement is being pumped, the hydrostatic pressure of the borehole fluid prevents gas entering the wellbore. Bu as soon as the mixture starts to harden, it loses its ability to transmit hydrostatic pressure and gas may migrate into hardened cement. Among the most commonly agents special lattices such as GAS-BIOK differs than others that coagulate at the gas – cement interface forming a membrane impermeable to gas (Michel et. al., 1989).

2. LITERATURE REVIEW

It is important to consider the compressive strength of oil-well cement for the purpose of securing the long – term integrity of wellbore. Strength development of cement becomes difficult issue since the cement slurry has been pumped down wellbore. During the early hydration time of the slurry in the wellbore strength development may not progress properly where secondary cementing operation can be demanded or it can be end up with the well damage (Ridha et al., 2013).

In cementing operation, at least 500 psi strength pressure is needed to continue further drilling operations (Backe K.R. et al., 2001). Duration until the pressure threshold is related directly to hydration time and generally is called wait – on – cement (WOC). Hence drilling cost per hour is extremely high longer waiting time due to strengthening of cement may cost a lot and shorter waiting time may lead to unsuccessfully completed cementing job in the wellbore (Ridha et al., 2013).

After being pumped cement slurry in the annulus, it starts to harden into a low – permeability annular seal. Factors like drilling fluid, spacer, chemical wash, cement, casing, rocks make these processes very complex and taking severe measurements becomes obligatory for the purpose of designing and optimizing cement jobs.

Tensile and shear strength of the cement slurry moderately build up as it hydrates by time. Tensile strength is defined as the maximum amount of tensile stress that a material can withstand before failure or without breaking apart. The unit of the tensile is Pa in SI units and psi in field units. In laboratories, tensile strength of the cement slurry is measured by injecting water at certain location inside the slurry. (Backe K.R. et al., 1999). Water is injected continuously at the stable rate and pressure is recorded during time. Then pressure is raised up till a fracture is appeared in the slurry. The figure for tensile strength of cement slurry has been recorded as high as 0.5 MPa. (Backe K.R. et al., 1999). In addition, the term of shear strength is defined as the maximum value of shear stress that the slurry can withstand without starting to flow or failing. Yield stress and shear strength of the cement equal to each other at pressures between 1 – 10 Pa while shear strength increases moderately as the slurry sets.

The pressure which is originated from the cement slurry in the annulus is a very serious problem whereby fluid influx can occur from the formation during cement setting. Experiments show that pressure decrease in a slurry column during setting can be highly worthwhile to take under consideration (Chenevert & Shrestha, 1991). Hydrostatic pressure which is formed by cement slurry may go down due to developing shear stresses between the slurry and the casing or rock. These stresses are limited by the yield stress of the slurry (Lavrov & Torsæter, 2016).

2.1 Properties of Cement

Annular cement sheath can be subjected to numerous factors such as heating and cooling cycles, reactive flows throughout the wellbore, mechanical stresses, vibrations and formation fluid influx during the life of well. Properties of hardened cement influence its sealing ability and therefore understanding them is important for maintaining well integrity. There are four different properties available for solid cement: mechanical, interfacial, thermal and hydraulic.

Mechanical properties essentially are explained the response of cement to deformations and mechanical loads. These also are subdivided into two segments: elastic properties and strength properties.

The specimen breaks down at the certain value of the uniaxial stress that this threshold is called unconfined compressive strength (UCS). It shows the capacity of the cement to carry load under compression. Depending on the composition and structure UCS may rise up to tens of megapascals. It could be relevant to remember that cement set in the annulus is accepted in a triaxial stress state.

Relationship between the maximum load, F_m, and tensile strength has been shown by the following equation (Fjaer E. et al,, 2008):

$$T_0 = \frac{2F_m}{\pi DL} \qquad (1)$$

Here D is diameter in meters and L is length of the cylinder in meters.

Compressive and tensile strength are both highly important properties for the cement's load – bearing capacity. Cement's tensile strength allow to control casing pressurization when an increase is observed in casing diameter. However, it would not be forgotten that annular cement does not be subjected to only tensile stress during its lifetime, it is exposed to many complicated stress paths and loading/unloading cycles. Annular cement is placed behind the casing where it confines with the formation as well. Therefore, its deformation originates from the deformations of the casing and the rock (Lavrov and Torsaeter, 2016).

2.1.1 Interfacial properties of cement

Like mechanical properties, interfacial properties of cement is play a pivotal role to control cement failure in wells. Potential weak spots in the wells occurs between cement and casing and between rock and cement. Problematic bonding places are detected by the lowering cement bond log into the well after the cement job is completed. Even so, bonding between the afore-mentioned surfaces are good it is possible to see lower the interfacial bonding strength compare than bulk cement strength. These problems are investigated in laboratories such realizing push – out experiments shown in the following Figure 2.1.

As be seen from the picture it is complex structure tool where specimen with a steel pipe or rock cylinder in the middle and cement around it. During the test time, certain amount of pressure is applied from the top of the rock or specimen in the direction of downward. As pressure increases up it causes to induce failure at the cement interface. The peak value of the loaded pressure is key to calculate the interfacial bonding strength between the outer of casing or steel and the surrounding cement. After these

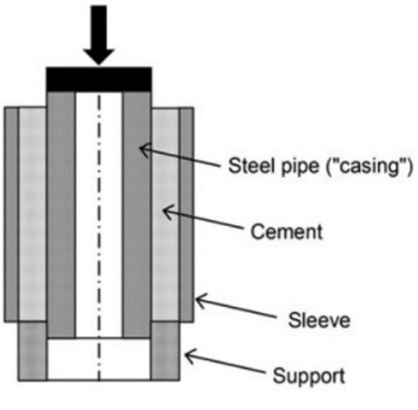

Figure 2.1: Principle of push – out testing for interfacial bond strength (Lavrov & Torsæter, 2016).

experiments, typical values have been determined for the shear bond strength that varies from 0.1 up to 1.0 MPa.

Besides bonding strength, hydraulic bonding properties of an interface can give good estimations regarding to any possible leakage. Hydraulic bonding can be quantified by applying fluid pressure at the interface between compound cement and steel or between cement and rock specimen (Nelson & Guillot, 2006).

2.1.2 Hydraulic properties of cement

Mechanical properties help to determine cement's resistance to mechanical loads. However, hydraulic features help to find out how leak is formed alongside the well or at what rate the cement sheath will be chemically degraded. Leakage can lead to having interconnections between geological horizons or even can evaluate formation fluids or particles to the surface. Particularly, microannulus, gas channels and micro fractures in cement is considered enough to have leakage throughout the cement sheath. The capacity of leakage is determined by cement's permeability.

2.1.3 Thermal properties of cement

Thermal properties have to be taken under consideration when problem is subjected to cement fractures. Possibility is high for having fractures or micro channels in the cement slurry during the heating and cooling in the well. Like mechanical properties, thermal properties also play a very crucial role, in particular the coefficient of thermal expansion and its difference between casing, cement and formation. "Typical" values of this parameter for steel, cement and sandstone has been given in the Table 2.1 (Lavrov & Torsæter, 2016).

Table 2.1: Example values of the coefficient of thermal expansion for steel, cement and rocks.

Material	Coefficient of thermal expansion (x 10^{-6} K^{-1})
Steel	10 – 16
Cement	10 – 12
Sandstone	10 – 12

2.2 Heat of Hydration

Mixing of water and Portland cement usually is observed by liberating of heat. Reaction between these components are exothermic type of chemical reaction and process is called heat of hydration (Url-12).

Heat is released with cement hydration caused by the breaking and making of chemical bonds while hydration. The heat liberation is depicted in Figure 2.2 as a function of time.

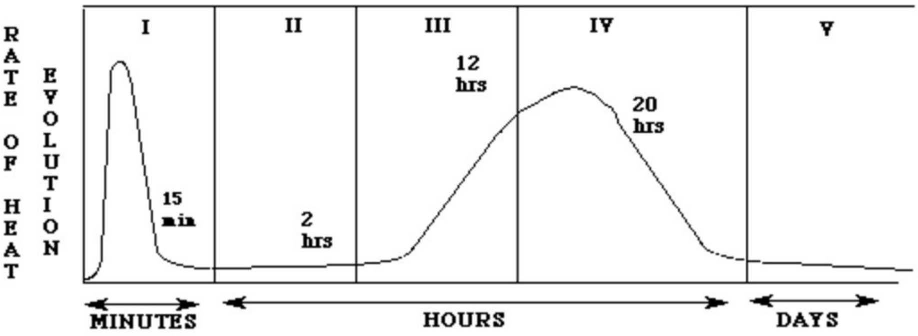

Figure 2.2: Rate of heat evolution during the hydration of Portland cement (Url-13).

Heat evolution is divided into 5 different stages. First stage is called Hydrolysis of the cement. Hydrolysis occurs fast with a temperature increase of several degrees. Stage II is the Dormancy period. The heat liberation slows dramatically in the Dormancy period stage. It is possible to place and transport the concrete easily without any major trouble due to its plastic state in this stage. Initial setting starts at the end of this stage as well. Hardening of the slurry and increment in the heat evolution is observed mainly in stages III and IV due primarily to the hydration of C_3S. After approximately 36 hours later the concrete reaches to the Stage V. The process is getting slower and process continues as long as water and unhydrated silicates are present (Url-13).

At high cement content mix temperature rises can be remarked up to 55 ^{0}C. An increment in temperature cause expansion while the slurry is hardening. If the temperature rise is significantly high and the concrete undergoes nonuniform or rapid cooling, stresses due to thermal contraction in conjunction with structural restraint can result in cracking before or after the concrete eventually cools to the surrounding temperature. It is not recommended in case the maximum temperature differential between the interior and exterior concrete is over 20 ^{0}C. Crack developments can be seen over 20 ^{0}C difference. Thermal crack basically depends on the tensile strength of the concrete, thermal expansion coefficient and temperature difference within concrete.

By choosing materials it is possible to adjust the heat of hydration depending on the need.

Having higher contents of tricalcium silicate and tricalcium aluminate in mixtures as well as higher fineness cause to higher rates of heat liberation than other cements. C_3S and C_3A chemically produce more heat and at a faster rate in comparison with C_2S or other cement compounds. Sulfate in cement mixtures serve to control the hydration of calcium aluminate, participates in the rate of heat release. Higher fineness means that greater surface area is available to be wetted, resulting in an acceleration of the chemical reaction between cement and water components. Higher fineness causes to increase at the rate of heat generation at the early ages, but may not influence the total amount of heat released over many years. Some factors such as cement content, water – cement ratio, placing and curing temperature, mineral and chemical admixtures also play a very important role in heat generation of cement (Url-18).

2.3 Effect of additives on cement properties

Temperature and pressure are very important factors and main influencers on the downhole performance of cement slurries. In deep and hot wells heat development from the cement during its hydration time can cause a substantial increase in the annulus. This issue has to be taken into account in the design of cement slurry at the surface. Temperature has more noticeable influence with regard to it.

At high temperatures the speed of setting is fastening and less time is required to complete cementing job in the well which costs less for the operators. Though high temperature in some cases is helpful but in many cases it leads to many severe problems inside the well, proper cementing work is demanded in particularly gas wells. Just as mentioned before while hydration proceeds some amount of heat is released from the cement slurry. If the heat from the formations would be taken consideration it makes the setting problem of cement more complicated as well (Kutasov and Eppelbaum, 2015).

According to A Lavrov and M. Torsaeter, heat generation during cement hydration causes the casing diameter to be slightly larger than it otherwise would be during cement setting. At the time when temperature start to fall back to its typical value, it is expected microchannels can be developed between the cement and the casing. Furthermore, generated heat during the hydration may have negative effect particularly in the permafrost wells. It may resulted in melting of the formation and poor bonding problems as well (Lavrov & Torsæter, 2016).

As mentioned above, as formation temperature goes up cement slurry hydrates and sets faster and gets strength more quickly. Designing cement slurry at the surface must be optimum that its rheological properties have to be enough to pump and place safely it in the well on time. At the same time the slurry cannot be designed overly retarded which can cause to get its compressive strength long time later. Thickening time of cement is the time that cement slurry remains in fluid state and keeps its pumping capability until end of cementing job. While retarders can extend the duration of thickening time, any change in temperature can alert properties of cement slurry in the place and thickening time can be swipe to another expected time (Kutasov and Eppelbaum, 2015).

Many techniques have been used to estimate temperature increment during cement hydration. Having detailed information about temperature behavior during hydration is important to verify how cement hardening happens and how long it takes before casing is released (Romero & Loizzo, 2000). Therefore, cement design has to be done properly at surface regarding to heat generation estimations in deep wells. Experimentally it is determined that heat development during hydration reaches at its peak point during the first 5 hours until 24 hours (Halliburton Cementing Tables, 1979). At these time intervals it is possible to observe maximum temperature change ΔT_{max} in the annulus. Field experience shows that temperature variations can lead to very essential problems caused by the generated heat during hydration in the well. It is vital to estimate the temperature variation while the cement is setting.

Importance of prediction temperature raise during cement setting can be helpful to determine the best time lapse between cementing and temperature survey. Temperature measurements during cementing operations are aimed to place the top of the cement column behind the casing. An increase in the temperature of ambient environment cause to goes up the rate of heat production. Change in the rate of heat generation regarding to different ambient temperatures has been proved by the laboratory tests for G Class cement. Tests were performed at two different temperatures 77 ^{0}F and 122 ^{0}F, the density of the slurry was 15.8 ppg (Romero & Loizzo, 2000). Following Figure 2.3 is obtained where graphic shows relationship between heat production and time. Blue line stands for test at 122 ^{0}F while pink is at 77 ^{0}F.

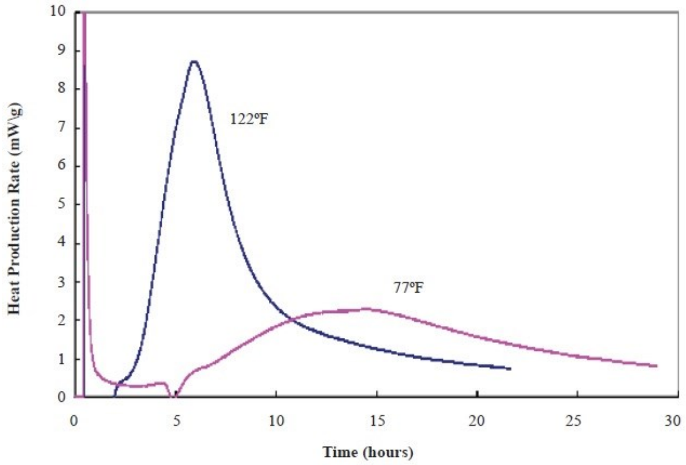

Figure 2.3: Heat production rate per unit of mass as a function of time for class "G" neat cement at two temperatures (Romero & Loizzo, 2000).

As mentioned earlier thickening time of the cement slurry at the known concentration of retarder is easily affected by change in temperature. Usually slurries are prepared for the conditions where high temperatures are dominated in the wellbore may have impermissible long duration to reach its typical value of strength at lower temperatures. Normally, at least 500 psi compressive strength is required to support casing during the first 24 hours (Romero & Loizzo, 2000). Following Figure 2.4 depicts the importance of temperature difference in the compressive strength. Though the difference between is only about 3.3^{0}C but compressive strength is affected significantly. It is possible and recommended to minimize the wait on cement (WOC) time by rising the outlet mud temperature. Particularly, this may reduce the cost associated with cementing of the conductor and surface casing (Kutasov I., 1999).

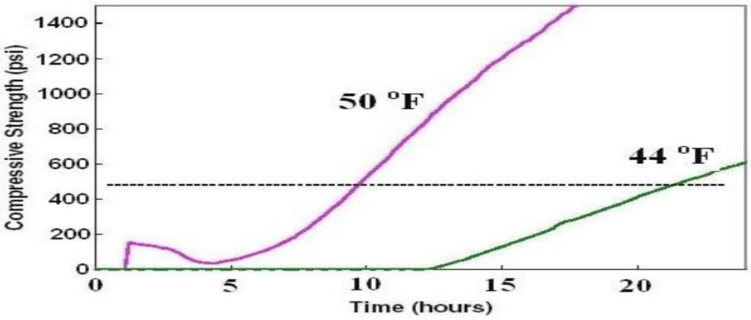

Figure 2.4: Compressive strength development for a deep-water (Kutasov and Eppelbaum, 2016).

3. PURPOSE OF STUDY

The utilization of additives in drilling industry has been increased substantially since the exploration wells goes deeper and drilling fluids requires more adjustments in order to provide their duties. Different type of additives is used for different purposes regarding to the encountered problems in the oil – gas wells. Though the additives help to accomplish well completion operations in a proper way while it may lead to some unexpected problems with themselves.

Well cementing is one of the important job during the drilling operations in the drilling fields to provide zonal isolation throughout the well. So that cement slurries are prepared at the surface and then pumped to between the formation and casing string. When cement is mixed with water it is followed by exothermic chemical reaction. Certain amount of heat is generated from the slurry during its setting time. Generated heat may cause to increase the temperature in the well. The cement slurry in the well contains not only water and cement but also some additives in order to regulate some properties of the well cement such as viscosity, fluid loss, strength, thickening time etc. The impact of these additives on the exothermic reaction is not clear. In many cases the effects are ignored. They also might affect the design of casing by causing some stress due to the heat liberation.

The purpose of this experimental study is to examine the effect of additives on the heat generation. Throughout the experiments it was intended to observe the effects of additives, particularly, friction reducer and fluid – loss agents on the cement slurry. Essentially, aim is to understand and monitor the change of temperature and determine to which additive is more severely impact on the contribution to generated heat at the different concentrations. Besides it is intended to observe the relation between the amount of additives and temperature change during setting by performing simple regression analysis to the obtained results. In addition, it is planned to check the effects of these temperature changes in the casing design using some obtained results from the experiments by calculating loaded stresses in the casing design regarding to the change in temperatures of cement compositions.

4. EXPERIMENTAL MEHTODS AND MATERIALS

Throughout the experiments Class G cement had been used. Experiments were fulfilled regarding to API 10B – Recommended Practice for Testing Well Cements, with a water to cement ratio of W/C=0.44. Cement samples were prepared by adding 264 cc water to 600 gr cement in the mixture. Two different additives – friction reducer and fluid loss controller were added to the cement slurries. Both additives are the product of Halliburton. As a friction reducer CFR–3™ which serves to reducing viscosity and improve the rheological parameters was put in the cement mixtures. Fluid – loss controller was Halad®–9 and this agent provided to maintain slurry density in the slurry as well.

4.1 Sample Cell

By using special mixer, these components were blended for 45 – 60 seconds in the laboratory. After being mixed, cement slurries were poured into the container as shown in Figure 4.1 which is insulated using isolation material to eliminate surrounding effect on temperature records. The volume of container is nearly 1000 ml in cubic shape (10 cm x 10 cm x 10 cm) and designed to keep cement slurry for 24 hours or more.

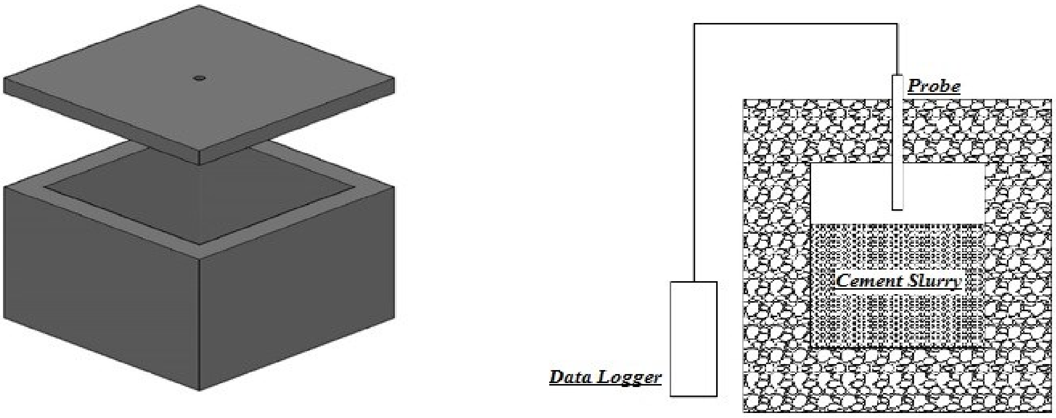

Figure 4.1: The visual view of isolated container.

4.2 Data Acquisition System

Temperature readings of each cement samples were realized by using portable data logger which is explained in the following paragraph. A probe of the data logger was securely inserted into the container, over the cement slurry throughout the lid of insulated plastic cover. Logger was programmed to record temperature readings at every 30 seconds time period. Collected data from the logger was transferred to the computer using data logger's special software.

Temperature measurements are realized by using a data logger. The data logger is the product of Ebro Company. Special software Winlog.basic is used to transfer all obtained data from the data logger to the computer. Portable data logger has been illustrated on the Figure 4.2.

Figure 4.2: View of EBI 310 type data logger.

First element is main body of the logger. On display it possible to check the current temperature while experiments are fulfilled. EBI 310 is widely used for transportation and storage monitoring purposes. It is easy to generate all obtained data from the experiments to PDF format automatically or direct USB readout gives opportunity to save data in excel sheet as well. Second element in the Figure 4.2 associate probe which is third element in the figure with the main body. It has two joints on itself where two different temperature readings from the experiment is deposited in the main body. Third element is called probe that is attached to the data logger. Data logger is able to collect data from – 200 ^{0}C up to maximum +400 ^{0}C with a resolution of 0.1 ^{0}C at each 30 second interval.

Programming of the device is done as in the following figures.

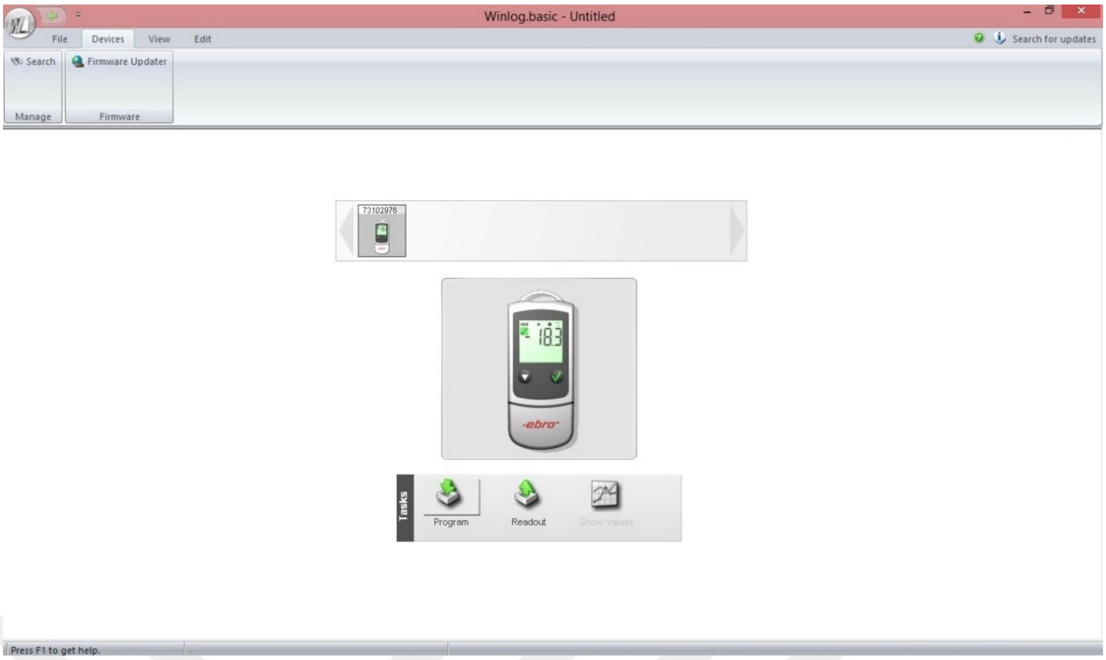

Figure 4.3: The main page of EBI 310 data logger.

By clicking “Program” it is possible to meet options of the software like shown in the Figure 4.3. After clicking to the “Program” button, users become eligible to arrange logger for experiments.

On this window as shown in the Figure 4.4 it is possible to see all possible alternatives such as “Endless mode measurement”, “Measure upon start time”, “Start immediately until end of memory”, “Start/Stop measurement”, “Don't measure / Start upon key pressed” for the purpose of preparing logger before use. “Endless mode measurement” has been selected to record instant temperature changes at every 30 second interval while experiments are done. Temperature scale is based on Celsius and TPX310 type external sensor is attached to data logger.

After being all arrangements done “Program logger” button is clicked to finish. In case, data logger is set successfully user is warned about that and by clicking “OK” button data logger can be detached from the logger.

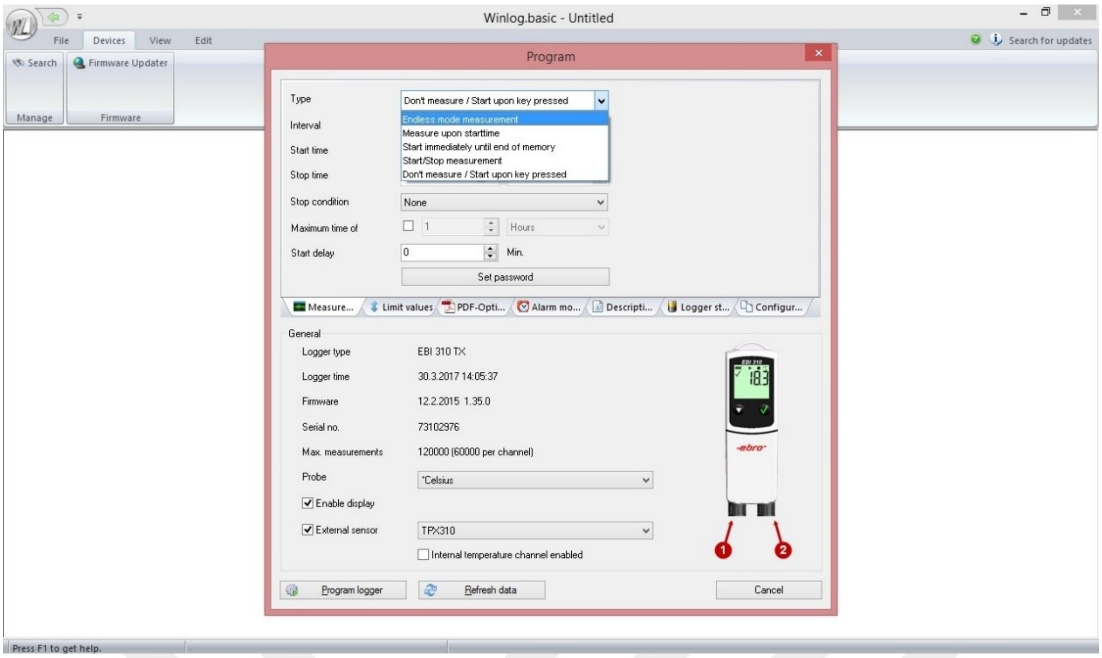

Type: Don't measure / Start upon key pressed
Interval
Start time
Stop time
Stop condition: None
Maximum time of: ☐ 1 Hours
Start delay: 0 Min.

General
Logger type: EBI 310 TX
Logger time: 30.3.2017 14:05:37
Firmware: 12.2.2015 1.35.0
Serial no.: 73102976
Max. measurements: 120000 (60000 per channel)
Probe: °Celsius
☑ Enable display
☑ External sensor: TPX310
☐ Internal temperature channel enabled

Figure 4.4: Options of the data logger for measurements.

After the data being collected throughout the experiments when USB part of logger is attached to the computer "Button of Readout" appears as depicted in the Figure 4.3.

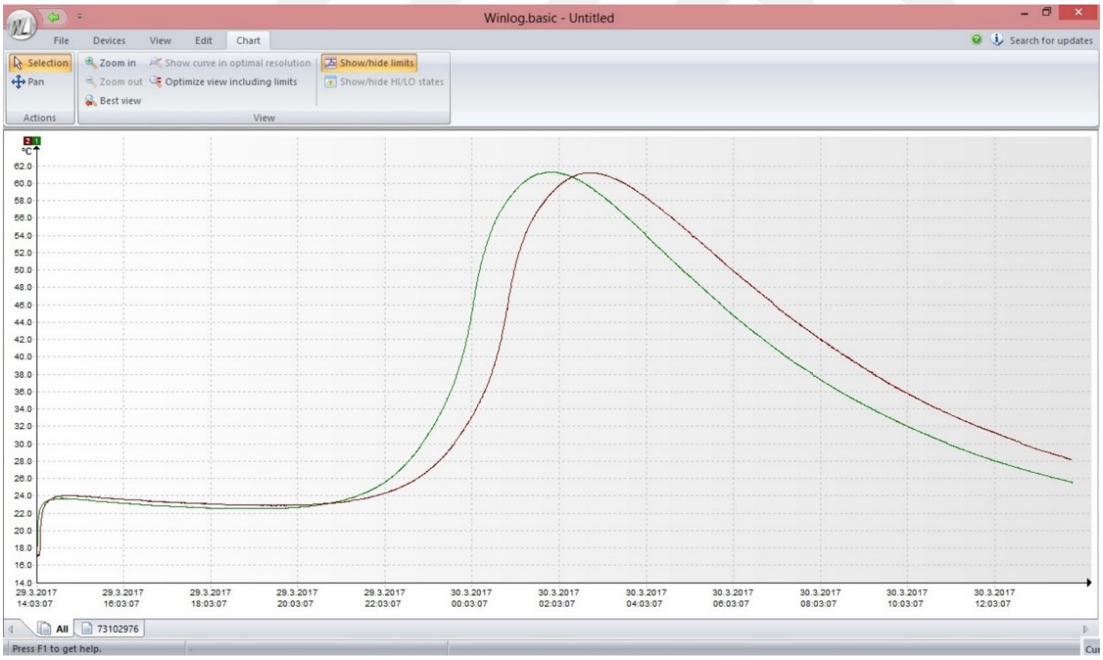

Figure 4.5: Launched graphics by EPI 310 data logger from the experiment.

Collected data through the logger is displayed by clicking to Readout button and results launched as in the following Figure 4.5.

To save the information in excel format it is needed to use convert function in the Winlog.Basic software. Information is exported by clicking “Export” button to the chosen file format, include excel (Figure 4.6).

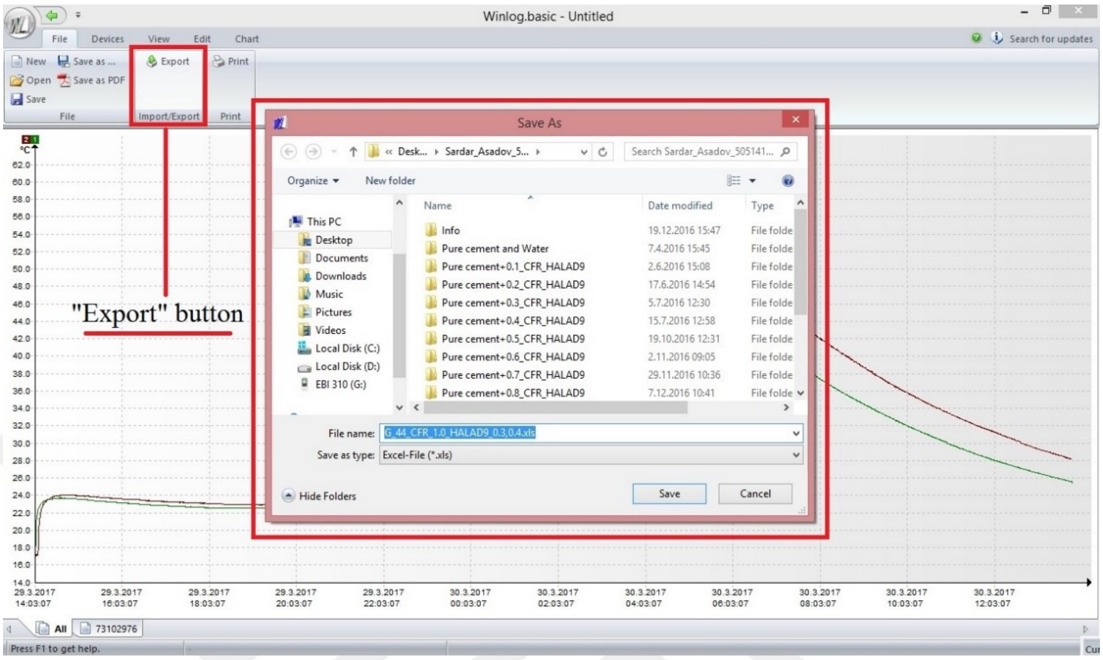

Name	Date modified	Type
Info	19.12.2016 15:47	File folde
Pure cement and Water	7.4.2016 15:45	File folde
Pure cement+0.1_CFR_HALAD9	2.6.2016 15:08	File folde
Pure cement+0.2_CFR_HALAD9	17.6.2016 14:54	File folde
Pure cement+0.3_CFR_HALAD9	5.7.2016 12:30	File folde
Pure cement+0.4_CFR_HALAD9	15.7.2016 12:58	File folde
Pure cement+0.5_CFR_HALAD9	19.10.2016 12:31	File folde
Pure cement+0.6_CFR_HALAD9	2.11.2016 09:05	File folde
Pure cement+0.7_CFR_HALAD9	29.11.2016 10:36	File folde
Pure cement+0.8_CFR_HALAD9	7.12.2016 10:41	File folde

File name: G_44_CFR_1.0_HALAD9_0.3,0.4.xls
Save as type: Excel-File (*.xls)

Figure 4.6: Saving data from data logger to the computer in excel sheet.

Experiments are coded regarding to the amount of water, cement and additives. On this picture G_44_CFR_1.0_HALAD9_0.3,0.4.xls provides information about the mixture in brief format. It says slurry is made CFR at 1% percent by weight of cement and HALAD9 at 0.3% and 0.4% by weight of cement in the mixture. Note that 0.3, 0.4 stands for two different experiments. More detailed information is given under “Coding of Samples” paragraph.

When transformation is done successfully then users are warned by the final message. In addition to that software is also suggest to save data in PDF format. So, it is enough to press Save as PDF button to convert information (Figure 4.7).

4.3 Experimental Conditions

Experiments were run at ambient conditions where pressure was nearly 14.7 psia and room temperature was 70 ^{0}F and for 24 hours. Several different compositions of slurry with the combination of the additives from 0 % to 1.0 % by weight of cement were tested.

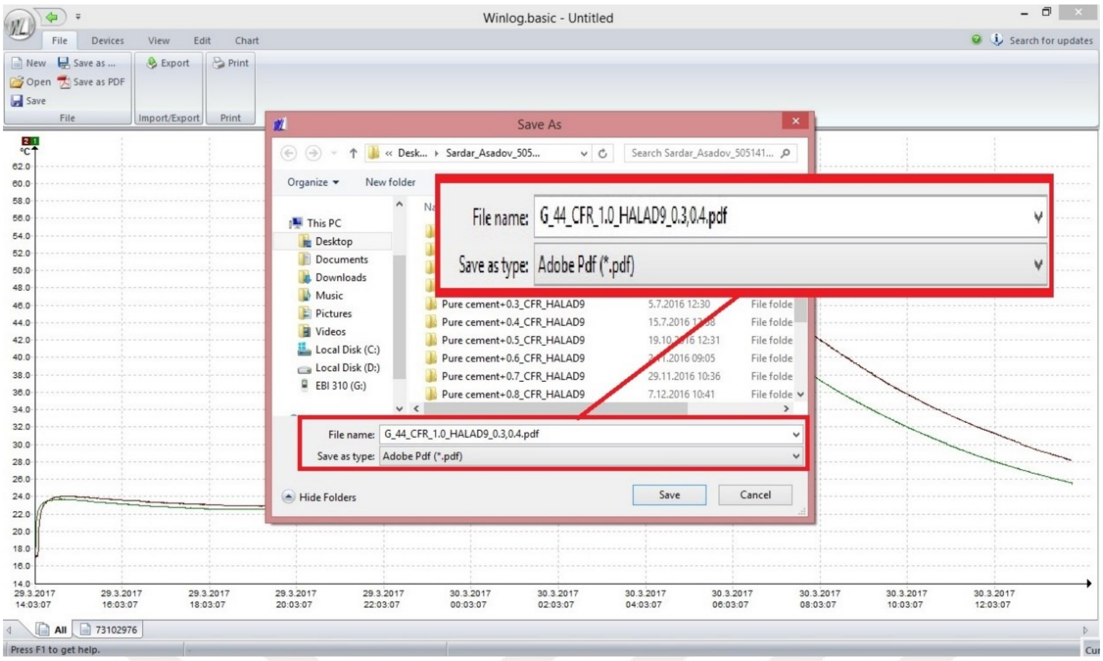

File name: G_44_CFR_1.0_HALAD9_0.3,0.4.pdf

Save as type: Adobe Pdf (*.pdf)

Figure 4.7: Saving data in PDF format by using Winlog.basic software.

4.4 Coding of Samples

Samples are named according to the materials added to the slurry. Name of all samples start to letter “G”. It stands for G class of Portland cement. The letter “G” is followed by the number of “0.44”. This number stands for volume of added water into the cement slurry. Next, the abbreviation of friction reducer as “CFR” follows them. Fractions of CFR is given nearby it. That fraction illustrates the amount of friction reducer is added to the composition. For instance, if the fraction is 0.3, it means that 1.8 gr additive used in the mixture. 1.8 gr is calculated 0.3 multiply the amount of cement: 1.8 gr =0.3*600/100. Then, HALAD9 is mentioned in the code. As friction reducer, the added amount of HALAD9 is mentioned in the name as in fractions. As an example, **G_0.44_CFR_0.5_HALAD9_0.9** depicts that 600 gr cement has been mixed with 264 cc tap water, 3 (=0.5*600/100) gr friction – reducer and 5.4 (=0.9*600/100) gr fluid – loss agent added to the slurry.

5. EXPERIMENTAL RESULTS AND STATISTICAL EVALUATION

First experiments performed with the slurries having only cement and water. The weight of Portland cement in the experiment is 600 grams where the volume of water is 264 cc (tap water). These measurements are based on API 10B – Recommended Practice for Testing Well Cements. Then, friction reducer and fluid loss control additives added merely to the composition to observe their individual effects on slurries. Finally, samples were prepared to test having both additives together in it.

Recorded temperature data for the cement and water mixture slurry was shown in Figure 5.1. Since the cement setting is an exothermic chemical reaction, temperature increment had been expected in the cell. It is clearly seen from Figure 5.1 that temperature raised up during first 8 hours and it peaked at 61.4 ^{0}C after 8.3 hours later. Gradual decrease was observed in temperature during the next following hours. Approximately after 16 hours later since temperature received its peak point it went down again to base temperature 20 ^{0}C. Nearly 40 ^{0}C increment was observed during the experiment.

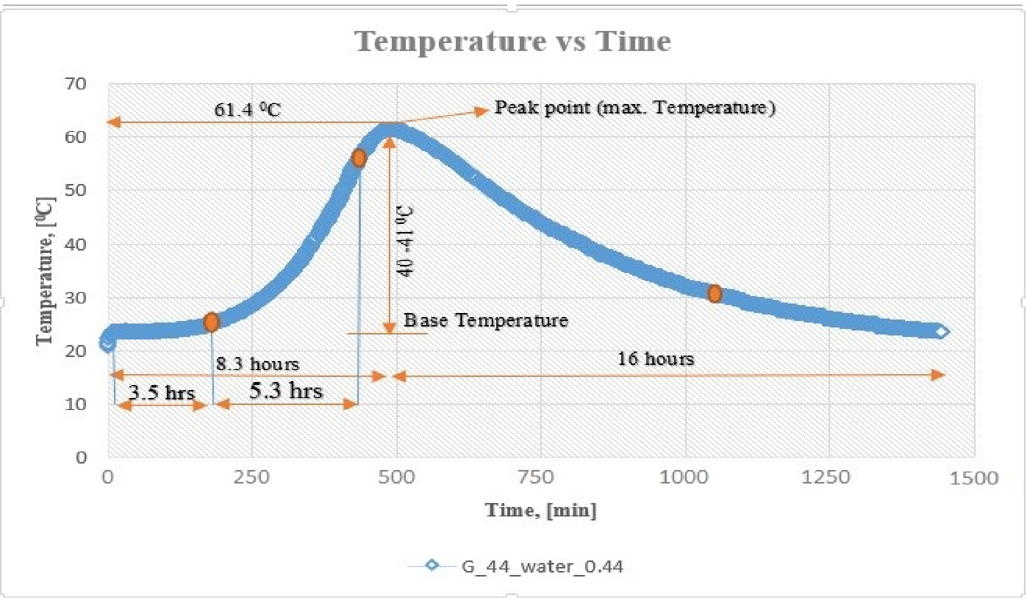

Figure 5.1: Heat of hydration of pure G class Portland cement with water.

First of all, heat evolution started with at dormancy period. Dormancy Period is explained when temperature stays constant at the time of first 2–4 hours. In this region cement slurry keeps its functions of pumpability and transportability to any desired place. At the end of this stage initial setting takes place and hydration accelerates. In this sample, the duration of the dormancy period is approximately 3 hours as shown in Figure 5.1. According to ASTM C 150 norms, initial setting time has to be more than 60 minutes and final setting time should not exceed 600 minutes regarding to Gillmore's results (Lowler et al., 2007). The orange colored point depicts the start of setting of slurry and at the same time, beginning of Stage III. Temperature increased substantially after that distinguished point and reached its peak, approximately at 61.4 ^{0}C. Length of time since beginning to the reaching maximum temperature constitutes 8.3 hours. While, time duration makes up nearly 5.3 hours since cement starts to set initially. Setting of cement finishes at the second orange colored point. Total time for setting is roughly 3.5 hours. Second orange colored point also indicates the end of Stage III and the starting point of Stage IV. Maximum heat generation usually is observed at the Stage IV due to the hydration of C_3S. Maximum temperature is at 61.4 ^{0}C and difference between maximum and base temperature is equal to 41.4 ^{0}C since base temperature is assumed as room temperature as 20 ^{0}C. Maximum temperature is also stands to stop heat liberation from the cement mixture. After that point process slows down and temperature goes down gradually. Specific time duration for Stage IV is accounted about 18–20 hours. In this Figure 5.1, it is not available to determine the starting point of Stage V but literature shows the stage can continue for many days.

Moreover, strength/stress development began at the point when setting starts and finished when temperature declined substantially. In this experiment, strength/stress development time was 16 hours.

Following Figure 5.2 depicts the composition of the cement with friction reducer. 264 cc water and 1.8 gr = (600×0.3/100) friction reducer were added to 600 gr Portland Cement. Composition was mixed for 45 sec – 1 min then poured into the isolated container. Temperature behavior was observed during 24 hours and following figures were obtained for 0.3, 0.9 and 1.0 per cent friction reducer BWOC.

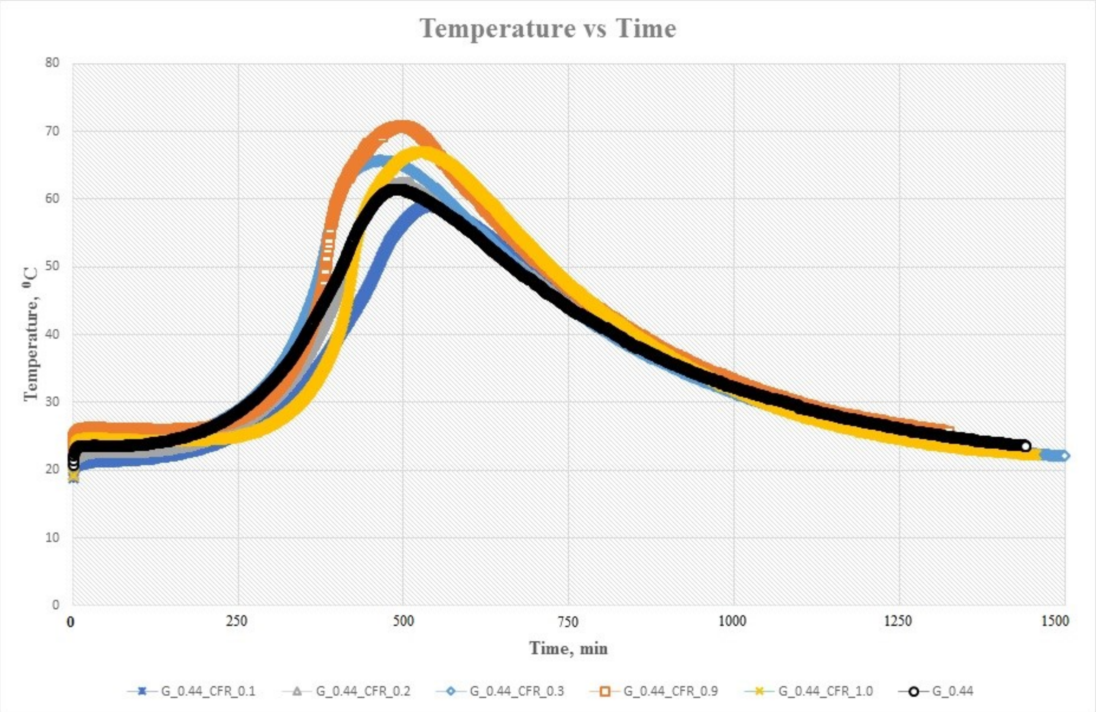

Figure 5.2: Heat of hydration of the cement slurry with friction reducers.

There are some striking similarities and some noticeable differences on the behavior of the cement slurry. The maximum temperature increased for each sample and as increasing weight of fluid – loss additive caused decrease in the temperature. Humps slightly slipped to the left side and temperature went up over 70 ^{0}C due to added fluid – loss agent. Furthermore, temperature track for the samples were recorded as CFR_0.1 climbed maximum at 59 ^{0}C, CFR_0.2 at 62.5 ^{0}C and CFR_0.3 at 65.7 ^{0}C. Maximum temperature among CFR samples observed at the CFR_0.9 sample by 70.8 ^{0}C. Then a dramatic decrease was seen in behavior of CFR_1.0 by 67 ^{0}C.

Time length also differs for each sample. 8 hours 58 minutes recorded for CFR_0.1 for reaching 59 ^{0}C, 8 hours 15 minutes for CFR_0.2 and 7 hours 42 minutes for CFR_0.3. Time duration until reaching peak temperature was 8 hours 15 minutes in CFR_0.9 sample. More or less same tendency was monitored for these samples during the experiment. 4 - 5 hours were spent for Dormancy period in each sample and maximum heat generations occurred in Stages III and IV. In these experiments it was surveilled that dormancy period ended lately whereas it was shorter in the pure cement and water composition. Base temperature was 20^{0}C and maximum temperature difference corresponds CFR_0.9 by 50.8 ^{0}C. Steady decrease was observed after hydration ended and approximately 16 hours were needed to get beginning temperature which is similar case as previous experiment.

Temperature difference was 11.8 ^{0}C between highest and lowest maximum temperature in the tests. Black colored graphic shows the temperature behavior of 600 gr cement and 264 cc water. Comparison shows CFR is dominant in temperature change when it is used in cement slurry.

Following Figure 5.3 illustrates effect of fluid – loss control agent in the cement slurries and temperature change alongside time. Experiments were performed at 10 different concentrations, starting from 0.1 % BWOC up to 1.0%. Slurries constituted fluid – loss additive at various amounts, 600 gr cement and 264 cc water.

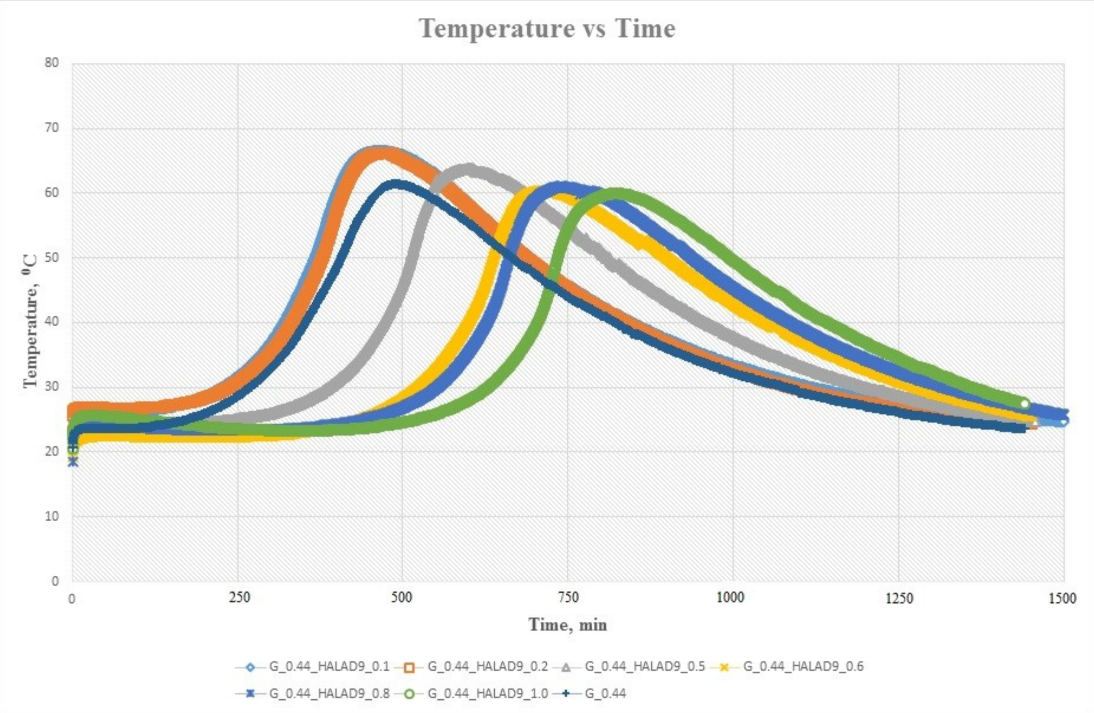

Figure 5.3: Heat of hydration of the cement slurry with fluid – loss additives.

It is obviously seen from the graphics that Halad9 strongly affect the properties of the cement slurry. The length of hydration time increased significantly after being added fluid – loss additive into the composition. Highest temperatures were seen at concentrations of 0.1% BWOC and 0.2% BWOC by 66.5 and 66.2 ^{0}C respectively. Halad9_0.1 and Halad_0.2 reached their maximum value almost at the same time, 7 hours 45 minutes later. Very short dormancy period was recorded for both samples. Results showed that roughly 4 hours were enough to start to hydration process at concentrations of 0.1 and 0.2.

Humps of other samples slipped notably to the right side. Reaching maximum temperature took more time in comparison with Halad9_0.1 and Halad9_0.2. Cement slurry at 0.5 % concentration started to hydration nearly 4 hours 45 minutes later where at that point dormancy period ended. After that time heat liberation accelerated until peak point of temperature. This process lasted 5 hours 30 minutes and maximum temperature recorded at 63.8 ^{0}C. In total, 9 hours 57 minutes were needed to come this point. During 15 – 16 hours after peak temperature, gradual lowering was monitored until base temperature.

Longest dormancy period was remarked for the concentrations at 0.6, 0.8 and 1.0 percent. These results can explain that addition of fluid – loss agent at these fractions can extend the pumpability and transferability of the slurry. 6 hours 20 minutes later since slurries were prepared heat generation started in these compositions. Top values of temperatures at these concentrations remarked by 60.4 ^{0}C at 0.6%, 61 ^{0}C at 0.8% and 59.9 ^{0}C at 1.0%. More than 13 hours needed to hit the peak temperature point at the concentration of 1.0% which is the longest time among these samples.

In the following figures, friction reducer and fluid – loss additive were added together in the cement slurries. Figure 5.4 illustrated that the fraction of the friction reducer was kept at 0.1% BWOC while the amount of fluid – loss additive varied from 0.1 BWOC up to 1. The weight of cement was taken 600 gr and 264 cc water used to prepare slurry.

In the Figure 5.4, only 4 different concentrations were taken for the explanation. Graphics obtained from other samples were given in the APPENDIX A.

Almost same behaviors were monitored for all samples and maximum temperatures did not exceed 70 ^{0}C threshold during hydration. The highest temperature was recorded at the CFR_0.1_Halad9_0.4 composition, by 67.3 ^{0}C. This temperature was obtained after 8 hours 41 minutes experiment began. Samples Halad9_0.7, Halad9_0.8 and Halad9_0.1 at fixed CFR_0.1 concentration followed each other at the same intervals. Temperature change was downward trend where 66.4 ^{0}C recorded for Halad9_0.7, 65.6 ^{0}C and 64.5 ^{0}C for 0.8 and 0.9% concentrations respectively. As fluid – loss agent increased hydration delayed by time. 10 hours 14 minutes duration was enough to reach peak at 0.7% fluid - loss concentration, 10 hours 57 minutes at 0.8% and 11 hours 56 minutes at 0.9%.

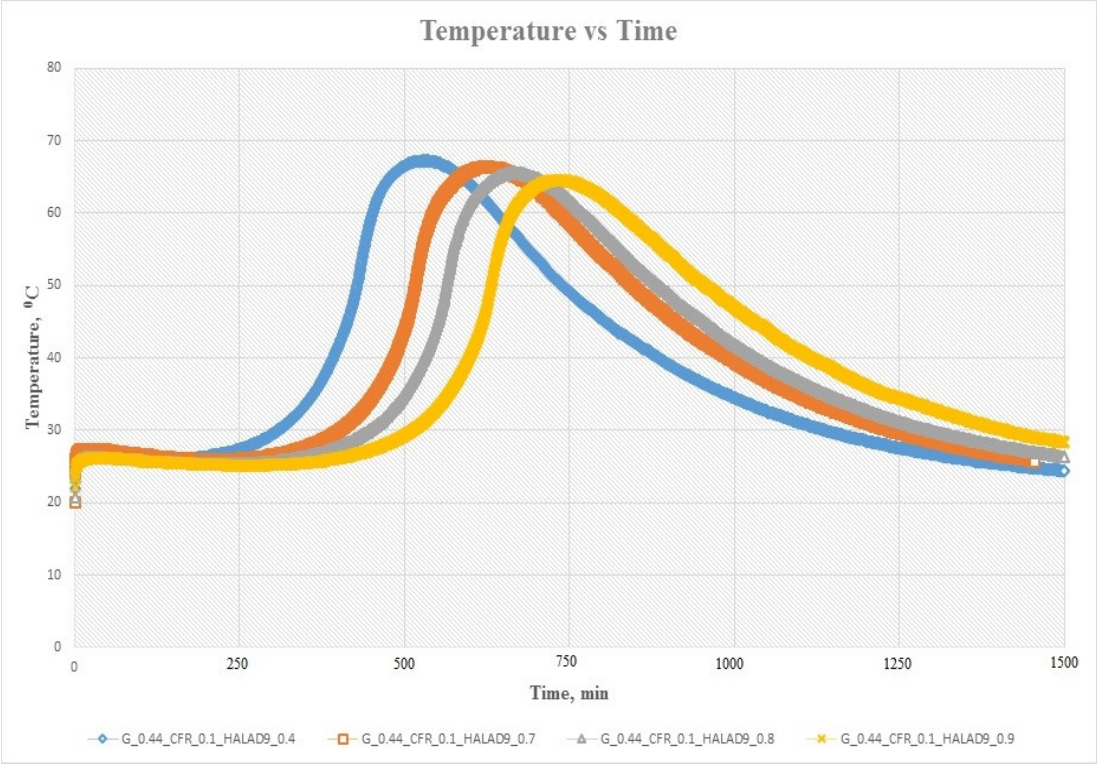

Figure 5.4: Heat of hydration of the cement slurry at the CFR concentration of 0.1 % BWOC and different fraction of Halad9 mixtures.

Almost same behaviors were monitored for all samples and maximum temperatures did not exceed 70 ^{0}C threshold during hydration. The highest temperature was recorded at the CFR_0.1_Halad9_0.4 composition, by 67.3 ^{0}C. This temperature was obtained after 8 hours 41 minutes experiment began. Samples Halad9_0.7, Halad9_0.8 and Halad9_0.1 at fixed CFR_0.1 concentration followed each other at the same intervals. Temperature change was downward trend where 66.4 ^{0}C recorded for Halad9_0.7, 65.6 ^{0}C and 64.5 ^{0}C for 0.8 and 0.9% concentrations respectively. As fluid – loss agent increased hydration delayed by time. 10 hours 14 minutes duration was enough to reach peak at 0.7% fluid - loss concentration, 10 hours 57 minutes at 0.8% and 11 hours 56 minutes at 0.9%.

Different behaviors of the hydration deceleration were observed in these experiments. Whereas the hydration acceleration was quicker than deceleration at the concentration of 0.4%. Heat liberation started nearly 5 hours 36 minutes later at the Halad9_0.7 and 0.8, but 6 hours 40 minutes later at Halad9_0.9.

However, after the highest temperatures being reached in the samples normal rate of decelerations were observed during more or less 15 hours for each composition.

6.9 ^{0}C temperature difference was obtained between the highest and lowest temperature points.

In the next Figure 5.5, the graphics were obtained at the concentrations of CFR 0.2% BWOC and Halad9 mixtures ranging 0.1 up to 1.0% BWOC.

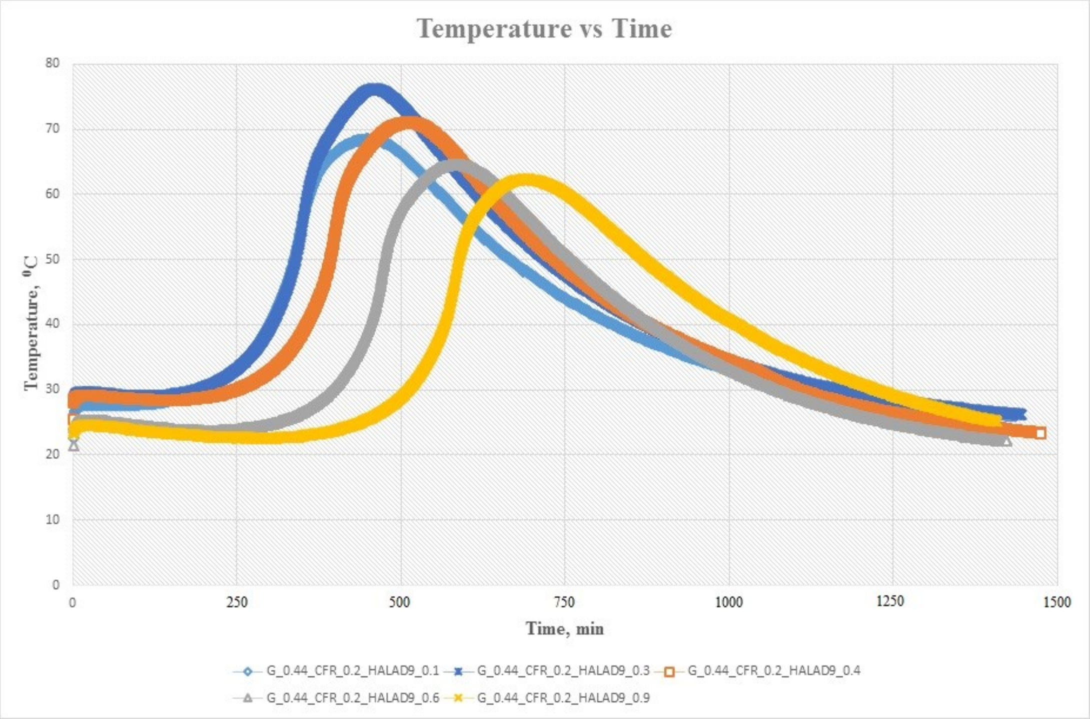

Figure 5.5: Heat of hydration of the cement slurry at the CFR concentration of 0.2 % BWOC and different fraction of Halad9 mixtures.

Results from these experiments are similar of the results from CFR_0.1_Halad9 compositions, however there are still some differences. At the first 4 samples maximum temperatures were around 70 degrees Celsius and at the concentration of Halad9_0.3 the degree was the highest by 76.3 ^{0}C. Halad9_0.3 climbed that point by following maximums of Halad9_0.1 and Halad9_0.2 by 68.5 ^{0}C and 69.7 ^{0}C respectively, whilst Halad9_0.4 followed them by descending at 71.1 ^{0}C. Then maximum temperatures followed downward trend: 64.6 ^{0}C at the concentration 0.6% BWOC and 62.3 ^{0}C at the 0.9%.

7 hours 8 minutes time was needed after composition poured in the container to reach peak point at the Halad9_0.3 and 8 hours 25 minutes was enough to Halad9_0.4 to do so. As increase the amount of fluid – loss additive in the cement slurry the time lapse until maximum temperatures extended as well. Longest time lapses were recorded for

Halad9_0.9 and Halad9_1.0 by having 11 hours 20 minutes and 11 hours 39 minutes correspondingly.

Furthermore, dormancy period lasted roughly 3 hours and half at the first 3 samples. Heat liberation performed quickly and mounted in a short time to the top. It means placing these compositions in the wells can be problematic due to their hardening time. In the rest of other samples initial setting began and/or Dormancy period finished 4 hours later after beginning the experiment. The rate of heat acceleration at the concentrations of 0.4%, 0.6% and 0.9% BWOC was slower compare than compositions at 0.1 and 0.3%. An increase at the amount of fluid – loss additive and the constant amount of friction reducer in the slurry caused to delay heat liberation during setting time. The length of time from beginning until the peak was 9 hours 38 minutes at the 0.6% fluid – loss agent by weight of cement in the cement slurry. As mentioned earlier, longest time lapses were seen at Halad9_0.9 and Halad9_1.0. Time till the initial temperatures also were long enough in the samples. For example, though 21 hours was required for the cement slurry having Halad9_0.3 in it, the figure for Halad9_0.9 was close to 24 hours.

Contrast between the highest and lowest temperatures were remarked by 14 ^{0}C.

Another set of experiments were held at the constant volume of friction reducer and varied amount of fluid – loss additives in the system. 2.4 gr (= 0.4×600/100) dispersant, Halad9 at the different 10 concentrations – starting from 0.1% BWOC up to 1.0%, 600 gr G class of Portland cement and 264 cc water were mixed and poured into the special container for the purpose of tracing temperature changes during 24 hours.

Graphics in these experiments as shown in the Figure 5.6 differ from others since they follow each other with the same manner in upward and downward trends. The highest temperatures were below 70 ^{0}C and as increasing fluid – loss agent in the cement slurry at the fixed volume of dispersant leaded to downward trend at the temperatures. On the other hand, fluid – loss additive also influenced to the time to start hydration.

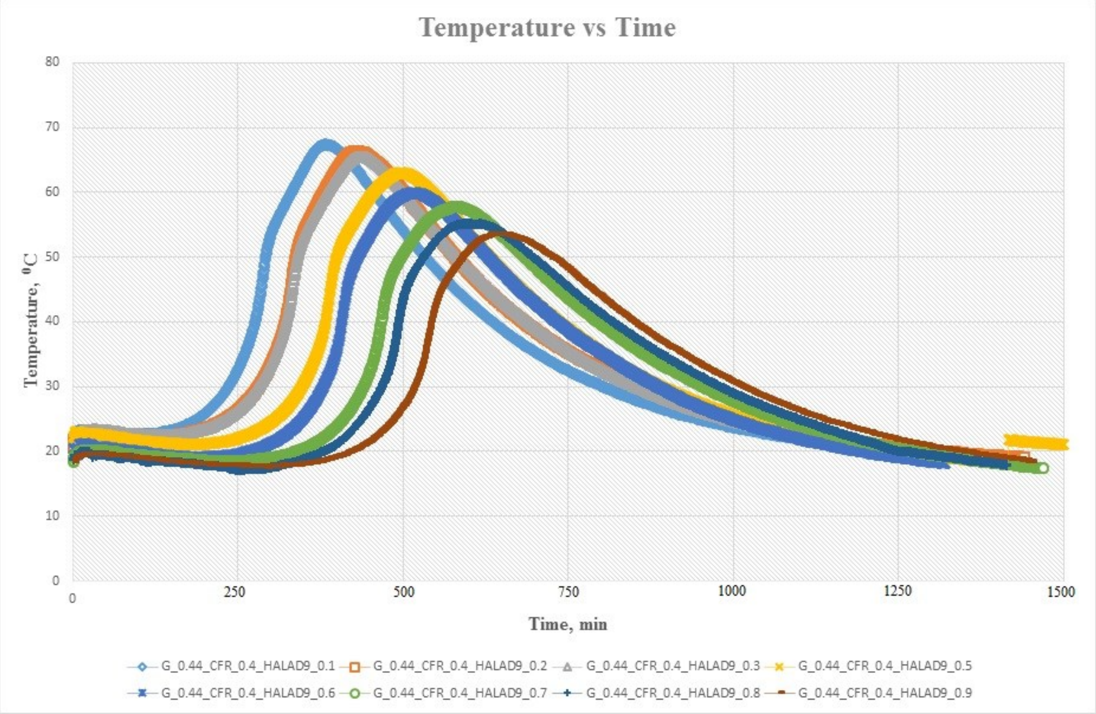

Figure 5.6: Heat of hydration of the cement slurry at the CFR concentration of 0.4 % BWOC and different fraction of Halad9 mixtures.

The highest temperature among these samples was recorded at the sample including 0.3% CFR and 0.1% Halad9 BWOC in the composition. CFR_0.4_Halad9_0.1 peaked at 67.4 ^{0}C during considerably short time, 6 hours 19 minutes. Dormancy period was the shortest at this sample and nearly 3 hours 40 minutes later reactions entered Stage III where hydration started and heat generated from the cement slurry. Heat acceleration occurred until the peak point during 2 hours 30 minutes time period. Initial strength/stress development took more than 8 hours at the Stages II and III together. The hydration deceleration which starts from the peak point until the base temperature lasted 18 hours 38 minutes. Strength/stress development prevailed about 12 hours 15 minutes at this particular sample.

Samples having higher content of fluid – loss additive put lower temperatures in a row. For example, 66.3 ^{0}C and 65.5 ^{0}C were surveilled at the composition having 0.2% and 0.3% Halad9 respectively. In contrast, heat generation delayed as increase of additive. As clearly be seen humps went to right side since the amount of Halad9 enlarged. The lowest maximum temperature was traced at the Halad9_0.9 sample by 53.6 ^{0}C. Approximately 11 hours 35 minutes time spent to strength/stress development process at the CFR_0.4_Halad9_0.9 sample.

Difference between the highest and lowest temperatures was 13.8 ^{0}C.

In the figures Figure 5.7 and Figure 5.8 friction reducer samples particularly at the fixed concentrations of 0.6% and 0.8% by weight of cement were compared. The weight of fluid – loss additive varied from 0.1% up to 1.0% BWOC in the cement slurry at the fixed volume of dispersant samples.

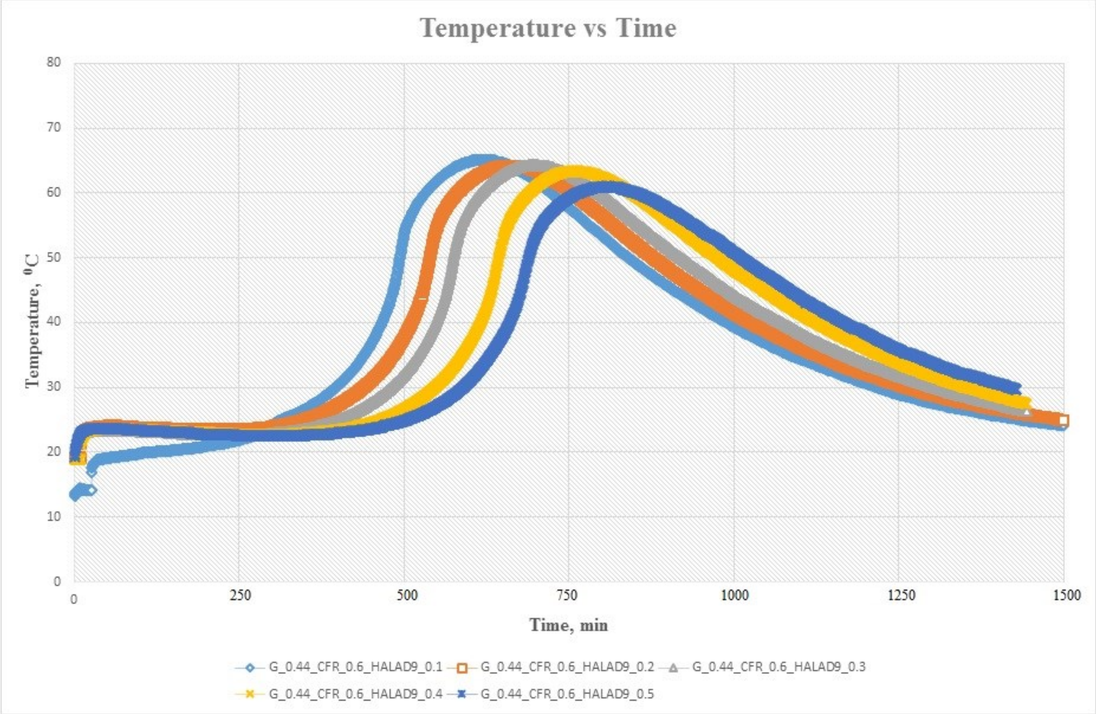

Figure 5.7: Heat of hydration of the cement slurry at the CFR concentration of 0.6 % BWOC and different fraction of Halad9 mixtures.

It can be inferred from the graphs that less amount of fluid – loss additive in the cement slurry lead to higher degree of temperatures which could give hint that at high temperatures dispersant predominantly cause to heat generation during chemical reactions. As a result, Halad9_0.1 peaked by 65.1 ^{0}C at the 0.6% CFR concentration and 68.7 ^{0}C at 0.8% BWOC. Decline were observed in both cement slurries after that maximum points and temperatures decreased moderately at the concentration of 0.6% dispersant samples and significantly at the other experiments.

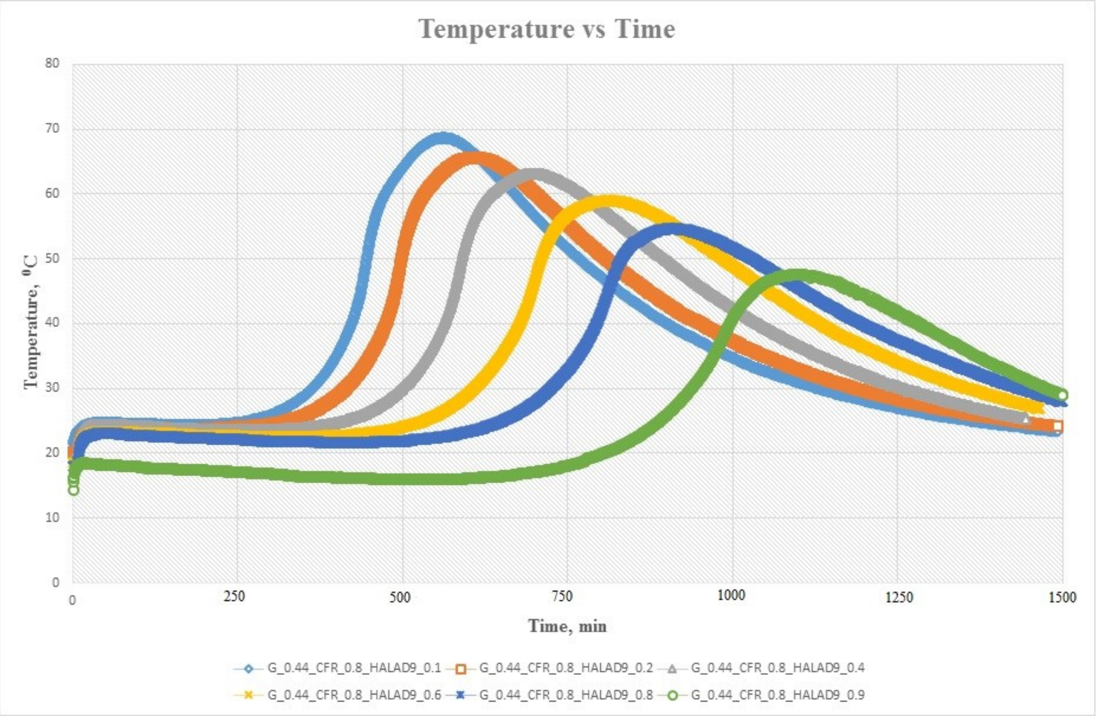

Figure 5.8: Heat of hydration of the cement slurry at the CFR concentration of 0.8 % BWOC and different fraction of Halad9 mixtures.

47.5 ^{0}C was the lowest temperature when cement and water mixed with 0.8 percent friction reducer and 0.9 percent fluid – loss agent by weight of cement. The lowest figure was 57 ^{0}C for 0.6% CFR and 1.0% Halad9 in the cement slurry.

The length of dormancy periods did not change severely as Halad9 increase up to 0.6% in the compositions including 0.6% CFR by weight of cement. Average time length remarked approximately 5 hours 50 minutes and during the first 4 hours in the Stage II and III hydration accelerations occurred and temperatures peaked. Normal rate of hydration decelerations for this particular concentration monitored as well. In the samples having 0.7-0.8-0.9-1.0 % Halad9 BWOC, humps slipped to the right noticeably as Halad9 raise at the fixed volume of CFR. Initial set points came upon 13 hours later since slurries were settled in the isolated container. The time length of heat decelerations also was abnormally long, the figures for decelerations were more than 15 hours at the last 4 samples. Temperature contrast was 8.1 ^{0}C between the peak points.

In addition to the samples at the concentration of 0.8% CFR by weight of cement, it can be deduced that Halad9 caused delay in the chemical reactions. Heat generations started at later time as fluid – loss agent increase in compositions. Moreover, Dormancy Periods extended and the longest period was seen by 12 hours and half in the sample having 1.0% Halad9. Heat deceleration time was recorded at least 11 hours 16 minutes. Difference between the highest and lowest temperatures was 18.9 ^{0}C.

In the APPENDIX A all the obtained graphics from the different experiments has been given. Observations were performed at the fixed friction reducer concentrations that range from 0.1% by weight of cement up to 1.0%. For each fixed concentration 10 different amount of fluid – loss additive was added. In total more than 100 experiments were completed where 10 set of tests and 10 different samples per set were fulfilled at the ambient conditions.

As it can be seen from the graphics that increment in the amount of fluid – loss additive in the cement slurries leads to delay heat generation. Specifically, heat generation started in the experiments after more or less 4 – 6 later when slurries were placed in the container. As stated, having high concentration of fluid – loss agent in the mixture reasoned to start heat generation lately. The longest time until heat liberation was in the sample having 0.9% CFR and 1.0% HALAD9 by 14 hours 36 minutes. Hydration acceleration occurred during first 2 – 3 hours and samples reached their maximum temperatures. Maximum heat generation were observed at the 0.3% CFR concentration by 76.7 ^{0}C at Halad9_0.1, duration until the peak was the shortest by 6 hours 14 minutes. Generally, lowest maximum temperatures were surveilled at the high concentrations of Halad9 agent in the compositions. The minimum figure was 45.5 ^{0}C in the sample of CFR_0.9_HALAD9_0.9.

Strength/stress development times which occurs in the Stages II and III were roughly 10 – 14 hours. In some experiments it was seen that fluid – loss additive could push the strength/stress development to the later hours. Especially CFR_0.8 and CFR_0.9 tests showed the reverse effect of fluid – loss agent.

Temperature contrast between the highest and lowest recorded point within sets also varied markedly. The biggest temperature contrast was monitored in the samples having 0.8% CFR by weight of cement by 21.2 ^{0}C. Interesting fact is that the smallest temperature difference was surveilled at the concentration of 1.0 % CFR mixtures by 5.1 ^{0}C.

Considering experimental results, it can be inferred that the additives have significant effect on increasing the setting temperature of well cement. Such situation must be considered during well cement design. As a result of this temperature increase, premature gelation, fractures on cement matrix and bonding problems might occur and might result in deteriorating the isolation duty of well cement.

5.1 Statistical Evaluation

Regression analysis is a statistical approach to estimate the relationship between variables. Linear regression computes an equation which minimizes the distance between the fitted line and all of the data points. Technically, ordinary least squares (OLS) regression minimizes the sum of the squared residuals.

R-squared is a statistical measure of how close the data are to the fitted regression line. It is also known as the coefficient of determination, or the coefficient of multiple determination for multiple regression.

The definition of R-squared is fairly straight-forward; it is the percentage of the response variable variation that is explained by a linear model. Or:

R-squared = Explained variation / Total variation

R-squared is always between 0 and 100%. 0% indicates that the model explains none of the variability of the response data around its mean. 100% indicates that the model explains all the variability of the response data around its mean (Url-14).

In the Figure 5.9 the results of regression analysis applied to all experimental results is shown. Regression analyze has been applied to temperature changes when temperature was maximum and base temperature was 20 ^{0}C.

It is obviously seen from the figure that the value of R – squared is small. Regression has been done among the maximum temperatures of all samples. It is not possible to predict the maximum temperature according to given amount of friction reducer and fluid – loss agent in the cement slurry. R squared is equal to approximately 0.48 or 48% which is 52 per cent less than maximum regression value. Although the experimental results exhibit that the amount of additives affects the exothermic reaction, the regression analyses did not provide a linear relation.

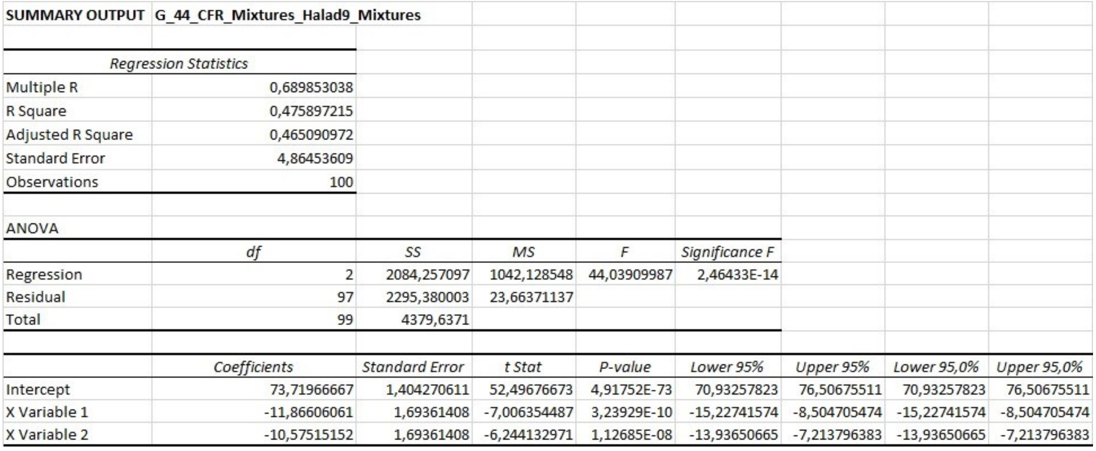

SUMMARY OUTPUT G_44_CFR_Mixtures_Halad9_Mixtures

Regression Statistics	
Multiple R	0,689853038
R Square	0,475897215
Adjusted R Square	0,465090972
Standard Error	4,86453609
Observations	100

ANOVA

	df	*SS*	*MS*	*F*	*Significance F*
Regression	2	2084,257097	1042,128548	44,03909987	2,46433E-14
Residual	97	2295,380003	23,66371137		
Total	99	4379,6371			

	Coefficients	*Standard Error*	*t Stat*	*P-value*	*Lower 95%*	*Upper 95%*	*Lower 95,0%*	*Upper 95,0%*
Intercept	73,71966667	1,404270611	52,49676673	4,91752E-73	70,93257823	76,50675511	70,93257823	76,50675511
X Variable 1	-11,86606061	1,69361408	-7,006354487	3,23929E-10	-15,22741574	-8,504705474	-15,22741574	-8,504705474
X Variable 2	-10,57515152	1,69361408	-6,244132971	1,12685E-08	-13,93650665	-7,213796383	-13,93650665	-7,213796383

Figure 5.9: Screenshot of the result of regression analysis applied to all data.

On the other hand, regression also has been performed for each sets that friction reducer is kept at the same concentration in the composition while the amount of fluid – loss additive is raised from 0.1% by weight of cement up to 1.0%. Results are tabulated in the following Table 5.1.

Table shows R squared values for each set of samples. The highest values are obtained at the friction reducer concentrations of 0.4, 0.5 and 0.8. The values for these set of samples are greater than 90%. Since results are higher than graphics followed almost same or familiar track during the heat of hydration. Highest R squared values belong to the composition of 0.5 % CFR and Halad9 mixtures, by 0.956 or 95.6%. CFR_0.4 set of samples follows CFR_0.5 by 0.955 or 95.5%. Lowest value of R – squared is obtained for CFR_0.7 samples by 0.106 or 10.6%. More detailed in APPENDIX B.

Table 5.1: Results of regression for each set of experiment.

Sample Code	R squared values
G_44_CFR_0,0_Halad9_Mixtures	0,455
G_44_CFR_Mixtures_Halad9_0,0	0,605
G_44_CFR_0,1_Halad9_Mixtures	0,449
G_44_CFR_0,2_Halad9_Mixtures	0,520
G_44_CFR_0,3_Halad9_Mixtures	0,880
G_44_CFR_0,4_Halad9_Mixtures	0,955
G_44_CFR_0,5_Halad9_Mixtures	0,956
G_44_CFR_0,6_Halad9_Mixtures	0,890
G_44_CFR_0,7_Halad9_Mixtures	0,106
G_44_CFR_0,8_Halad9_Mixtures	0,934
G_44_CFR_0,9_Halad9_Mixtures	0,593
G_44_CFR_1,0_Halad9_Mixtures	0,574

6. CASING DESIGN APPLICATION

Temperature changes have pivotal role in the designing of casing during completion operations. Casings are affected due to several factors when they placed in the well. Pressure and temperature changes are one of these kind of factors. Changes in temperature and pressure may cause to extra loads such a compressive and tensile stresses once casing is placed. Particularly, at the early time of cement setting temperature raises significantly. Temperature jumps in the cement slurry impact the casing design. To see the effects of temperature changes in the casing design it is relevant to choose three different type of casings and estimate loads generated from the temperature.

Strains can arise regarding to temperature change without causing a stress or temperature change can cause a stress without a strain. In the following Figure 6.1 two different type of casing strings were illustrated.

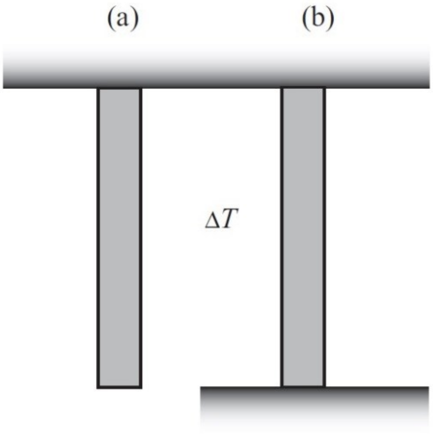

Figure 6.1: Thermal effects (a) suspended bar, (b) constrained bar (Byrom, Ted G., 2007

Generated certain amount of ΔT in the wellbore may cause to expand and get longer casing strings as shown in the Figure 6.1 – a. Casing string is only constrained at the top end and free at the bottom end. Temperature change possibly may cause to expansion in this kind of casing design. However, same temperature change can generate stress in this casing string where both ends are constrained as shown in the Figure 6.1 – b. To understand thermal effects in casing, let us apply temperature change for casing string illustrated in Figure 6.1 – b. For simplicity it is assumed that constant temperature throughout the length of casing string dominates, casing string is truly vertical – no any inclination, no any friction in the bore hole. The casing was hanging by its own weight before the lower end was constrained. After being assumed these assumptions, axial stress at any point will be calculated in the direction of z as follows:

$$\sigma_z = \sigma_o + E(\varepsilon_z - \alpha\Delta T) = \frac{F_o}{A_t} - \left(\frac{\omega}{A_t}\right)z - E\alpha\Delta T \tag{2}$$

Here σ_z is uniaxial stress in z – direction, σ_o is initial stress, ε_z is uniaxial stress due to change in depth, ΔT is temperature change, E is Young's elastic modulus, A_t is the cross – sectional area of the metal bar, α is the thermal expansion coefficient.

If casing string is constrained then $\varepsilon_z = 0$ in Equation (2).

In the above equation ω is nominal weight (Ib_m/ft) and α is the thermal expansion coefficient and its value in calculations is 0.69×10^{-5} [°F^{-1}]. F_o is tensile force at the top:

$$F_o = \omega \times l = \ [Ib_f] \tag{3}$$

Our general equation modifies and become as follow:

$$\sigma_z = \frac{F_1}{A_{t_1}} - \left(\frac{\omega}{A_{t_1}}\right)z - E\alpha\Delta T \tag{4}$$

After all, it is easy to estimate thermal loads by using Equation (4) in the casing design. Highest temperatures were recorded at the concentrations of friction reducer 0.2% by weight of cement and in our calculations 73 ^{0}C will be taken. Since base temperature is assumed 20 ^{0}C, then ΔT will be equal to 53 ^{0}C.

First of all, it would be useful to see how temperature change affect to K – 55 type of casing. Diameter of casing is 7″ and its nominal weight is 20 (Ib_m/ft).

$$\sigma_{z_1} = \frac{F_1}{A_{t_1}} - \left(\frac{\omega}{A_{t_1}}\right) z - E\alpha\Delta T$$

$$= \frac{60000\, Ib_f}{38.48\, in^2} - \left(\frac{20\frac{Ib_m}{ft}}{38.48\ in^2} \times 0\right) - 30 \times 10^6 \times (0.69 \times 10^{-5}) \times 53 \tag{5}$$

$$= 1560 - 10971 = -9411\ {}^{Ib_f}/_{in^2}$$

In Equation (5), F_1 is tensile force for and its value at 3 000 ft long casing string is:

$$F_1 = \omega \times l = 20 \times 3000 = 60\,000\ [Ib_f] \tag{6}$$

However, axial stress at the top was found as $\sigma_z = -9411\, psi$ by Equation (4) but axial stress at the 3000 ft. will be found as follows:

$$\sigma_{z_1} = \frac{F_1}{A_{t_1}} - \left(\frac{\omega}{A_{t_1}}\right) z - E\alpha\Delta T$$

$$= \frac{60000\, Ib_f}{38.48\, in^2} - \left(\frac{20\frac{Ib_m}{ft}}{38.48\ in^2} \times 3000\right) - 30 \times 10^6 \times (0.69 \times 10^{-5}) \tag{7}$$

$$\times 53 = 1560 - 1560 - 10971 = -10971\ {}^{Ib_f}/_{in^2}$$

As be seen from the Equation (7) axial stress at the bottom increased, $\sigma_{z_2} = -10971\, psi.$

Negative sign shows that casing is in compression, while positive value stands for tension. So, at the early times of cement setting K – 55 type of casing with 7″ diameter and 20 (Ib_m/ft) nominal weight is in compression at the top and bottom.

In the following calculations temperature change will be constant at 53 ^{0}C and the length of casing string will increase up to 10 000 ft. for this particular case.

Tensile force will increase as:

$$F_2 = \omega \times l = 20 \times 10\,000 = 200\,000\ [Ib_f] \tag{8}$$

And axial stress at the top will be:

$$\sigma_{z_2}=\frac{F_2}{A_{t_1}}-\left(\frac{\omega}{A_{t_1}}\right)z-E\alpha\Delta T=$$

$$=\frac{200000\,Ib_f}{38.48\,in^2}-\left(\frac{20\frac{Ib_m}{ft}}{38.48\ in^2}\times 0\right)-30\times 10^6\times(0.69\times 10^{-5})\times 53 \tag{9}$$

$$=5197-10971=-5774\ {}^{Ib_f}/_{in^2}$$

Axial stress at the bottom of the well where length of string is 10 000 ft. (Eq.10) will be given as follows:

$$\sigma_{z_2}=\frac{F_2}{A_{t_1}}-\left(\frac{\omega}{A_{t_1}}\right)z-E\alpha\Delta T$$

$$=\frac{200\,000\,Ib_f}{38.48\,in^2}-\left(\frac{20\frac{Ib_m}{ft}}{38.48\ in^2}\times 100\,000\right)-30\times 10^6\times(0.69*10^{-5}) \tag{10}$$

$$\times 53=5197-5197-10971=-10971\ {}^{Ib_f}/_{in^2}$$

Axial stress at the bottom of the casing was equal to the – 10971 psi. It can be explained that depth did not change the value of compression at the bottom while it affects to the stress at the surface. Axial stress has changed due to change in the length of casing and its value increased noticeable from –9411 psi to –5774 psi. However, axial stress at the bottom of the casing has not changed and stayed constant at – 10971 psi.

To see the effect of temperature, in the following calculations casing length will be constant at 3 000 ft. while temperature change will decrease from 53 ^{0}C to 40 ^{0}C for K – 55 type of casing having 7″ diameter and 20 (Ib_m/ft) nominal weight.

So axial stress at the top will be as follows:

$$\sigma_{z_1}=\frac{F_1}{A_{t_1}}-\left(\frac{\omega}{A_{t_1}}\right)z-E\alpha\Delta T$$

$$=\frac{60000\,Ib_f}{38.48\,in^2}-\left(\frac{20\frac{Ib_m}{ft}}{38.48\ in^2}\times 0\right)-30\times 10^6\times(0.69\times 10^{-5})\times 40 \tag{11}$$

$$=1560-8280=-6720\ {}^{Ib_f}/_{in^2}$$

And at the bottom of casing:

$$\sigma_{z_2} = \frac{F_1}{A_{t_1}} - \left(\frac{\omega}{A_{t_1}}\right) z - E\alpha\Delta T$$

$$= \frac{60000\, Ib_f}{38.48\, in^2} - \left(\frac{20 \frac{Ib_m}{ft}}{38.48\ in^2} \times 3000\right) - 30 \times 10^6 \times (0.69 \times 10^{-5}) \tag{12}$$

$$\times 40 = 1560 - 1560 - 8280 = -8280\, {}^{Ib_f}/_{in^2}$$

It is clearly seen that decrease in the temperature change caused to increase at the axial stress. At the surface value of the stress is – 6720 psi but at the bottom it equals to – 8280 psi. Comparison with the temperature change by 53 ^{0}C shows that compressive stress decreased and tensile stress increased at the same depth of the well.

Calculations for other cases where the diameter of the casing increased and other nominal weights are used will be given in the following tables.

Table 6.1 shows temperature effects on the K – 55 type of casing. It is obvious that temperature change at the early times of cement setting has significant impact on the casing.

Axial stresses at the bottom do not change due to change of casing diameter or nominal weight, only it depends on temperature change. Relationship between temperature drop and axial stress at the bottom of the casing is inversely proportional. Stress at the 3000 ft. depth is –10971 psi regarding to 53 ^{0}C temperature change. This figure is constant for whole K – 55 type casing products unless temperature change is different. However, axial stress at the top depends on nominal weight of the casing, length of the string and temperature change at the same time. When temperature drop is constantly 53 ^{0}C, as increase of nominal weight the axial stress at the top increases or in other words compression decreases but tension increases. Moreover, length of the casing string has also severe impact at the values of axial stress. The increment in the length of casing cause to increase of tension at the top.

Table 6.1: Thermal load results of K – 55 grade casing at the three different temperature differences.

K-55 [Ib/ft]	$\Delta T = 53$						$\Delta T = 40$						$\Delta T = 25$					
↓	0 ft	3000 ft	0 ft	10000 ft	0 ft	15000 ft	0 ft	3000 ft	0 ft	10000 ft	0 ft	15000 ft	0 ft	3000 ft	0 ft	10000 ft	0 ft	15000 ft
20	-9411.93	-10971	-5774.1	-10971	-3176.66	-10971	-6720.93	-8280	-3083.1	-8280	-484.66	-8280	-3615.93	-5175	21.8961	-5175	2620.344	-5175
23	-9178.07	-10971	-4994.57	-10971	-2006.35	-10971	-6487.07	-8280	-2303.57	-8280	684.65	-8280	-3382.07	-5175	801.43	-5175	3789.646	-5175
26	-8944.21	-10971	-4215.57	-10971	-837.053	-10971	-6253.21	-8280	-1524.04	-8280	1853.95	-8280	-3148.21	-5175	1580.97	-5175	4958.95	-5175
36	-9486.66	-10971	-6023.21	-10971	-3549.32	-10971	-6795.66	-8280	-3332.21	-8280	-858.31	-8280	-3690.66	-5175	-227.21	-5175	2246.68	-5175
40	-9321.74	-10971	-5473.46	-10971	-2724.69	-10971	-6630.74	-8280	-2782.46	-8280	-33.69	-8280	-3525.74	-5175	322.54	-5175	3071.31	-5175
54.5	-9807.3	-10971	-7092.01	-10971	-5152.51	-10971	-7116.3	-8280	-4401.01	-8280	-2461.51	-8280	-4011.3	-5175	-1296.01	-5175	643.49	-5175
61	-9668.51	-10971	-6629.37	-10971	-4458.56	-10971	-6977.51	-8280	-3938.37	-8280	-1767.56	-8280	-3872.51	-5175	-833.374	-5175	1337.44	-5175
68	-9519.05	-10971	-6131.16	-10971	-3711.23	-10971	-6828.05	-8280	-3440.16	-8280	-1020.23	-8280	-3723.05	-5175	-335.155	-5175	2084.77	-5175

Comparing results between the temperatures at 53 ^{0}C and 40 ^{0}C give information that temperature increase puts more thermal loads in the casing string. As a results the compression increases. Figures show that the magnitude of the compressive stress due to 25 ^{0}C temperature change is –3616 psi for 3 000 ft casing string at the surface. However, this figure decreases remarkably due to increase in temperature change from 25 ^{0}C up to 40 ^{0}C, by –3105 psi. At 53 ^{0}C the temperature difference the axial stress at the top for this particular case becomes very high by – 9411 psi.

Highest compression is observed at the surface by – 9487 psi when diameter of the casing string is 13⅜ ″ and nominal weight 54.5 (Ib_m/ft) having 53 ^{0}C temperature drop and highest axial stress is – 10971 psi at the bottom of casing string when temperature drop is 53 ^{0}C.

Furthermore, axial stresses have been determined for another type of casing, namely C – 95. Axial stresses at the top of string and end of the string are determined by the same way of K – 55 samples do so. First of all, it would be useful to see how temperature change affects to C – 95 type of casing. Diameter of casing is 7″ and its nominal weight is 35 (Ib_m/ft).

$$\sigma_{z_1} = \frac{F_1}{A_{t_1}} - \left(\frac{\omega}{A_{t_1}}\right) z - E\alpha\Delta T =$$

$$= \frac{105000\, Ib_f}{38.48\, in^2} - \left(\frac{20\frac{Ib_m}{ft}}{38.48\ in^2} \times 0\right) - 30 \times 10^6 \times (0.69 \times 10^{-5}) \qquad (13)$$

$$\times 53 = 2729 - 10971 = -8242\ {}^{Ib_f}/_{in^2}$$

In Equation (12), $F_1 = \omega \times l$=35×3000=105000 [Ib$_f$] and axial stress at the top is – 8242 psi when temperature drop is 53 ^{0}C.

And at the bottom of the casing string the axial stress is equal to (Equation 13):

$$\sigma_{z_1} = \frac{F_1}{A_{t_1}} - \left(\frac{\omega}{A_{t_1}}\right) z - E\alpha\Delta T =$$

$$= \frac{105000\, Ib_f}{38.48\, in^2} - \left(\frac{20\frac{Ib_m}{ft}}{38.48\ in^2} \times 3000\right) - 30 \times 10^6 \times (0.69 \times 10^{-5}) \qquad (14)$$

$$\times 53 = 2729 - 2729 - 10971 = -10971\ {}^{Ib_f}/_{in^2}$$

Table 6.2: Thermal load results of C – 95 grade casing at the three different temperature differences.

C-95 [Ib/ft]	$\Delta T = 53$						$\Delta T = 40$						$\Delta T = 25$					
↓	0 ft	3000 ft	0 ft	10000 ft	0 ft	15000 ft	0 ft	3000 ft	0 ft	10000 ft	0 ft	15000 ft	0 ft	3000 ft	0 ft	10000 ft	0 ft	15000 ft
23	-9178	-10971	-4994	-10971	-2006	-10971	-6487	-8280	-2304	-8280	-685	-8280	-3382	-5175	801	-5175	3789	-5175
26	-8944	-10971	-4215	-10971	-837	-10971	-6253	-8280	-1524	-8280	1854	-8280	-3148	-5175	1580	-5175	4958	-5175
29	-8710	-10971	-3435	-10971	332	-10971	-6019	-8280	-744	-8280	3023	-8280	-2914	-5175	2360	-5175	6128	-5175
32	-8476	-10971	-2656	-10971	1501	-10971	-5785	-8280	35	-8280	4192	-8280	-2681	-5175	3140	-5175	7297	-5175
35	-8242	-10971	-1876	-10971	2670	-10971	-5551	-8280	814	-8280	5361	-8280	-2447	-5175	3920	-5175	8466	-5175
38	-8008	-10971	-1097	-10971	3840	-10971	-5318	-8280	1595	-8280	6531	-8280	-2213	-5175	4699	-5175	9636	-5175
40	-9321	-10971	-5473	-10971	-2724	-10971	-6630	-8280	-2782	-8280	-34	-8280	-3526	-5175	322	-5175	3071	-5175
43.5	-9177	-10971	-4992	-10971	-2003	-10971	-6486	-8280	-2301	-8280	688	-8280	-3381	-5175	803	-5175	3792	-5175
47	-9033	-10971	-4511	-10971	-1281	-10971	-6342	-8280	-1820	-8280	1409	-8280	-3237	-5175	1284	-5175	454	-5175
53.5	-9765	-10971	-3618	-10971	58	-10971	-6074	-8280	-927	-8280	2750	-8280	-2970	-5175	2177	-5175	5854	-5175
68	-9519	-10971	-6131	-10971	-3711	-10971	-6828	-8280	-3440	-8280	-1020	-8280	-3723	-5175	-335	-5175	2084	-5175
72	-9433	-10971	-5846	-10971	-3284	-10971	-6743	-8280	-3155	-8280	-593	-8280	3637	-5175	-50	-5175	2512	-5175

Result obtained for the bottom of C – 95 type of casing string is – 10971 psi which is the same figure with K – 55. In addition to results it can be commented that stresses are in compression at the both ends. Calculations are done for each product of C – 95 type of casing and tabulated in the Table 6.2.

From the Table 6.2 it is noticeable that highest figures for compression are obtained for the casing having 9⅝″ diameter and 53.5 (Ib_m/ft) nominal weight. –9765 is the highest axial stress at the top of the casing string regarding to 53 ^{0}C temperature change. As increasing the length of casing the axial stresses declined when the other features stayed constant for this particular case. Change of temperature substantially impacted to the compressive stress at the top of the casing bar. For instance, at the same length of string axial stresses increased from –9765 psi at ΔT=53 ^{0}C to – 2970 psi at ΔT=25 ^{0}C. Difference is nearly 6800 psi. Besides, at the lower temperatures in many applications, axial stresses jumped from the compression to tension due to change in the length. These tendency is seen among results at the 25 ^{0}C temperature difference.

Especially, at the depth of 10 000 and 15 000 ft, all stresses are at the top of casing string are in tension unlike at other temperature drops. It is commonly seen in all type of casings. Huge gap is observed at the C – 95 type of casing having 7″ diameter and 38 (Ib_m/ft) nominal weight. Whereas tension at the top is 9636 psi and however compression at the bottom is – 5175 psi regarding to 15 000 ft long bar.

Figures in the Table 6.2 demonstrate that when temperature difference getting lower then compression at the top of bar decreases while higher temperature changes cause to compressions.

Nominal weights also play an important role in compression and tension. At the top of the long casing bars the axial stress becomes higher for the casings which have lower nominal weights and majority is loaded by tensile stresses.

Finally, effects of temperature originated during the hydration of cement will be analyzed as follow. Like K – 55 and C – 95 types of casing, P – 110 type casing also shows familiar results (Table 6.3). Lower temperature changes keep the casing in tension at the top of string while bottom mostly feel compression. The highest figures for tension are seen at the casing which is 7″ diameter. Due to the length of the strings at ΔT=25 ^{0}C axial stresses vary from – 4959 psi up to 9636 psi, while at the end of the casing string stresses are – 5175 psi which is compressive stresses. In case, temperature difference would be raised to 40 ^{0}C still it is possible to see predominant tensile stresses at the top of the casing due to length of string unlike K – 55 and C – 95. Casings having 7″ diameter at the depth of 15000 ft. are in tension at the top. Minimum tensile stress at the top is 1853 while it goes up to 6531 psi.

Lowest axial stress can be seen at the casing which have heavier nominal weights. For example, 13⅜″ casing with 68 (Ib_m/ft) nominal weight showed maximum compressive stress by – 9515 psi.

To sum up, thermal loads usually lead to have more compression in the casing designing. To determine and predict thermal loads in the wells it is supposed to know the several factors in the wells. Major factor for the purpose of giving correct prediction about thermal loads is temperature change definitely. In these calculations the importance of the temperature change due to heat generation while hydration is clearly be seen. Results show that at the higher temperature drops casings become in compression at the both ends. However, other factors such as nominal weight, diameter and length of the casings may play an important role to predict thermal loads. Heat generation from the cement slurry in the well loads casings with higher stresses.

Table 6.3: Thermal load results of P – 110 grade casing at the three different temperature differences.

P–110 [Ib/ft]	$\Delta T = 53$						$\Delta T = 40$						$\Delta T = 25$					
↓	0 ft	3000 ft	0 ft	10000 ft	0 ft	15000 ft	0 ft	3000 ft	0 ft	10000 ft	0 ft	15000 ft	0 ft	3000 ft	0 ft	10000 ft	0 ft	15000 ft
26	-8944	-10971	-4215	-10971	-837	-10971	-6253	-8280	-1524	-8280	1853	-8280	-3148	-5175	1581	-5175	-4959	-5175
29	-8710	-10971	-3435	-10971	332	-10971	-6019	-8280	-744	-8280	3023	-8280	-2914	-5175	2360	-5175	6128	-5175
32	-8476	-10971	-2656	-10971	1501	-10971	-5785	-8280	35	-8280	4192	-8280	-2680	-5175	3140	-5175	7297	-5175
35	-8243	-10971	-1876	-10971	2671	-10971	-5551	-8280	814	-8280	5361	-8280	-2446	-5175	3920	-5175	8466	-5175
38	-8008	-10971	-1097	-10971	3840	-10971	-5318	-8280	1594	-8280	6531	-8280	-2212	-5175	4700	-5175	9636	-5175
43.5	-917	-10971	-4992	-10971	-2003	-10971	-6486	-8280	-2301	-8280	687	-8280	-3381	-5175	804	-5175	3792	-5175
47	-9033	-10971	-4511	-10971	-1281	-10971	-6342	-8280	-1820	-8280	1409	-8280	-3237	-5175	1285	-5175	4514	-5175
53.5	-8765	-10971	-3618	-10971	58	-10971	-6074	-8280	-927	-8280	2750	-8280	-2669	-5175	2177	-5175	5854	-5175
68	-9515	-10971	-6131	-10971	-3711	-10971	-6828	-8280	-3440	-8280	-1020	-8280	-3723	-5175	-335	-5175	2084	-5175
72	-9434	-10971	-5846	-10971	-3285	-10971	-6743	-8280	-3155	-8280	-593	-8280	-3637	-5175	-50	-5175	2511	-5175

7. CONCLUSIONS

This experimental study aimed to examine the effect of additives, particularly, friction reducer and fluid – loss agents on the heat generation. Obtained results were examined by simple regression analysis in order to determine the relation between the amount of additives in the cement sample and the change in exothermic reaction peak temperature. Moreover, the obtained temperature data was used to calculate stresses loads in the casing design regarding to the maximum temperatures of cement compositions.

The following results have been obtained from this experimental study on investigation the effect of additives on exothermic heat generation of the well cement:

1. The exothermic reaction of cement and water mixture was expectedly observed.
2. The additive CFR increases the change in temperature and affects the time to reach the peak temperature when used alone in cement sample.
3. Maximum temperature among cement samples with only CFR observed as 70.8 ^{0}C. (Cement sample with 0.9 % CFR)
4. The individual effect of the additive HALAD9 on temperature increase is less dominant, however, it retards considerably the time to reach the peak temperature.
5. Maximum temperature among cement samples with only HALAD9 observed as 66.5 ^{0}C. (Cement sample with 0.1 % HALAD9)
6. The required time to reach the maximum reaction temperature was retarded approximately 1 hour in cement samples having only 0.1 % HALAD9. This required time increased with increasing amount of HALAD9 in the composition (Approximately 6.7 hours of retardation for the cement sample with 1.0 % HALAD9).
7. When used together, increasing the amount of CFR increase the maximum reaction temperature, however, increasing the amount of HALAD9 slightly decrease the maximum reaction temperature (up to 0.3 % BWOC). Maximum

reaction temperature obtained approximately 77 ^{0}C for cement sample with 0.3 % CFR and 0.1 % HALAD9.

8. When used together over 0.3% BWOC, increasing the amount of both additives cause a decrease in maximum reaction temperature. Lowest maximum reaction temperature obtained approximately 46 ^{0}C for cement sample with 0.9 % CFR and 0.9% HALAD9.
9. Using both additives with up to 0.3 % in cement slurry, more severely increases the maximum reaction temperature compared to that of the water-cement mixture.
10. Depending on the regression analysis, it is not possible to predict the maximum temperature according to given amount of friction reducer and fluid – loss agent in the cement slurry since the obtained R-square value is low. Further, the statistical evaluation of the experimental results reveals that the effect of additive CFR on cement setting temperature is more dominant.
11. For the regression performed for each sets in which CFR concentration is kept constant while the amount of HALAD9 is raised from 0.1% by weight of cement up to 1.0%, the highest values are obtained at the friction reducer concentrations of 0.4, 0.5 and 0.8. The values for these sets of samples are close 100%. For these experimental sets, that is obvious that increasing the amount of additives affect proportionally the maximum reaction peak temperature.
12. Additional axial casing stress values were performed considering that the casings (K-55, C-95, and P-110 grades) were exposed to maximum temperature changes of 53 ^{0}C, 40 ^{0}C and 25 ^{0}C for different casing lengths. The maximum additional compression in casing were obtained as 9765 psi at a temperature change of 53 ^{0}C for C-95 53.5 lbm/ft grade casing (at 3000 ft. casing length).
13. Heat generation from the cement slurry in the well causes higher additional axial stresses on casing strings.

The additives have significant effect on setting temperature of well cement. The change in temperature might also have an early time impact on casing loads. Such situation may deteriorate the cement matrix by causing premature gelation, micro/macro fractures (or channels) and bonding problems.

The obtained results from this study might create an awareness on considering the effect of additives on the cement heat of hydration as an important aspect at any well cement design related works.

RECOMMENDATIONS FOR FUTURE WORKS

These experiments have been conducted at the ambient conditions in the laboratory. To prevent the heat transfer, between cement slurry and its surroundings the special isolation materials were used in the design of container. It is certain that there was still heat transfer through surroundings. It could be recommended that using two probes and compare the obtained results from them might provide more confident recording temperature data. One of these probes could be placed into container to observe temperature behavior of cement slurries and another probe might be used to notice the temperature of environment throughout the experiment. Relationship between these records can give us better approach to cognize the effects of additives on heat hydration of cement slurries. The impact of these additives on well cement setting temperature can be examined by applying different method where one of the probe can be used to measure temperatures of cement slurries having additives in it and other probe could record temperature behaviors of cement and water mixture without any additive at the same period.

Furthermore, some other numerical analyze tools can be applied for recorded temperature data to build strong statistical evaluation among them. CFD might be used in the future for this purpose.

Finally, it is also recommended to re – run these experiments at the different temperature and pressure conditions in order to simulate in – situ environments.

REFERENCES

Audibert, A., Argillier, J.-F., Bailey, L., & Reid, P. I. (1997, September 23). *USA Patent No. US5669456.* Retrieved from http://www.google.tl/patents/US5669456

Backe , K. R., Lile, O. B., & Lyomov, S. K. (2001, December). Characterizing Curing Cement Slurries by Electrical Conductivity. *SPE Drilling & Completion, 16*(04), 207-207. doi:https://doi.org/10.2118/74694-PA

Backe, K. R., Lile, O. B., Lyomov, S. K., Elvebakk, H., & Skalle, P. (1999, September). Characterizing Curing-Cement Slurries Permeability, Tensile Strength, and Shrinkage. *SPE Drilling & Completion, 14*(03), 162-167. doi:https://doi.org/10.2118/57712-PA

Bogue, R. H. (1929). *Calculation of Compunds in Portland Cement.* Washington,D.C.: Portland Cement Association Fellowship.

Boukadi, F., Yaghi, B., Al-Hadrami, H., Bemani, A., Babadagli, T., & De Mestre, P. (2004). A Comparative Study of Lost Circulation Materials. *Energy Sources, 26*, 1043-1051. doi:10.1080/00908310490494612

Bourgoyne, A. T., Millheim, K. K., Chenevert, M. E., & Young, F. J. (1991). *Applied Drilling Engineering* (2nd ed.). Texas, USA: Society of Petroleum Engineers, Richardson.

Byrom, T. G. (2007). *Casing and Liners for Drilling and Completion.* Houston, Texas, USA: Gulf Publishing Company.

Cartalos, U., & Lecourtier, J. (1993). *Cementing Technology and Procedures.* Paris, France: Editions Technip.

Chang, F. F., & Parlar, M. (1999, November 9). *USA Patent No. US5981447.* Retrieved from https://www.google.ch/patents/US5981447

Chenevert, M. E., & Shrestha, B. K. (1991, March). Chemical Shrinkage Properties of Oilfield Cements. *SPE Drilling Engineering, 6*(01), 37-43. doi:https://doi.org/10.2118/16654-PA

Eckel, E. C. (1905). *Cement Materials and Industry of the United States.* Washington, D.C., USA: Washingron Government Printing Office.

Fjar, E., Holt, R. M., Raaen, A. M., Risnes, R., & Horsrud, P. (2008). *Petroleum Related Rock Mechanics* (2nd ed., Vol. 53). Amsterdam, The Netherlands: Elsevier Science. Retrieved from https://www.elsevier.com/books/petroleum-related-rock-mechanics/fjar/978-0-444-50260-5

Hewlett, P. (2001). *Lea's Chemistry of Cement and Concrete* (4th ed.). Washington, D.C., USA: Elsevier Ltd.

Isaacs, N. (2008, June/July). Cementing History. *Journal BUILD*, 50-54.

Kutasov, I. M. (1999). *Applied Geothermics for Petroleum Engineers* (1st ed., Vol. 48). Amsterdam - New York - London, The Netherlands: Elsevier Ltd.

Kutasov, I. M., & Eppelbaum, L. V. (2015). *Pressure and Temperature Well Testing.* Boca Ralton - London - New York, NW, USA: CRC Press, Taylor & Francis Group LLC.

Lavrov, A., & Torsæter, M. (2016). *Physics and Mechanics of Primary Well Cementing.* (D. Stow, M. Bentley, J. Gholinezhad, L. Akanji, K. M. Sabil, & S. Agar, Eds.) Trondheim, Norway: SpringerBriefs in Petroleum Geoscience & Engineering. doi:10.1007/9783319431659

Lowler, J. S., Connoly, J. D., Krauss, P. D., Tracy, S. L., & Ankenman, B. E. (2007). *Guidelines for Concrete Mixtures Containing Supplementary Cementitious Materials to Enhance Durability of Bridge Decks.* National Cooperative Highway Research Program. Washington,D.C.: Transportation Research Board. doi:10.17226/23181

Michaux, M., Nelson, E., & Vidick, B. (1989, April). Cement Chemistry and Additives. *Schlumberger Oilfield Review, 1*.

Nelson, E. B., & Guillot, D. (2006). *Well Cementing* (2nd ed.). Paris, France: Schlumberger.

Nelson, E. B., Schlumberger, D., Michaux, M., & Benoit Vidick. (1990). *Well Cementing.* Amsterdam, The Netherlands: Elsevier Science Publishers B.V.

Nguyen, P. D., Weaver, J. D., Cole, C. R., & Schulze, C. R. (1996, October 6-9). Development and Field Application of New Fluid - Loss Control Material. *SPE Annual Technical Conference and Exhibition*, p. 9. doi:https://doi.org/10.2118/36676-MS

Parlar, M., Ali, S. A., & Cromb, J. (1998, February 18-19). Development of a new crosslinked - HEC (hydroxyethylcellulose) fluid loss control pill for highly-overbalanced,highpermeability and/or high temperature formations. *SPE International Symposium on Formation Damage Control*, pp. 215-227.

Patel, B. (1990, June 13). *Bartlesville, OK Patent No. EP 0372469.* Retrieved from http://www.google.at/patents/EP0372469A2?cl=en

Portland Cement Association, & Skokie, I. (1969). *Portland Cements.* USA: Portland Cement Association.

Rahman, S. S., & Chilingarian, G. V. (1995). *Casing Design Theory and Practice* (1st ed., Vol. Developments in Petroleum Science 42). (G. V. Chilinagarian, Ed.) Amsterdam - Lausanne - New York - Oxford - Shannon - Tokyo, The Netherlands: Elsevier Ltd. Retrieved from https://www.elsevier.com/books/casing-design-theory-and-practice/rahman/978-0-444-81743-3

Ridha, S., Irawan, S., & Ariwahjoedi, B. (2013, December). Strength prediction of Class G oilwell cement during early ages by electrical conductivity. *Journal of Petroleum Exploration and Production Technology, 3*(4), 303-311. doi:10.1007/s13202-013-0075-9

Romero, J., & Loizzo, M. (2000, October 1-4). The Importance of Hydration Heat on Cement Strength Development for Deep Water Wells. *SPE Annual Technical Conference and Exhibition*, p. 8. doi:https://doi.org/10.2118/62894-MS

Taylor, H. F. (1990). *Cement Chemistry.* London, United Kingdom: Academic Press.

Url–1 <https://en.wikipedia.org/wiki/Colosseum#/media/File:Roma06(js).jpg> date retrieved 27.04.2017

Url–2 <*http://www.dartfordarchive.org.uk/*> date retrieved 19.03.2017

Url–3 <*http://cembureau.eu/*> date retrieved 25.02.2017

Url–4 <*https://www.cemex.com/*> date retrieved 15.03.2017

Url–5 <*http://www.civilology.com/*> date retrieved 03.04.2017

Url–6 <*https://theconstructor.org/building/*> date retrieved 29.03.2017

Url–7 <*http://www.golchhapigments.com/*> 29.03.2017

Url–8 <*http://www.halliburton.com/*> date retrieved 17.04.2017

Url–9 <*http://petrowiki.org/*> date retrieved 15.03.2017

Url–10 <*http://www.messinachemicals.com/*> date retrieved 15.03.2017

Url–11 <*http://www.slb.com/*> date retrieved 16.03.2017

Url–12 <*http://www.philadelphia.edu.jo/*> date retrieved 25.04.2017

Url–13 <*Http://matse1.matse.illinois.edu/*> date retrieved 16.03.2017

Url–14 <*http://blog.minitab.com/blog/adventures-in-statistics-2/regression-analysis-how-do-i-interpret-r-squared-and-assess-the-goodness-of-fit*> date retrieved 27.04.2017

APPENDICES

APPENDIX A: Graphics of CFR and Halad9 Mixtures

APPENDIX B: Regression Results

APPENDIX A

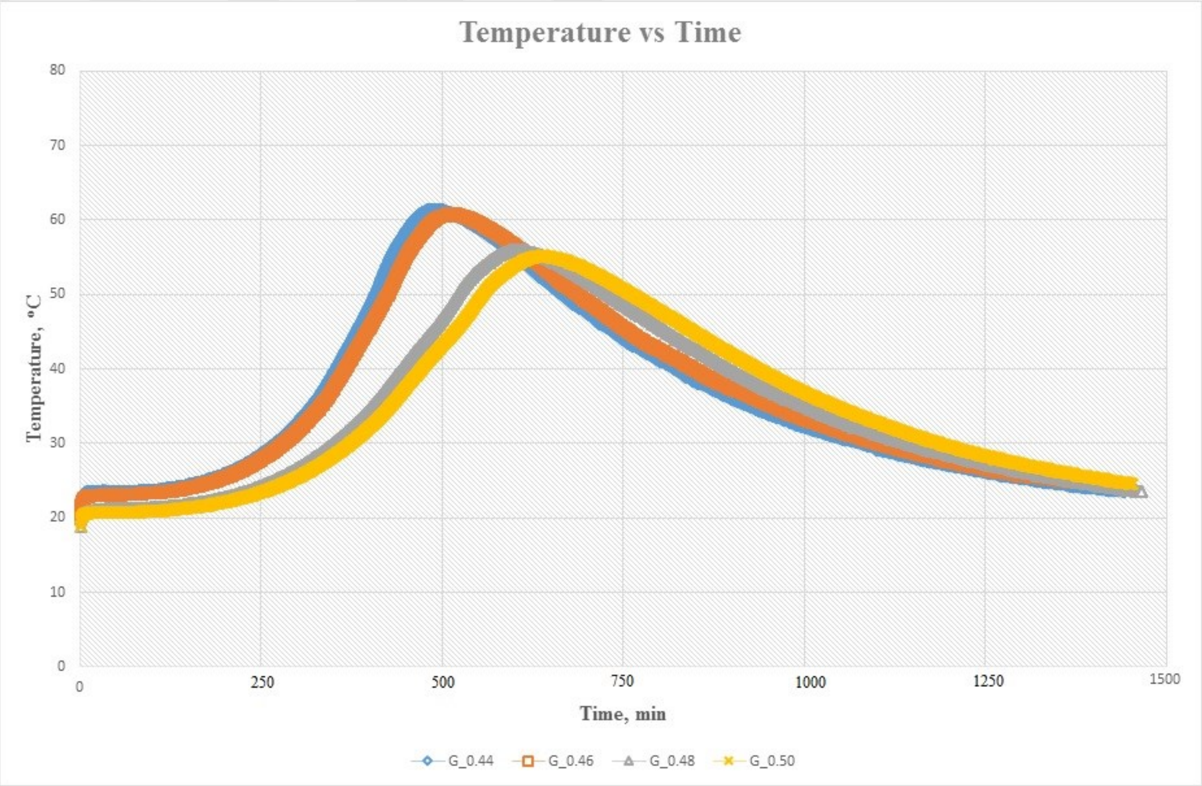

Figure A. 1: Heat of hydration of G class cement with water at different concentrations.

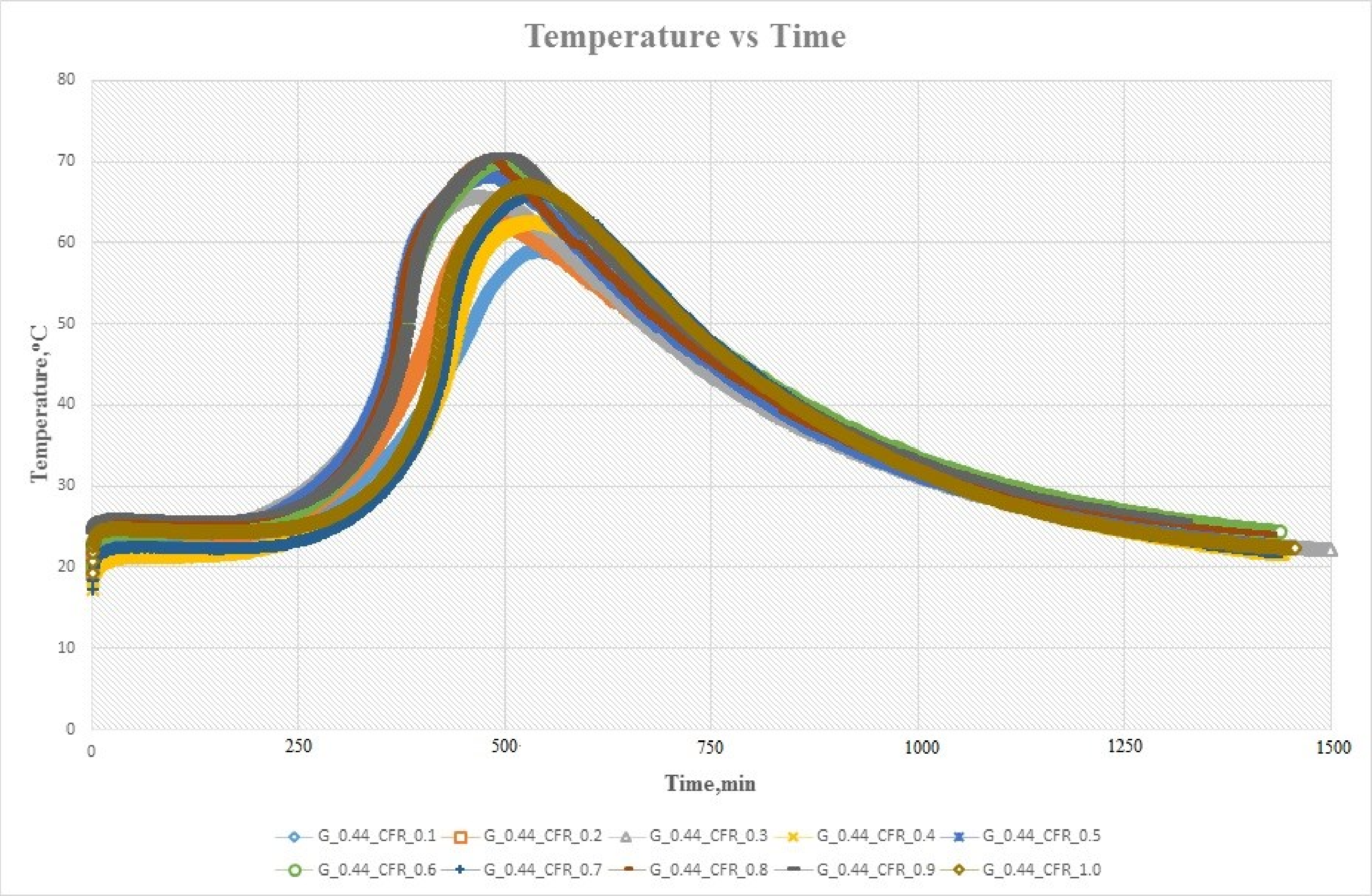

Figure A. 2: Heat of hydration of the cement slurry with CFR.

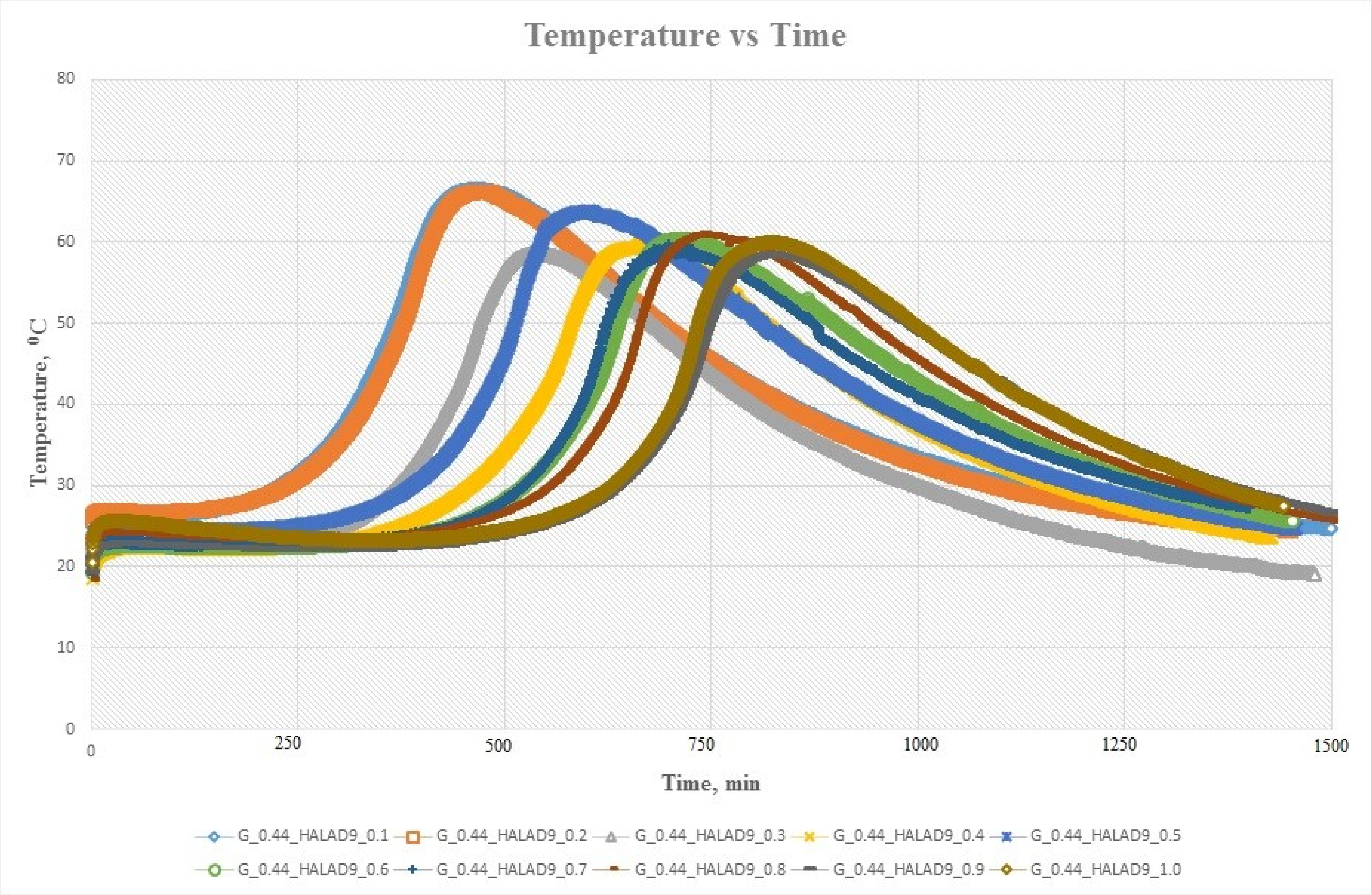

Figure A. 3: Heat of hydration of the cement slurry with fluid – loss additives.

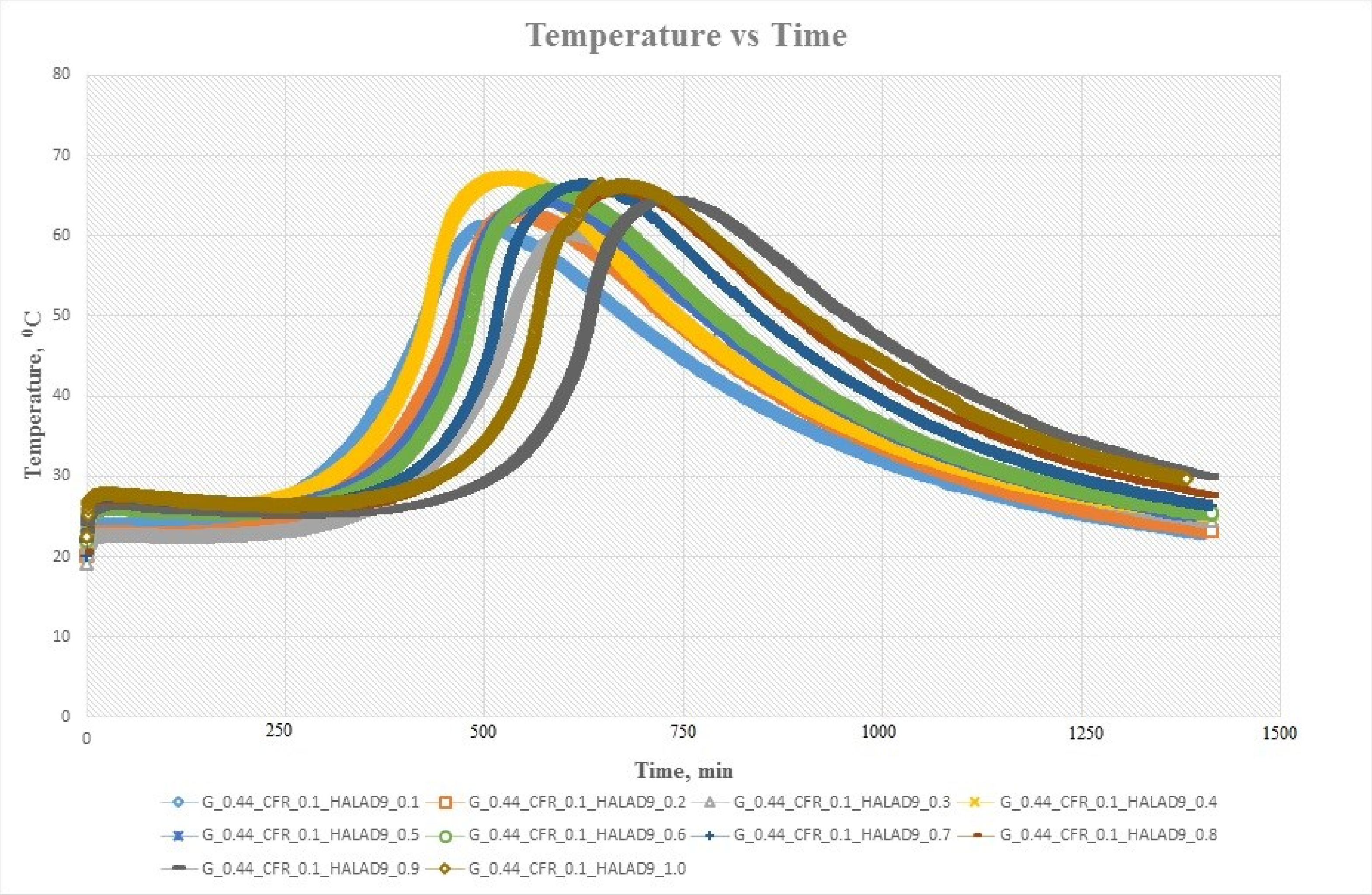

Figure A. 4: Heat of hydration of the cement slurry at the CFR concentration of 0.1 % BWOC and different fraction of Halad9 mixtures.

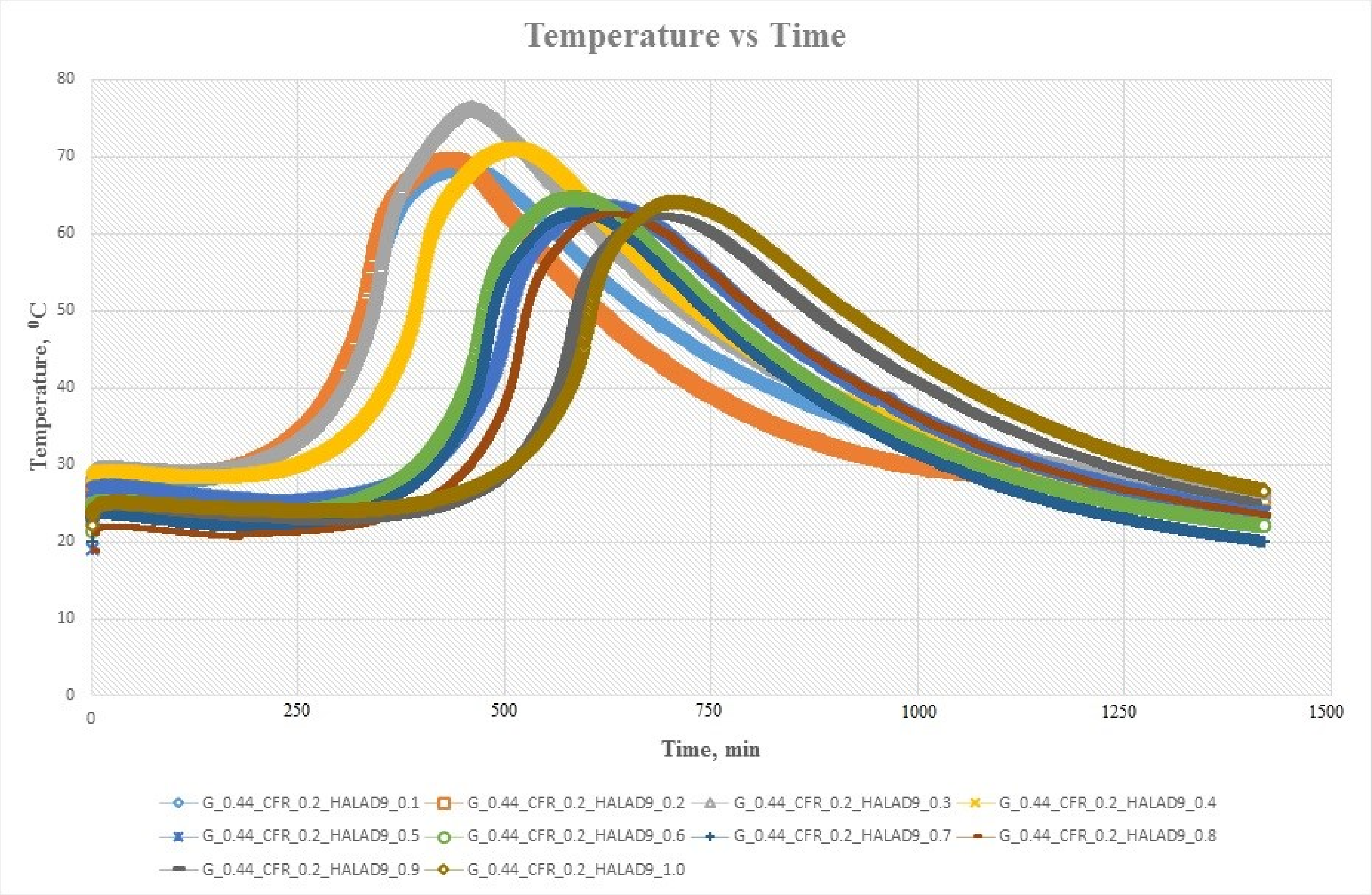

Figure A. 5: Heat of hydration of the cement slurry at the CFR concentration of 0.2 % BWOC and different fraction of Halad9 mixtures.

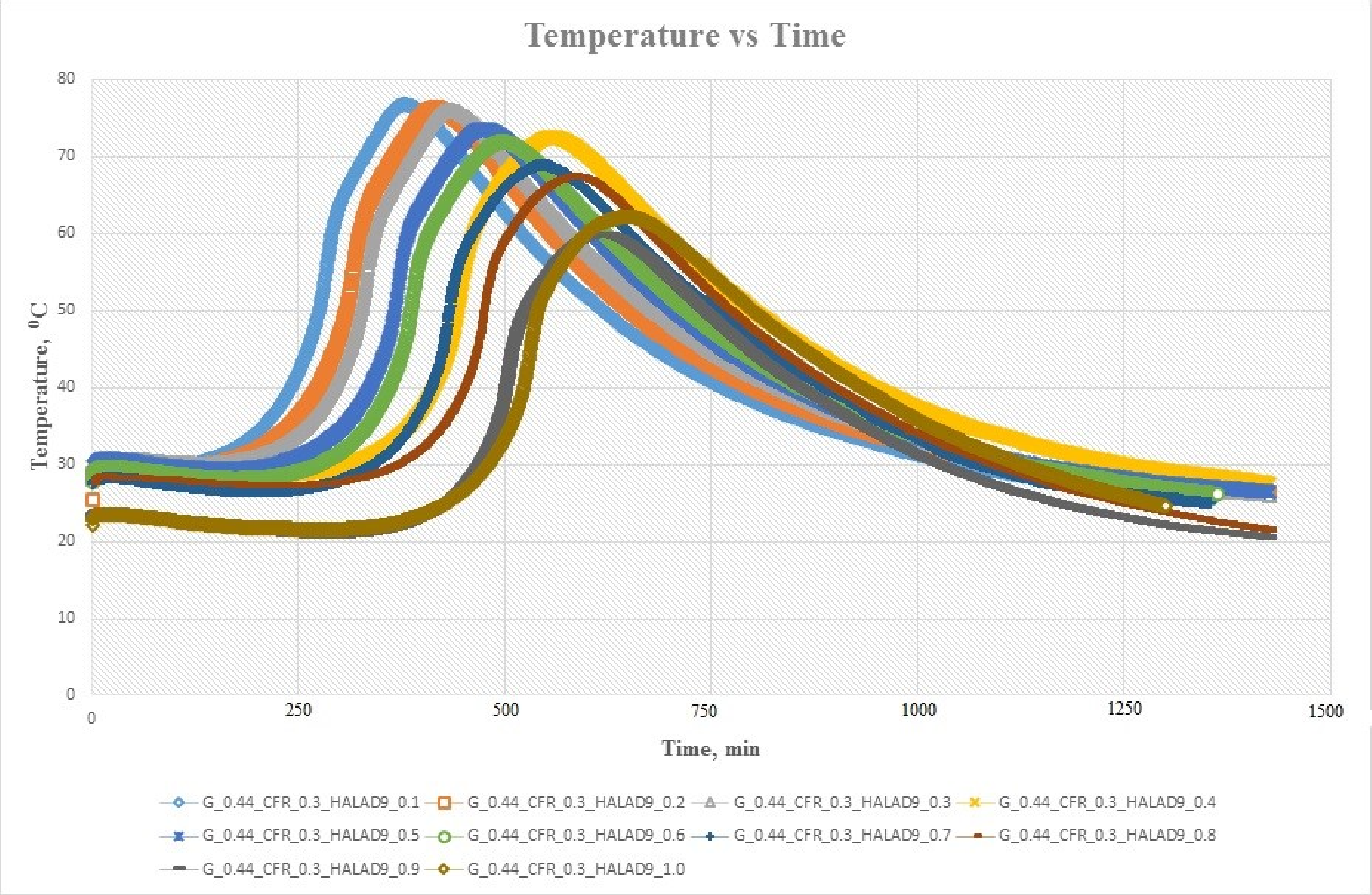

Figure A. 6: Heat of hydration of the cement slurry at the CFR concentration of 0.3 % BWOC and different fraction of Halad9 mixtures.

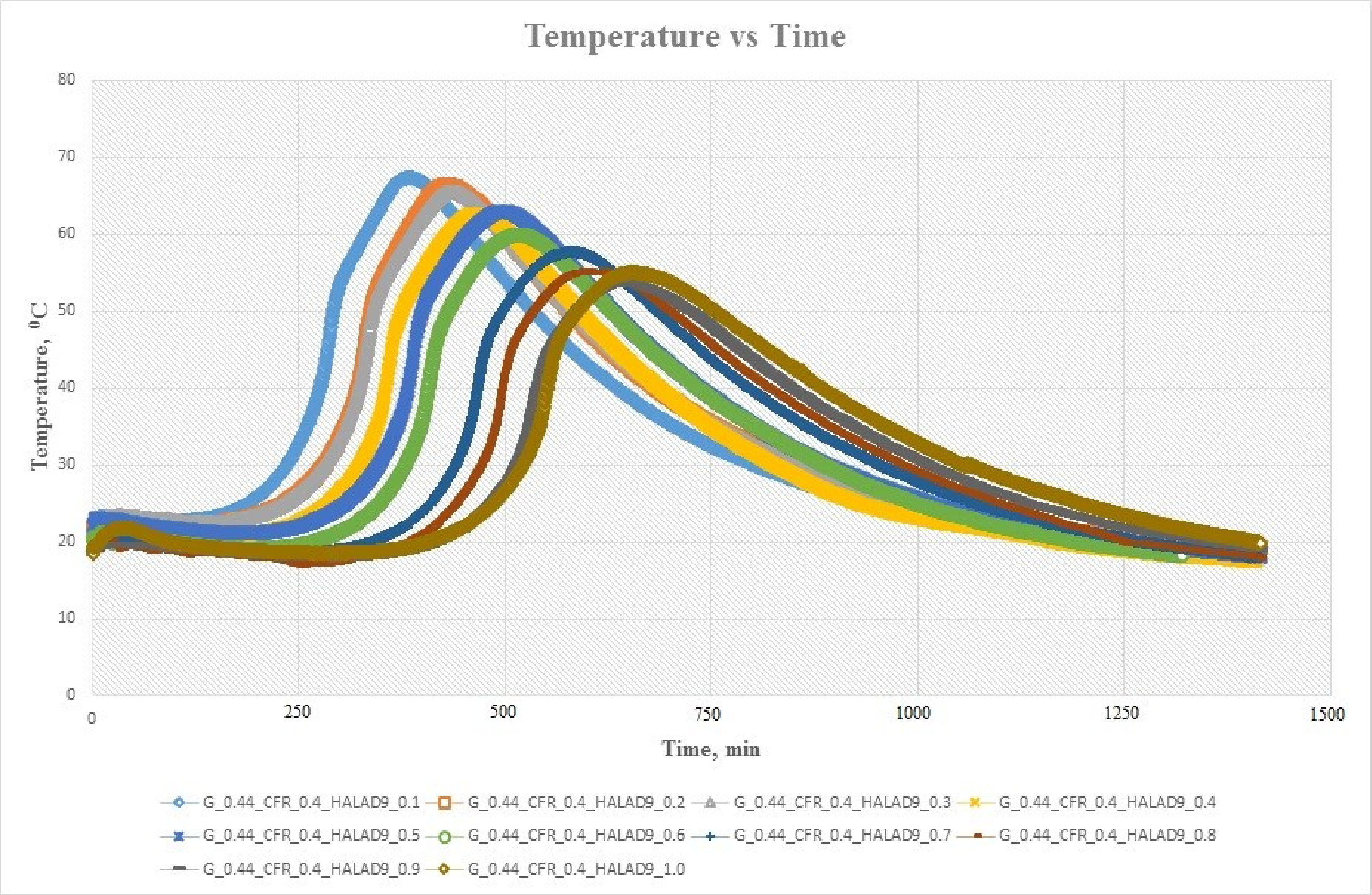

Figure A. 7: Heat of hydration of the cement slurry at the CFR concentration of 0.4 % BWOC and different fraction of Halad9 mixtures.

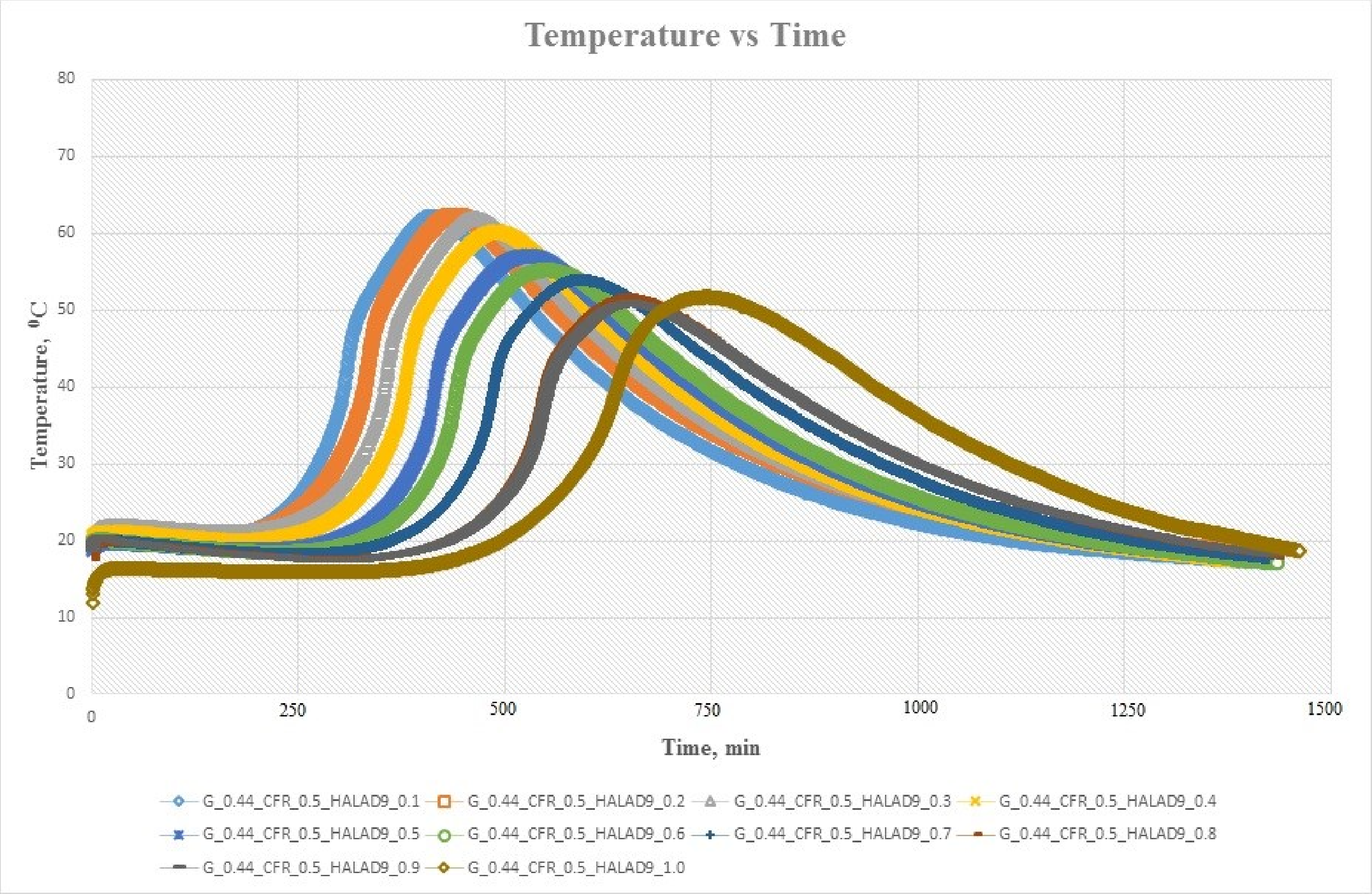

Figure A. 8: Heat of hydration of the cement slurry at the CFR concentration of 0.5 % BWOC and different fraction of Halad9 mixtures.

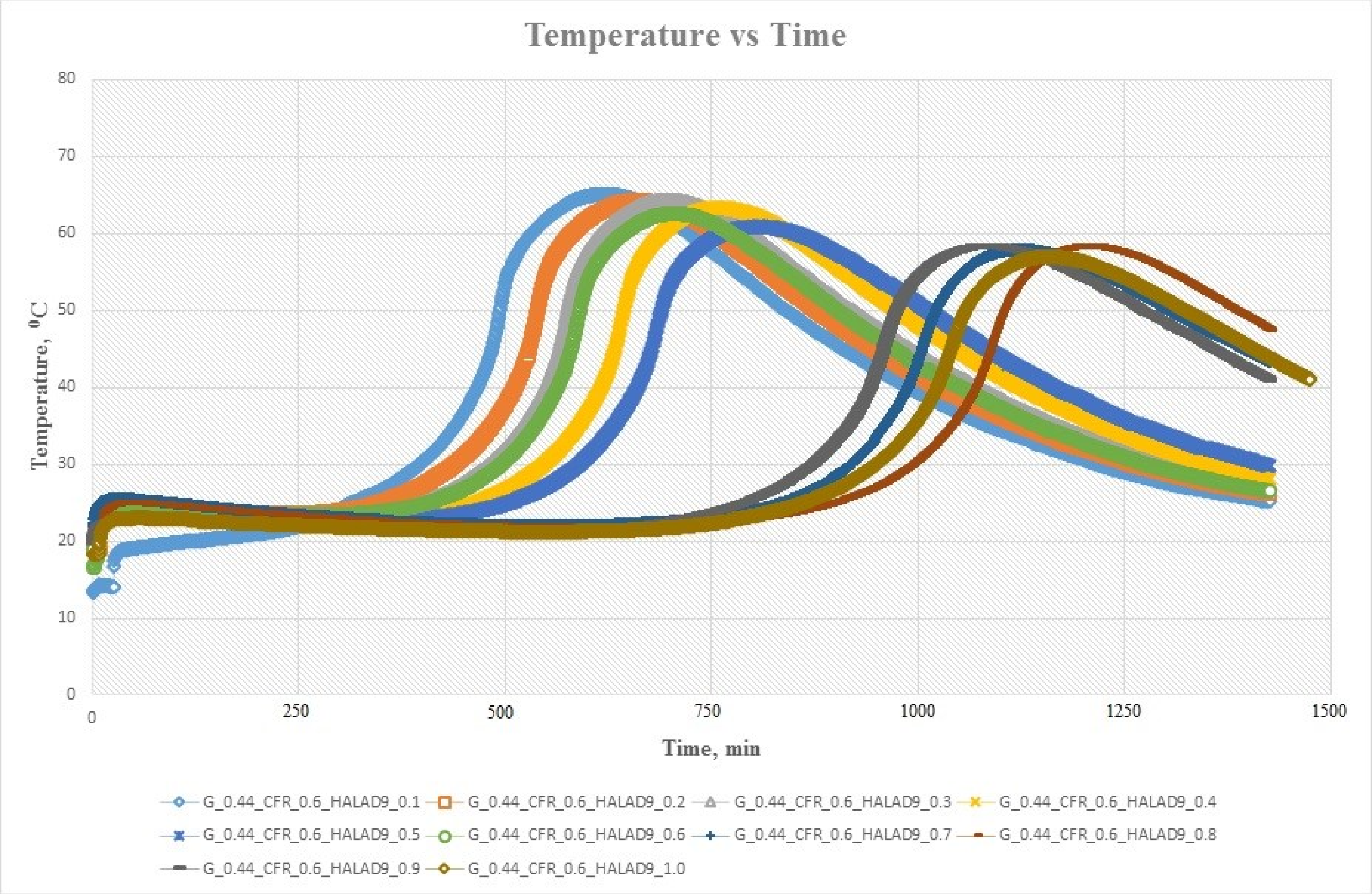

Figure A. 9: Heat of hydration of the cement slurry at the CFR concentration of 0.6 % BWOC and different fraction of Halad9 mixtures.

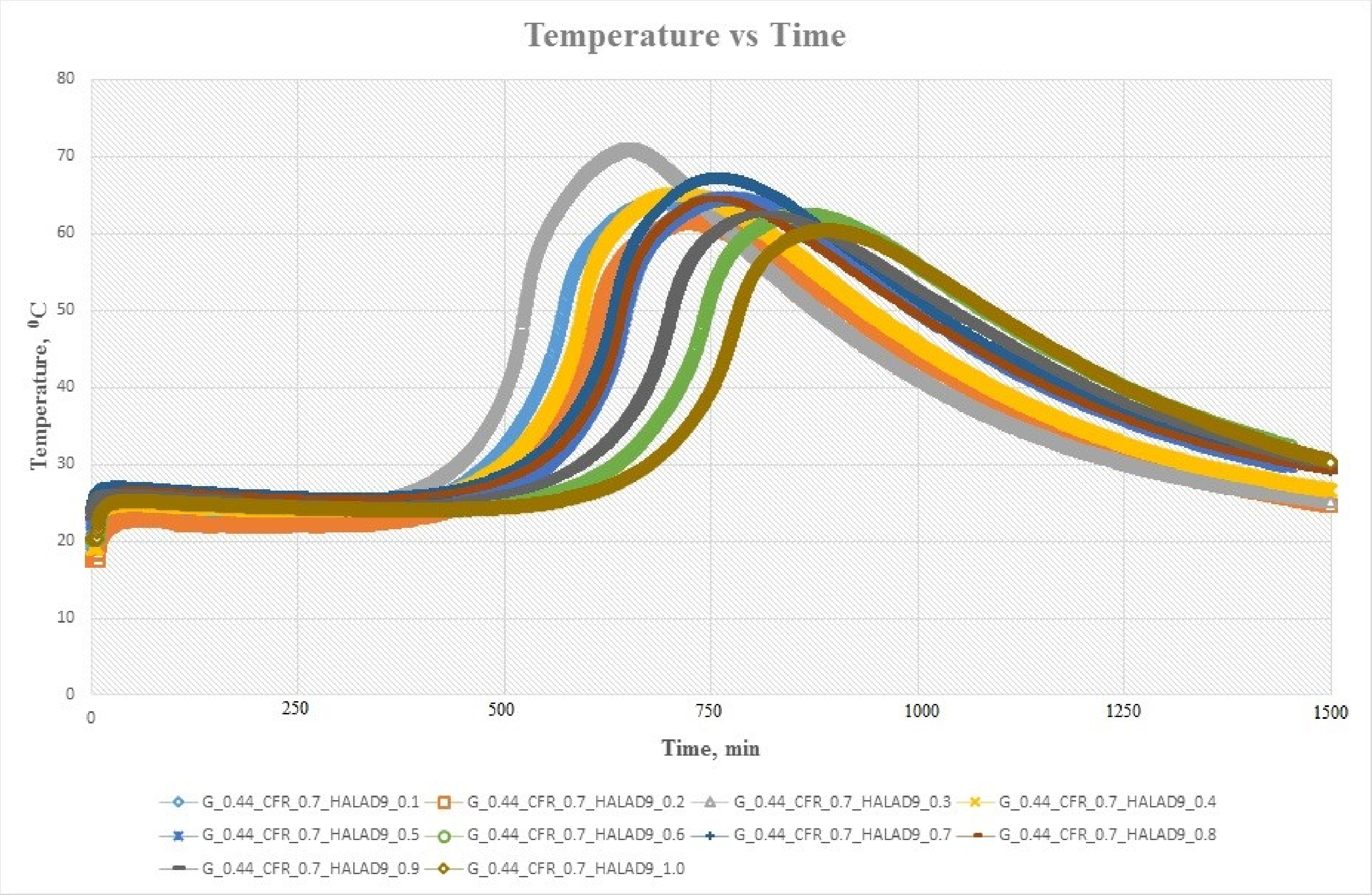

Figure A. 10: Heat of hydration of the cement slurry at the CFR concentration of 0.7 % BWOC and different fraction of Halad9 mixtures.

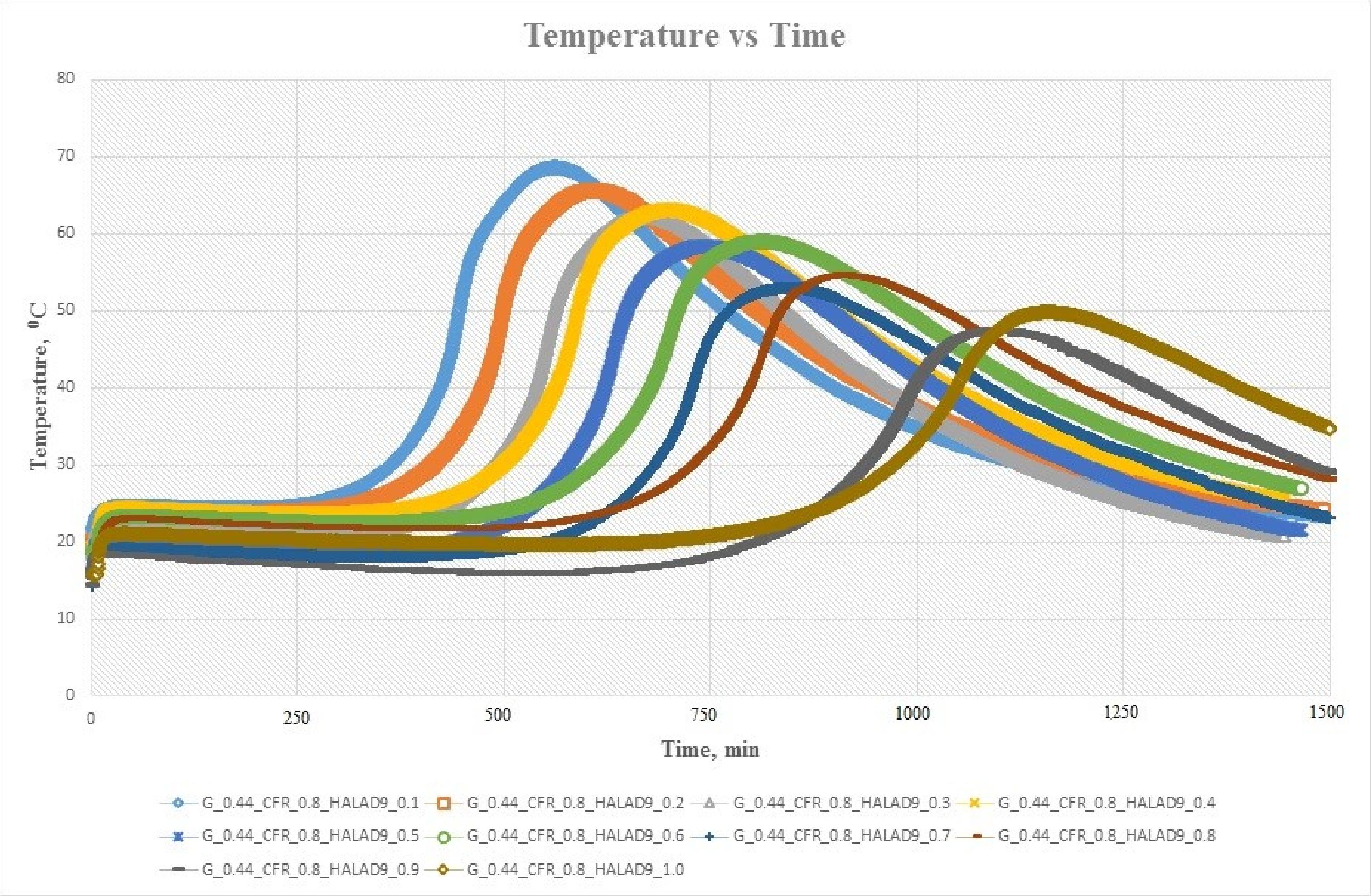

Figure A. 11: Heat of hydration of the cement slurry at the CFR concentration of 0.8 % BWOC and different fraction of Halad9 mixtures.

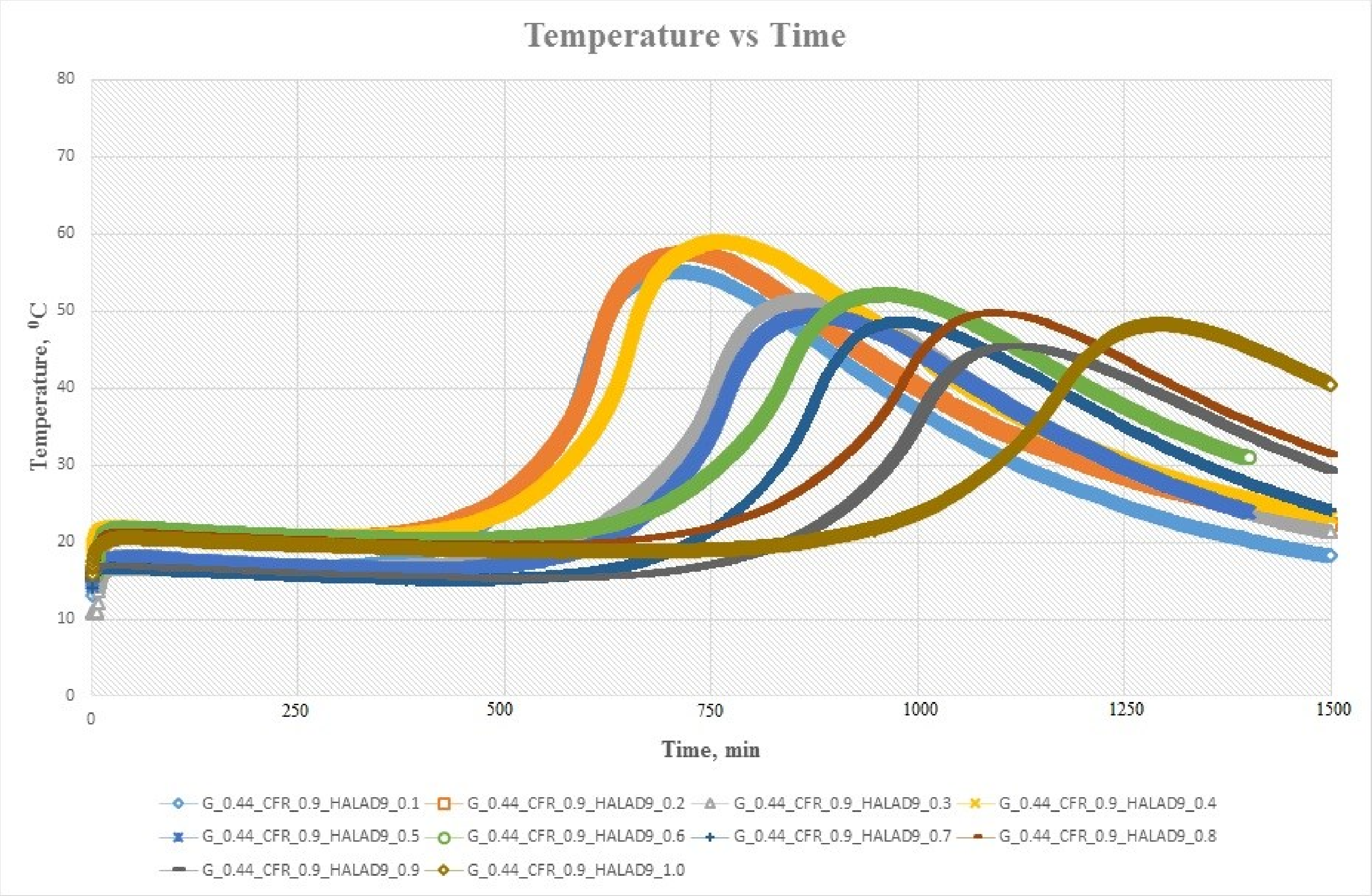

Figure A. 12: Heat of hydration of the cement slurry at the CFR concentration of 0.9 % BWOC and different fraction of Halad9 mixtures.

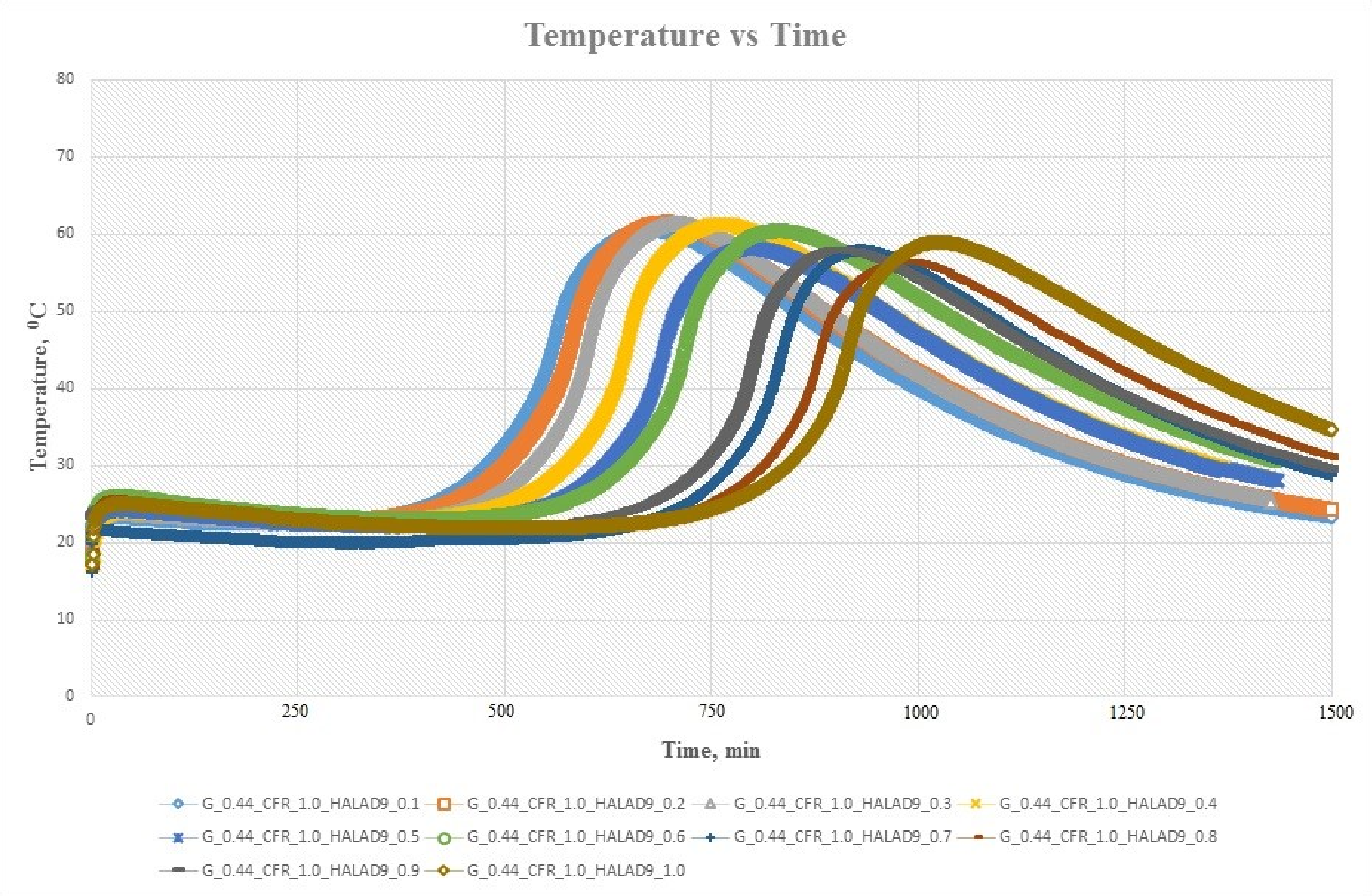

Figure A. 13: Heat of hydration of the cement slurry at the CFR concentration of 1.0 % BWOC and different fraction of Halad9 mixtures.

APPENDIX B

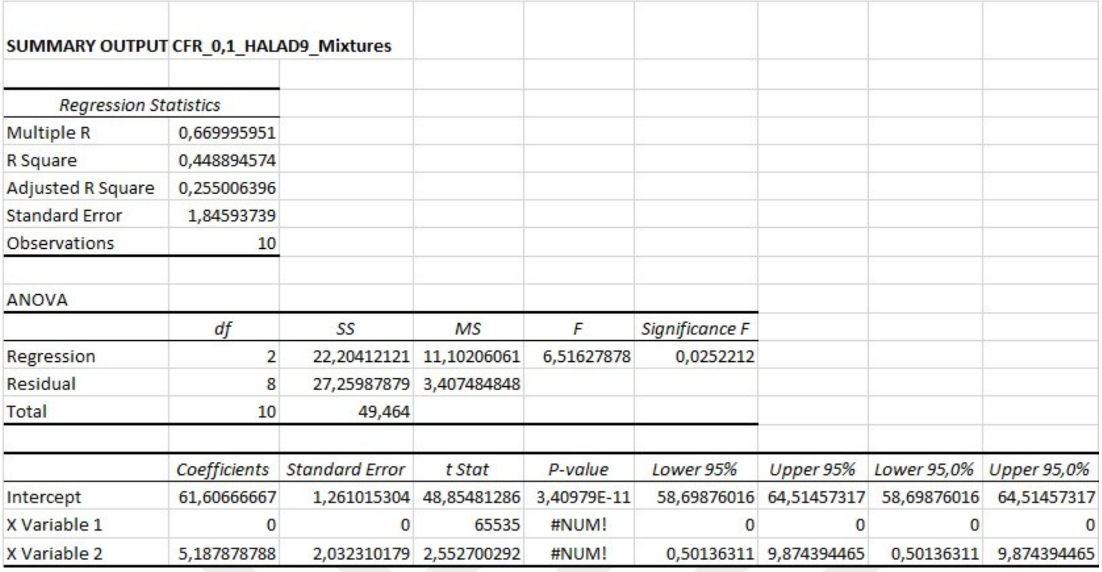

SUMMARY OUTPUT CFR_0,1_HALAD9_Mixtures

Regression Statistics	
Multiple R	0,669995951
R Square	0,448894574
Adjusted R Square	0,255006396
Standard Error	1,84593739
Observations	10

ANOVA

	df	*SS*	*MS*	*F*	*Significance F*
Regression	2	22,20412121	11,10206061	6,51627878	0,0252212
Residual	8	27,25987879	3,407484848		
Total	10	49,464			

	Coefficients	*Standard Error*	*t Stat*	*P-value*	*Lower 95%*	*Upper 95%*	*Lower 95,0%*	*Upper 95,0%*
Intercept	61,60666667	1,261015304	48,85481286	3,40979E-11	58,69876016	64,51457317	58,69876016	64,51457317
X Variable 1	0	0	65535	#NUM!	0	0	0	0
X Variable 2	5,187878788	2,032310179	2,552700292	#NUM!	0,50136311	9,874394465	0,50136311	9,874394465

(a)

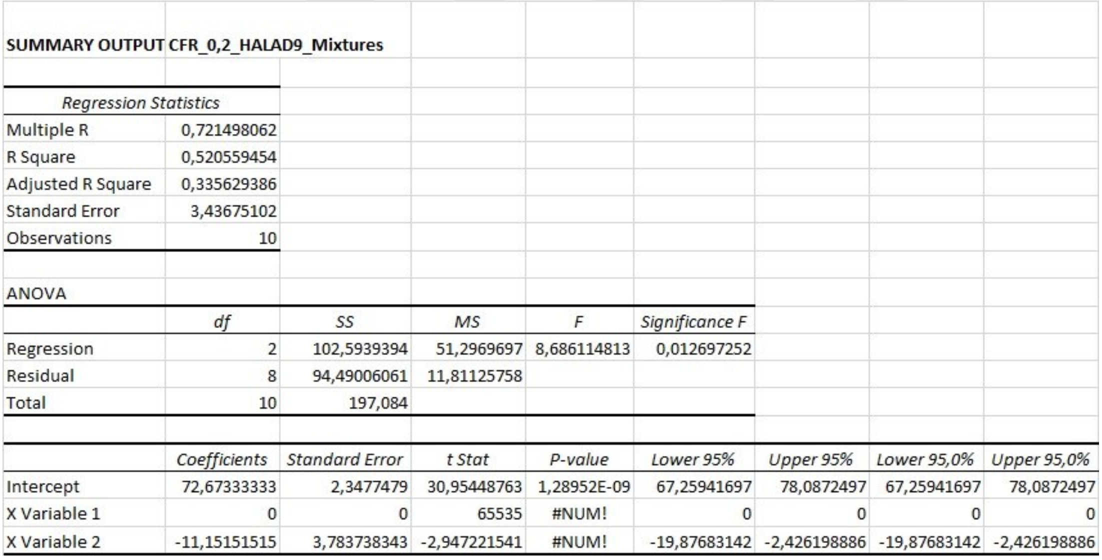

SUMMARY OUTPUT CFR_0,2_HALAD9_Mixtures

Regression Statistics	
Multiple R	0,721498062
R Square	0,520559454
Adjusted R Square	0,335629386
Standard Error	3,43675102
Observations	10

ANOVA

	df	*SS*	*MS*	*F*	*Significance F*
Regression	2	102,5939394	51,2969697	8,686114813	0,012697252
Residual	8	94,49006061	11,81125758		
Total	10	197,084			

	Coefficients	*Standard Error*	*t Stat*	*P-value*	*Lower 95%*	*Upper 95%*	*Lower 95,0%*	*Upper 95,0%*
Intercept	72,67333333	2,3477479	30,95448763	1,28952E-09	67,25941697	78,0872497	67,25941697	78,0872497
X Variable 1	0	0	65535	#NUM!	0	0	0	0
X Variable 2	-11,15151515	3,783738343	-2,947221541	#NUM!	-19,87683142	-2,426198886	-19,87683142	-2,426198886

(b)

Figure B. 1: Screenshot of the result of regression analysis applied to CFR_0.1 (a) and CFR_0.2 (b) compositions.

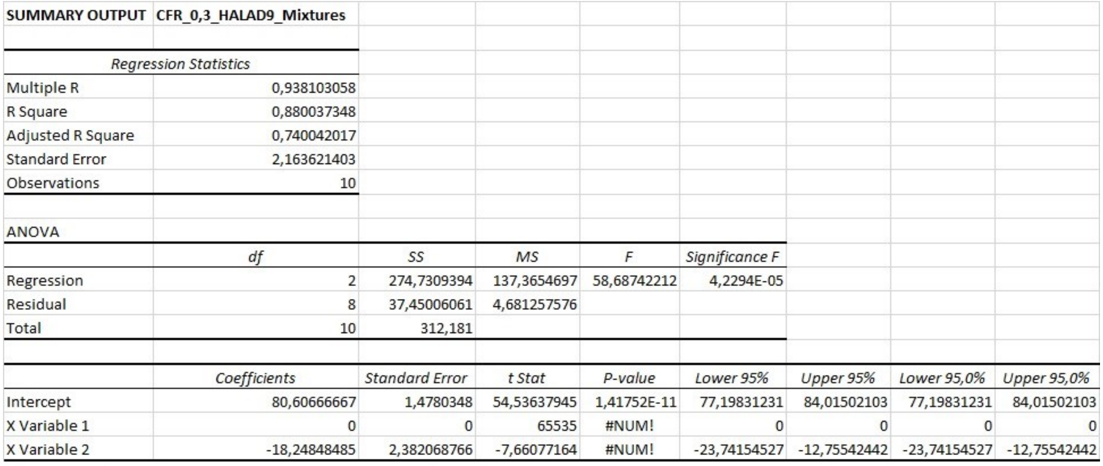

SUMMARY OUTPUT **CFR_0,3_HALAD9_Mixtures**

Regression Statistics	
Multiple R	0,938103058
R Square	0,880037348
Adjusted R Square	0,740042017
Standard Error	2,163621403
Observations	10

ANOVA

	df	*SS*	*MS*	*F*	*Significance F*
Regression	2	274,7309394	137,3654697	58,68742212	4,2294E-05
Residual	8	37,45006061	4,681257576		
Total	10	312,181			

	Coefficients	*Standard Error*	*t Stat*	*P-value*	*Lower 95%*	*Upper 95%*	*Lower 95,0%*	*Upper 95,0%*
Intercept	80,60666667	1,4780348	54,53637945	1,41752E-11	77,19831231	84,01502103	77,19831231	84,01502103
X Variable 1	0	0	65535	#NUM!	0	0	0	0
X Variable 2	-18,24848485	2,382068766	-7,66077164	#NUM!	-23,74154527	-12,75542442	-23,74154527	-12,75542442

(a)

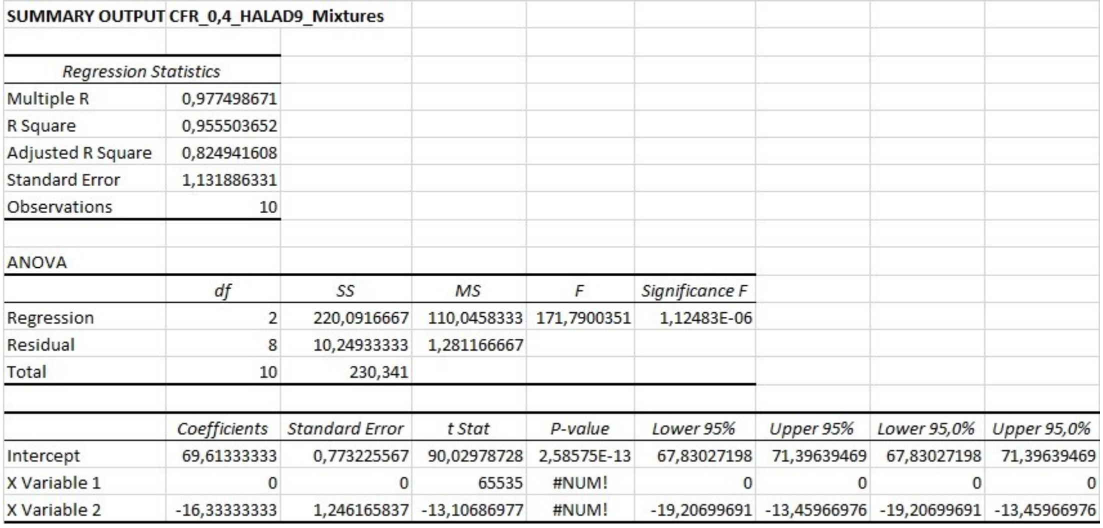

SUMMARY OUTPUT **CFR_0,4_HALAD9_Mixtures**

Regression Statistics	
Multiple R	0,977498671
R Square	0,955503652
Adjusted R Square	0,824941608
Standard Error	1,131886331
Observations	10

ANOVA

	df	*SS*	*MS*	*F*	*Significance F*
Regression	2	220,0916667	110,0458333	171,7900351	1,12483E-06
Residual	8	10,24933333	1,281166667		
Total	10	230,341			

	Coefficients	*Standard Error*	*t Stat*	*P-value*	*Lower 95%*	*Upper 95%*	*Lower 95,0%*	*Upper 95,0%*
Intercept	69,61333333	0,773225567	90,02978728	2,58575E-13	67,83027198	71,39639469	67,83027198	71,39639469
X Variable 1	0	0	65535	#NUM!	0	0	0	0
X Variable 2	-16,33333333	1,246165837	-13,10686977	#NUM!	-19,20699691	-13,45966976	-19,20699691	-13,45966976

(b)

Figure B. 2: Screenshot of the result of regression analysis applied to CFR_0.3 (a) and CFR_0.4 (b) compositions.

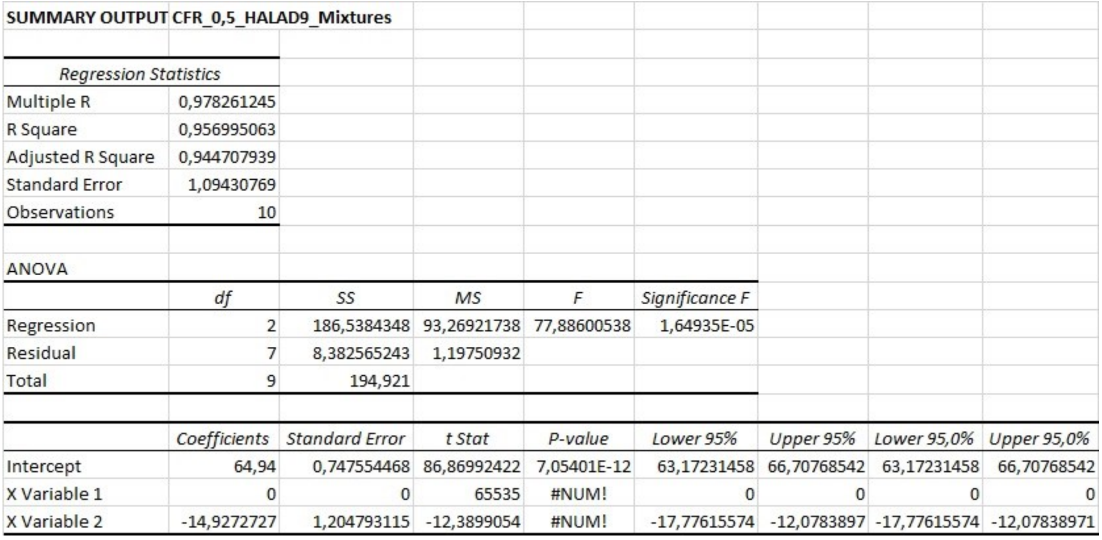

SUMMARY OUTPUT CFR_0,5_HALAD9_Mixtures

Regression Statistics	
Multiple R	0,978261245
R Square	0,956995063
Adjusted R Square	0,944707939
Standard Error	1,09430769
Observations	10

ANOVA

	df	*SS*	*MS*	*F*	*Significance F*
Regression	2	186,5384348	93,26921738	77,88600538	1,64935E-05
Residual	7	8,382565243	1,19750932		
Total	9	194,921			

	Coefficients	*Standard Error*	*t Stat*	*P-value*	*Lower 95%*	*Upper 95%*	*Lower 95,0%*	*Upper 95,0%*
Intercept	64,94	0,747554468	86,86992422	7,05401E-12	63,17231458	66,70768542	63,17231458	66,70768542
X Variable 1	0	0	65535	#NUM!	0	0	0	0
X Variable 2	-14,9272727	1,204793115	-12,3899054	#NUM!	-17,77615574	-12,0783897	-17,77615574	-12,07838971

(a)

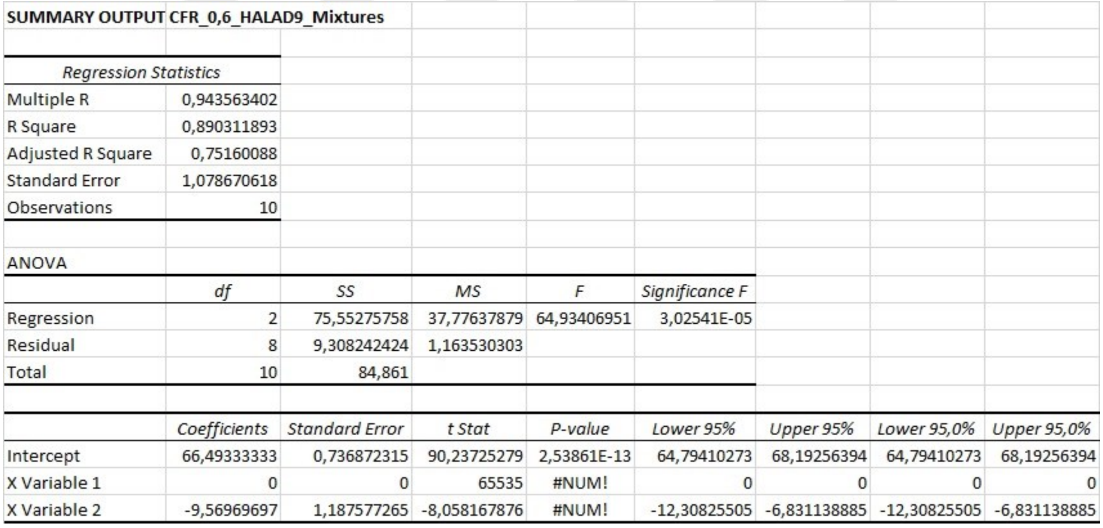

SUMMARY OUTPUT CFR_0,6_HALAD9_Mixtures

Regression Statistics	
Multiple R	0,943563402
R Square	0,890311893
Adjusted R Square	0,75160088
Standard Error	1,078670618
Observations	10

ANOVA

	df	*SS*	*MS*	*F*	*Significance F*
Regression	2	75,55275758	37,77637879	64,93406951	3,02541E-05
Residual	8	9,308242424	1,163530303		
Total	10	84,861			

	Coefficients	*Standard Error*	*t Stat*	*P-value*	*Lower 95%*	*Upper 95%*	*Lower 95,0%*	*Upper 95,0%*
Intercept	66,49333333	0,736872315	90,23725279	2,53861E-13	64,79410273	68,19256394	64,79410273	68,19256394
X Variable 1	0	0	65535	#NUM!	0	0	0	0
X Variable 2	-9,56969697	1,187577265	-8,058167876	#NUM!	-12,30825505	-6,831138885	-12,30825505	-6,831138885

(b)

Figure B. 3: Screenshot of the result of regression analysis applied to CFR_0.5 (a) and CFR_0.6 (b) compositions.

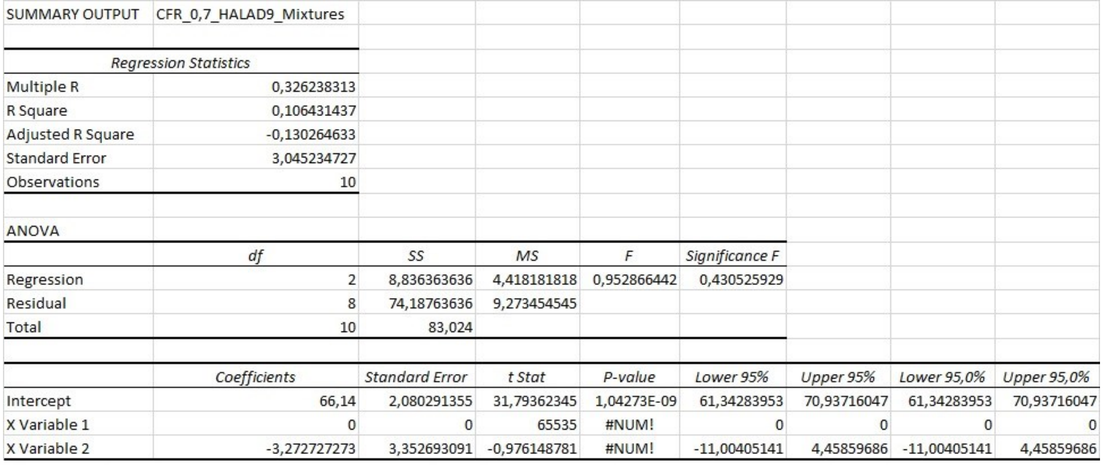

SUMMARY OUTPUT CFR_0,7_HALAD9_Mixtures

Regression Statistics	
Multiple R	0,326238313
R Square	0,106431437
Adjusted R Square	-0,130264633
Standard Error	3,045234727
Observations	10

ANOVA

	df	*SS*	*MS*	*F*	*Significance F*
Regression	2	8,836363636	4,418181818	0,952866442	0,430525929
Residual	8	74,18763636	9,273454545		
Total	10	83,024			

	Coefficients	*Standard Error*	*t Stat*	*P-value*	*Lower 95%*	*Upper 95%*	*Lower 95,0%*	*Upper 95,0%*
Intercept	66,14	2,080291355	31,79362345	1,04273E-09	61,34283953	70,93716047	61,34283953	70,93716047
X Variable 1	0	0	65535	#NUM!	0	0	0	0
X Variable 2	-3,272727273	3,352693091	-0,976148781	#NUM!	-11,00405141	4,45859686	-11,00405141	4,45859686

(a)

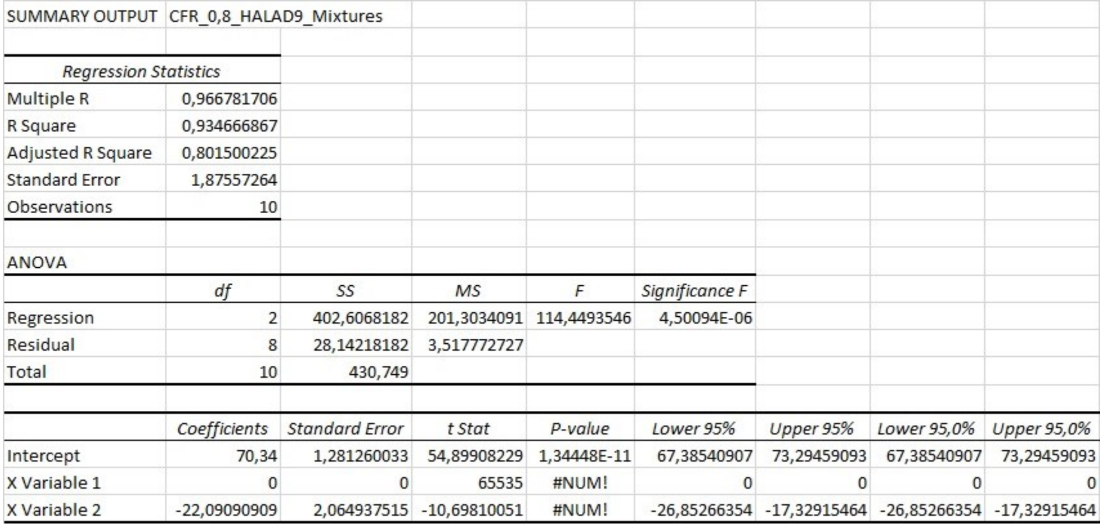

SUMMARY OUTPUT CFR_0,8_HALAD9_Mixtures

Regression Statistics	
Multiple R	0,966781706
R Square	0,934666867
Adjusted R Square	0,801500225
Standard Error	1,87557264
Observations	10

ANOVA

	df	*SS*	*MS*	*F*	*Significance F*
Regression	2	402,6068182	201,3034091	114,4493546	4,50094E-06
Residual	8	28,14218182	3,517772727		
Total	10	430,749			

	Coefficients	*Standard Error*	*t Stat*	*P-value*	*Lower 95%*	*Upper 95%*	*Lower 95,0%*	*Upper 95,0%*
Intercept	70,34	1,281260033	54,89908229	1,34448E-11	67,38540907	73,29459093	67,38540907	73,29459093
X Variable 1	0	0	65535	#NUM!	0	0	0	0
X Variable 2	-22,09090909	2,064937515	-10,69810051	#NUM!	-26,85266354	-17,32915464	-26,85266354	-17,32915464

(b)

Figure B. 4: Screenshot of the result of regression analysis applied to CFR_0.7 (a) and CFR_0.8 (b) compositions.

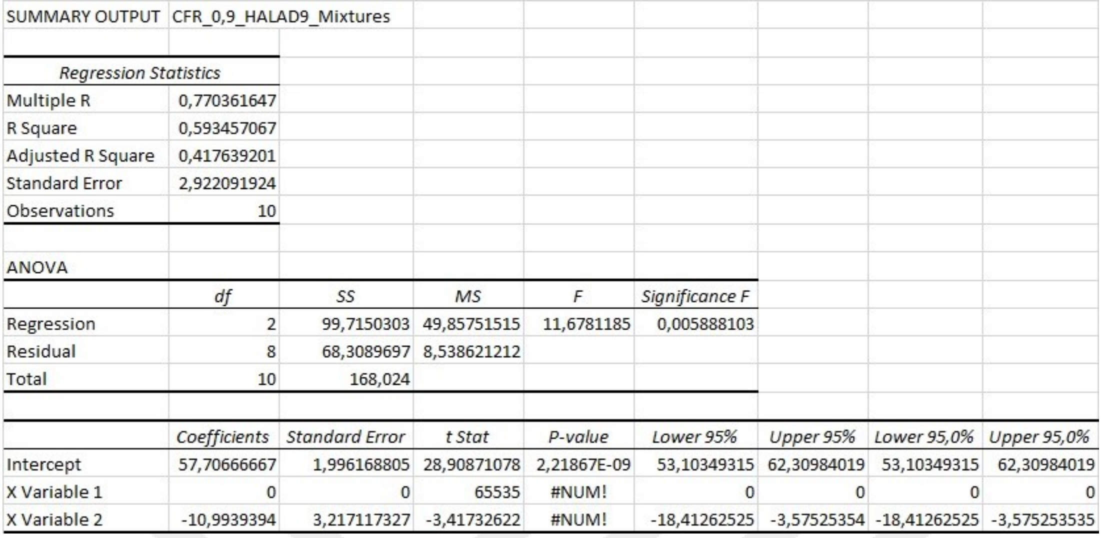

SUMMARY OUTPUT CFR_0,9_HALAD9_Mixtures

Regression Statistics	
Multiple R	0,770361647
R Square	0,593457067
Adjusted R Square	0,417639201
Standard Error	2,922091924
Observations	10

ANOVA

	df	*SS*	*MS*	*F*	*Significance F*
Regression	2	99,7150303	49,85751515	11,6781185	0,005888103
Residual	8	68,3089697	8,538621212		
Total	10	168,024			

	Coefficients	*Standard Error*	*t Stat*	*P-value*	*Lower 95%*	*Upper 95%*	*Lower 95,0%*	*Upper 95,0%*
Intercept	57,70666667	1,996168805	28,90871078	2,21867E-09	53,10349315	62,30984019	53,10349315	62,30984019
X Variable 1	0	0	65535	#NUM!	0	0	0	0
X Variable 2	-10,9939394	3,217117327	-3,41732622	#NUM!	-18,41262525	-3,57525354	-18,41262525	-3,575253535

(a)

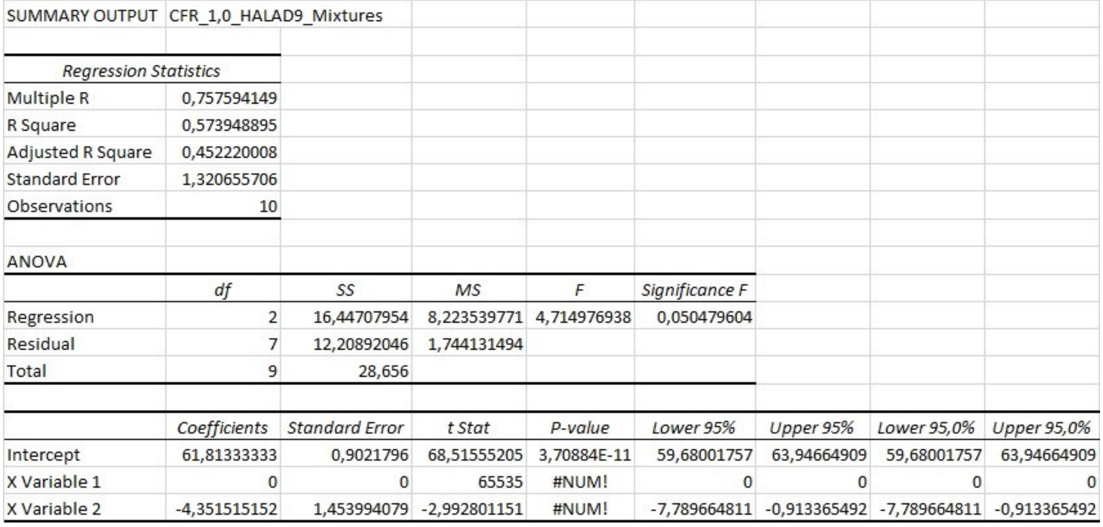

SUMMARY OUTPUT CFR_1,0_HALAD9_Mixtures

Regression Statistics	
Multiple R	0,757594149
R Square	0,573948895
Adjusted R Square	0,452220008
Standard Error	1,320655706
Observations	10

ANOVA

	df	*SS*	*MS*	*F*	*Significance F*
Regression	2	16,44707954	8,223539771	4,714976938	0,050479604
Residual	7	12,20892046	1,744131494		
Total	9	28,656			

	Coefficients	*Standard Error*	*t Stat*	*P-value*	*Lower 95%*	*Upper 95%*	*Lower 95,0%*	*Upper 95,0%*
Intercept	61,81333333	0,9021796	68,51555205	3,70884E-11	59,68001757	63,94664909	59,68001757	63,94664909
X Variable 1	0	0	65535	#NUM!	0	0	0	0
X Variable 2	-4,351515152	1,453994079	-2,992801151	#NUM!	-7,789664811	-0,913365492	-7,789664811	-0,913365492

(b)

Figure B. 5: Screenshot of the result of regression analysis applied to CFR_0.9 (a) and CFR_1.0 (b) compositions.

CURRICULUM VITAE

Name Surname : **Sardar Asadov**

Place and Date of Birth : **Tovuz, Azerbaijan 07.02.1993**

E-Mail : **esedov.serdar@gmail.com**

Linkedin : **https://www.linkedin.com/in/esedovserdar**

EDUCATION

- **B.Sc.** : 2014, **Azerbaijan State Oil Academy**, Oil–Gas–Mining Faculty, Transportation and Storage of Oil & Gas

PUBLICATIONS :

- Mustafa Hakan Ozyurtkan, Azimjan Dovletyarov, Sulayman Matkuliyev,Sardar Asadov **“Investigation the effect of additives on well cement’s exothermic heat development throughout setting period”**, WMESS (World Multidisciplinary Earth Sciences Symposium), 5 – 9 September 2016, Prague, Czech Republic.
- Sardar Asadov, Mustafa Hakan Ozyurtkan **“Modelling the Effect Additives on Exothermic Heat Development of Well Cement”**, ARMA (American Rock Mechanics Association), 51st U.S. Rock Mechanics/Geomechanics Symposium, 25 – 28 June 2017, San Francisco, California, USA.